

UNIVERSIDAD DE CUENCA

Facultad de Ingeniería

Doctorado en Recursos Hídricos

Unraveling evapotranspiration dynamics and processes in tropical Andean tussock grasslands

Trabajo de titulación previo a la obtención del título de Doctora en Recursos Hídricos

Autora:

Ana Elizabeth Ochoa Sánchez

CI: 0104162243

Director:

Dr. Rolando Célleri Alvear

CI: 0602794406

Codirector:

Dr. Patricio Crespo Sánchez

CI: 0102572773

Cuenca, Ecuador

15-octubre-2019

Jury Committee

Prof. Dr. Luis Timbe (Universidad de Cuenca, Ecuador)

Prof. Dr. Jan Feyen (KU Leuven, Belgium)

Prof. Dr. Bradford Wilcox (Texas A&M University, USA)

Director:

Prof. Dr. Rolando Célleri Alvear.

Department of Water Resources and Environmental Sciences University of Cuenca

Co-director:

Prof. Dr. Patricio Crespo Sánchez.

Department of Water Resources and Environmental Sciences University of Cuenca

Dean

Prof. Eng. Julver Pino Velázquez

Rector

Prof. Dr. Pablo Vanegas Peralta

Spanish translation of the title:

Dinámicas y procesos de la evapotranspiración en los pajonales andinos.

Please refer to this work as follows:

Ochoa-Sánchez, A, 2019. Unraveling evapotranspiration dynamics and processes in tropical Andean tussock grasslands. PhD thesis, Universidad de Cuenca, Escuela Politécnica Nacional and Universidad Técnica Particular de Loja, Ecuador.

This research was conducted under the financial support of the University of Cuenca, through a grant awarded to the author.

Resumen

El páramo proporciona recursos hídricos para importantes ciudades andinas. Estos recursos son utilizados para agua potable, agricultura, generación de energía hidroeléctrica y para sostener ecosistemas acuáticos. A pesar de que las zonas de montaña presentan dificultades por su locación remota; y, en consecuencia, escasez de datos, el conocimiento acerca del funcionamiento de este bioma ha mejorado últimamente. El monitoreo de precipitación (P) y escorrentía ha incrementado dramáticamente, pero no así el de evapotranspiración (ETa). A fin de comprender los componentes del ciclo hidrológico, este estudio tiene como objetivo entender el proceso de evapotranspiración en este importante bioma, a través de tres objetivos específicos: (1) cuantificar la intercepción, la transpiración y su contribución a la evapotranspiración, (2) encontrar métodos adecuados para medir y estimar la evapotranspiración e (3) investigar los controles de la evapotranspiración.

Los resultados mostraron la alta contribución de la intercepción al proceso de evapotranspiración. La capacidad máxima de los pajonales para interceptar agua fue de 2 mm. Durante eventos pequeños (P < 2 mm), la precipitación fue interceptada entre 100 y 80 % y regresó en forma de vapor a la atmósfera; mientras que, durante eventos largos (P > 2 mm), la pérdida por intercepción decreció desde 80 a 10 %. La intercepción fue principalmente controlada por la cantidad de precipitación y en menor grado por la humedad relativa. Durante periodos secos, las tasas de transpiración fueron en promedio 1.7 mm/día (en un rango de 0.7 y 2.7 mm/día). Incluso durante esos periodos secos, la neblina y el rocío fueron retenidos por la vegetación y contribuyeron a la evapotranspiración.

Para la medición de la evapotranspiración, se encontró que el método de eddy-covariance es el más preciso y el de mejor resolución. Sin embargo, debido a la complejidad de instalación, operación y mantenimiento, se encontraron como alternativas para la estimación diaria de evapotranspiración, dos modelos hidrológicos (HBV-light y PDM) y la ecuación calibrada de Penman-Monteith. Estos métodos alternativos son precisos, están disponibles gratuitamente y son fáciles de implementar. Este estudio demostró, además, que el método de balance hídrico, usado comúnmente, no es aceptable para la estimación de la evapotranspiración a escala diaria o mensual.

Finalmente, se encontró que el páramo tiene una tasa de evapotranspiración relativamente baja (ETa/P = 0.5, agregación anual) y que es un sitio limitado por la cantidad de energía, donde la radiación neta es el principal control de la evapotranspiración (ETa/Rn = 0.47,

agregación anual). Los controles secundarios que se encontraron fueron la velocidad del viento, la conductancia superficial y la conductancia aerodinámica, los cuales fueron especialmente importantes durante periodos secos.

Palabras clave: Páramo. Andes. Pajonal. Evapotranspiración. Intercepción. Evaporación. Transpiración.

Abstract

The páramo biome provides water resources for many cities in the Andes. These resources are used for drinking water, irrigation, hydropower generation and for sustaining aquatic ecosystems. Notwithstanding mountainous terrains place difficulties for their study, due to its remoteness and data scarcity, knowledge about the functioning of this biome has improved lately. Precipitation (P) and runoff monitoring has increased dramatically, but this was not the case for evapotranspiration (ETa). In order to understand the components of the hydrological cycle, this study aimed at understanding the evapotranspiration process of this important biome by pursuing the following three objectives: (1) to quantify interception, transpiration and their contribution to evapotranspiration, (2) to find suitable methods for measuring and estimating evapotranspiration, and (3) to investigate the controls on evapotranspiration.

Results show the high contribution of interception to the evapotranspiration process. The maximum capacity of tussock grasslands to intercept water was 2 mm. During small events (P < 2 mm), between 100 and 80 % of precipitation was intercepted and released back to the atmosphere as vapour; while during large events (P > 2 mm), interception loss decreased from 80 to 10 %. Interception was mainly driven by precipitation amount and secondary by relative humidity. During dry periods, transpiration rates were on average 1.7 mm/day (ranging between 0.7 and 2.7 mm/day) and on top, the fog and dew harvested by the vegetation contributed to the evapotranspiration in around 30 %.

For measuring evapotranspiration, the eddy-covariance method is considered the most accurate and with the highest resolution. However, given the high cost of the method, complex installation, operation and maintenance, two hydrological models (HBV-light and PDM) and the calibrated Penman-Monteith equation were found robust alternative methods for the daily estimation of evapotranspiration. These alternative methods are accurate (Pearson's correlation coefficient > 0.7 and bias percentage < 20 %), freely available and easy to implement. This study also showed that the commonly used water balance method was not suitable for estimating evapotranspiration at daily or monthly scale.

Finally, it was found that the páramo biome has a relatively low evapotranspiration rate (annual ETa/P = 0.5) and is an energy-limited site, where net radiation is the primer control on evapotranspiration (annual ETa/Rn = 0.47). The secondary controls were wind speed, surface and aerodynamic conductance, especially important during dry periods.

Keywords: Páramo. Andes. Tussock grasslands. Evapotranspiration. Interception. Evaporation.

Contents

Resume	1	i
Abstract	<u> </u>	iii
Content	S	V
List of F	igures	viii
List of T	ables	xi
Acknow	ledgements	xvii
1. Inti	oduction	1
1.1	Importance of the study	1
1.2	Objectives	2
1.3	Outline of the doctoral thesis	4
1.4	Study area	4
2. Qua	antification of rainfall interception	7
2.1	Introduction	8
2.2	Materials and methods	11
2.2.1	Data	11
2.2.2	Interception loss calculation	13
2.	2.2.1 Events selection	13
2.2.3	Effective rainfall and interception loss calculated with a disdrometer vs. a raingauge	14
2.2.4	Relationship between interception loss and meteorological variables	14
2.2.5	Estimation of interception loss from meteorological variables	16
2.3	Results and discussion	17
2.3.1	Effective rainfall and interception loss calculated with a disdrometer vs. a raingauge	17
2.3.2	Quantification of interception loss	19
2.3.3	Relationship between interception loss and meteorological variables	20
2.3.4	Estimation of interception loss	22
2.4	Conclusions	25

3.	Qua	nntification of transpiration	27
	3.1	Introduction	28
	3.2	Materials and methods	29
	3.2.1	Data	29
	3.2.2	Quantification of transpiration	29
	3.3	Results and discussion	30
	3.4	Conclusions	32
4.	_	antification of actual evapotranspiration: comparison of measurement and	
est	timati	on methods	35
	4.1	Introduction	36
	4.2	Materials and methods	38
	4.2.1	Methods for measuring and estimating actual evapotranspiration	38
		2.1.1 Eddy-covariance method (ETa _{EC})	
		2.1.2 Lysimeters installation and methodology	
		2.1.3 Water balance method	
	4.	2.1.4 Energy balance method	43
	4.	2.1.5 Potential evapotranspiration equation calibrated with eddy-covariance measurements	
	4.	2.1.6 Hydrological models	45
	4.2.2	Comparison of actual evapotranspiration measurements and estimates	46
	4.3	Results	48
	4.3.1	Measuring daily actual evapotranspiration with the eddy-covariance method	48
	4.3.2	Comparison of methods for the estimation and measurement of actual evapotranspiration	49
	4.4	Discussion	53
	4.4.1	Actual evapotranspiration and its environmental controls	53
	4.4.2	Sources of uncertainty in the ETa estimation methods	54
	4.	4.2.1 The eddy-covariance technique	54
	4.	4.2.2 Lysimeters	55
	4.	4.2.3 Water balance	56
	4.	4.2.4 Energy balance	58
	4.	4.2.5 The calibrated evapotranspiration equation	59
	4.	4.2.6 The hydrological models	60
	4.5	Summary and conclusions	61
5.	Cor	trols on actual evapotranspiration	65

5.1	Introduction	66
5.2	Methods	67
5.2.	.1 Data	67
5.2.	.2 Evapotranspiration and meteorological variables seasonality and their differ	rence between wet
and	dry periods	68
5.2.	.3 Controls on evapotranspiration	70
5	5.2.3.1 Events selection	71
5.3	Results	71
5.3.	.1 Evapotranspiration seasonality	71
5.3.	.2 Evapotranspiration controls	74
5.4	Discussion	76
5.5	Conclusions	78
6. Co	onclusions	81
6.1	Synthesis	81
6.2	Future research	83
Referen	nces	85
Append	lix A	97
About t	the author	101

List of Figures

Figure 1.1. The paramo biome located above the 3300 m a.s.l. This map was elaborated by T.
Distler and provided by C. Ulloa, Missouri Botanical Garden3
Figure 1.2. Outline of the doctoral thesis
Figure 1.3. Zhurucay Ecohydrological Observatory located in Southern Ecuador. Three
main microcatchments within the Zhurucay Observatory are numbered from M1 to M3 and
five raingauges are numbered from P1 to P5.
Figure 2.1. CS616 WCR calibration curve and its 95 % confidence interval
Figure 2.2. Effective rainfall (ER) vs. cumulative precipitation (P) calculated from: a) the
disdrometer and b) the raingauge; where RSS corresponds to the residual sum of squares and
R^2 to the coefficient of determination. c) Event duration vs. cumulative precipitation from
events selected with the disdrometer and raingauge. d) P, ER and interception loss (IL) box
plots calculated from the disdrometer and raingauge records
Figure 2.3. a) Interception loss relative to cumulative precipitation (IL/P) calculated from the
disdrometer and WCRs observations and b) IL/P estimated from the multiple linear
regression expressed in equation 1.4 (red dots).
Figure 2.4. The most important variables in the IL process according to the RF algorithm
have the highest reduction in the mean square error (MSE) and the highest reduction in the
node impurity presented as percentages. The variables are cumulative precipitation
(Prcpacum), maximum rainfall intensity (MI), mean rainfall intensity in the eighteen hours
before the event (WI18), cumulative precipitation eighteen hours before the event (Pacum18),
weighted wind speed (WS), and weighted mean rainfall intensity (WI)21
Figure 2.5. Regression tree for interception loss. In each node: IL mean, number of items in
the node, and percentage of data included in the node. Each split is determined by a variable
with its threshold. 23
Figure 3.1. Example of the soil volumetric water content signal (VWC) during a 6-day dry
event. Daylight hours are coloured in grey
Figure 3.2. Transpiration (Transp) against actual evapotranspiration (ETa) for zero-
precipitation events. Blue dots are events with dew, light blue dots are events without dew
and white dots are events where dew temperature could not be calculated due to missing data.
31

Figure 3.3. Dry event including the following variables: precipitation (P), soil volumetric
water content (VWC), vapour pressure deficit (VPD), temperature (Temp), surface
conductance (g _s), aerodynamic conductance (g _a), wind speed (u ₂), net radiation (Rn) and
actual evapotranspiration (ETa). Shadow bars show daylight hours from 7 am to 7 pm32
Figure 4.1. Eddy-covariance tower at the supersite in Zhurucay (3765 m a.s.l.). Photograph:
Galo Carrillo-Rojas40
Figure 4.2. a) Lysimeters installed at the study site before they were covered by soil and
vegetation. Sensors shown are T8 tensiometers. b) Illustration of the lysimeter
instrumentation (WCR = water content reflectometers, DWP = dielectric water potential
sensors, T8 = tensiometers). Dimensions are shown in centimetres. Photograph: Galo
Carrillo-Rojas. Illustration: Juan Pablo Córdova42
Figure 4.3. Daily actual evapotranspiration measured with the eddy-covariance method
(ETa _{EC} in mm/day) shown for every month together with the median potential
evapotranspiration (ETo in mm/day) estimated with the Penman-Monteith equation and
median net radiation (Rn in mm/day). Additionally, monthly precipitation (P in mm/month),
soil volumetric water content (VWC), and relative humidity (RH in percentage) are shown. 48
Figure 4.4. Cumulative daily actual evapotranspiration measured by the eddy-covariance
(EC) and lysimeters and estimated by the PDM and HBV-light hydrological models, the
water balance (WB) and energy balance (EB) methods, the calibrated evapotranspiration
equation (PMCal), and the potential evapotranspiration (ETo). Cumulative precipitation (P) is
also shown50
Figure 4.5. Daily actual evapotranspiration measured by the eddy-covariance method (EC)
and estimated by the HBV-light and PDM models, the calibrated evapotranspiration equation
(PMCal), the energy balance (EB) and the water balance methods (WB)51
Figure 4.6. Daily differences in evapotranspiration between the methods and the eddy-
covariance. Methods include: PDM and HBV-light hydrological models, lysimeters (Lys),
energy balance (EB), water balance (WB), and the calibrated evapotranspiration equation
(PMCal)52
Figure 4.7. Cumulative evapotranspiration measured with the four lysimeters every 7 days,
cumulative precipitation, and the change in soil water storage (ΔS)56
Figure 4.8. Differences between the mean water balance estimates (without the change in
storage term) with EC measurements (orange line) and the differences between the mean
water balance estimates (including the change in storage term) and the EC measurements
(black line)

Figure 4.9. Energy fluxes measured with the eddy-covariance method vs. energy fluxes
estimated with the energy balance method. Energy balance method is highly dependent on the
variance of the temperature (σT)
Figure 4.10. Soil volumetric water content observed with a water content reflectometer
(VWC), soil water storage modelled with the PDM (PDM S), and soil water storage modelled
with the HBV-light model (HBV S)60
Figure 5.1. Seasonality of the average values of actual evapotranspiration (ETa),
precipitation (P), vapour pressure deficit (VPD), temperature (Temp), surface conductance
(g _s), aerodynamic conductance (g _a) and net radiation (Rn). Precipitation bars correspond to
the minimum and maximum monthly value. Bars for the remaining variables correspond to
the first and the third quartile of the daily values. The grey shadow covers the dry periods of
September, October and November according to the Budyko analysis73
Figure 5.2. Evapotranspiration ratio (ETa/P) as a function of the dryness index (ETo/P) for
three-month periods. D1, D2 and D3 correspond to dry periods (09/2016 - 11/2016, 09/2017
– 11/2017 and 09/2018 – 11/2018)
Figure 5.3. Actual evapotranspiration observations and estimations for the validation events.
Bars correspond to the 95 % confidence intervals75
Figure 5.4. Wet event including the following variables: precipitation (P), soil volumetric
water content (VWC), vapour pressure deficit (VPD), temperature (Temp), surface
conductance (g _s), aerodynamic conductance (g _a), wind speed (u ₂), net radiation (Rn) and
actual evapotranspiration (ETa). Shadow bars show daylight hours from 7 am to 7 pm76

List of Tables

Table 1.1. M1, M2 and M3 microcatchment characteristics. Soil type correspond to Andosol
(AN), Histosol (HN) and Leptosol (LP). Vegetation coverage correspond to tussock grass
(TG), cushion plants (CP), Polylepis forest (QF) and pine forest (PF). Soil and vegetation
characteristics were calculated from the corresponding microcatchments in Mosquera et al.
(2015). However, names M1, M2 and M3 differ from Mosquera et al. (2015)6
Table 2.1. Meteorological variables included in this chapter 16
Table 2.2. Bibliographical revision of studies reporting interception loss estimations for short
vegetation around the world: Interception loss relative to cumulative precipitation (IL / P),
canopy storage capacity (S), and positive (+) or negative (-) relations between interception
loss and meteorological variables. "No cor" corresponds to no correlation of the variable to
IL
Table 4.1. Spatial and temporal resolution of the actual evapotranspiration measurement and
estimation methods used in this study
Table 4.2. Zhurucay microcatchments soil characteristics where vegetation cover
corresponds to tussock grasslands
Table 4.3. Bias percentage (pbias), normalized root mean square error (nRMSE), Pearson's
correlation coefficient (r), volumetric efficiency (ve), and coefficient of determination (R2)
for the actual evapotranspiration estimated with the HBV-light and PDM models, the
calibrated evapotranspiration equation (PMCal), the lysimeters (Lys), the energy balance
(EB), and water balance (WB) methods against the eddy-covariance measurements51
Table 4.4. Bias percentage (pbias), normalized root mean square error (nRMSE), Pearson's
correlation coefficient (r), volumetric efficiency (ve), and coefficient of determination (R2)
for the ETa estimates from the water balance closure in three catchments against the eddy-
covariance measurements
Table 4.5. General advantages and disadvantages of the actual evapotranspiration
measurement and estimation methods.
Table 5.1. Variables used in this study. Sensors or equations used for each variable. Mean,
maximum and minimum daily values for the three-years study period $(03/2016 - 02/2019)69$
Table 5.2. Annual averages, seasonal averages, and percentage increase during dry months
compared to the wet months value of the actual evapotranspiration (ETa) and its main
controlling variables: precipitation (P), net radiation (Rn), vapour pressure deficit (VPD).

temperature (Temp), surface conductance (g_s) and aerodynamic conductance (g_a) . Bold numbers are seasonal daily averages that are significantly different from each other at the 0.05 significance level according to the t-test. Dry periods correspond to the D1, D2 and D3 points in Figure 5.2 (09/2016-11/2016,09/2017-11/2017) and 09/2018-11/2018).......74

Cláusula de licencia y autorización para publicación en el Repositorio Institucional

Ana Elizabeth Ochoa Sánchez en calidad de autora y titular de los derechos morales y patrimoniales del trabajo de titulación "Unravelling evapotranspiration dynamics and processes in tropical Andean tussock grasslands", de conformidad con el Art. 114 del CÓDIGO ORGÁNICO DE LA ECONOMÍA SOCIAL DE LOS CONOCIMIENTOS, CREATIVIDAD E INNOVACIÓN reconozco a favor de la Universidad de Cuenca una licencia gratuita, intransferible y no exclusiva para el uso no comercial de la obra, con fines estrictamente académicos.

Asimismo, autorizo a la Universidad de Cuenca para que realice la publicación de este trabajo de titulación en el repositorio institucional, de conformidad a lo dispuesto en el Art. 144 de la Ley Orgánica de Educación Superior.

Cuenca, 15 de octubre del 2019.

Ana Elizabeth Ochoa Sánchez

Just 12 betha

C.I: 0104162243

Cláusula de Propiedad Intelectual

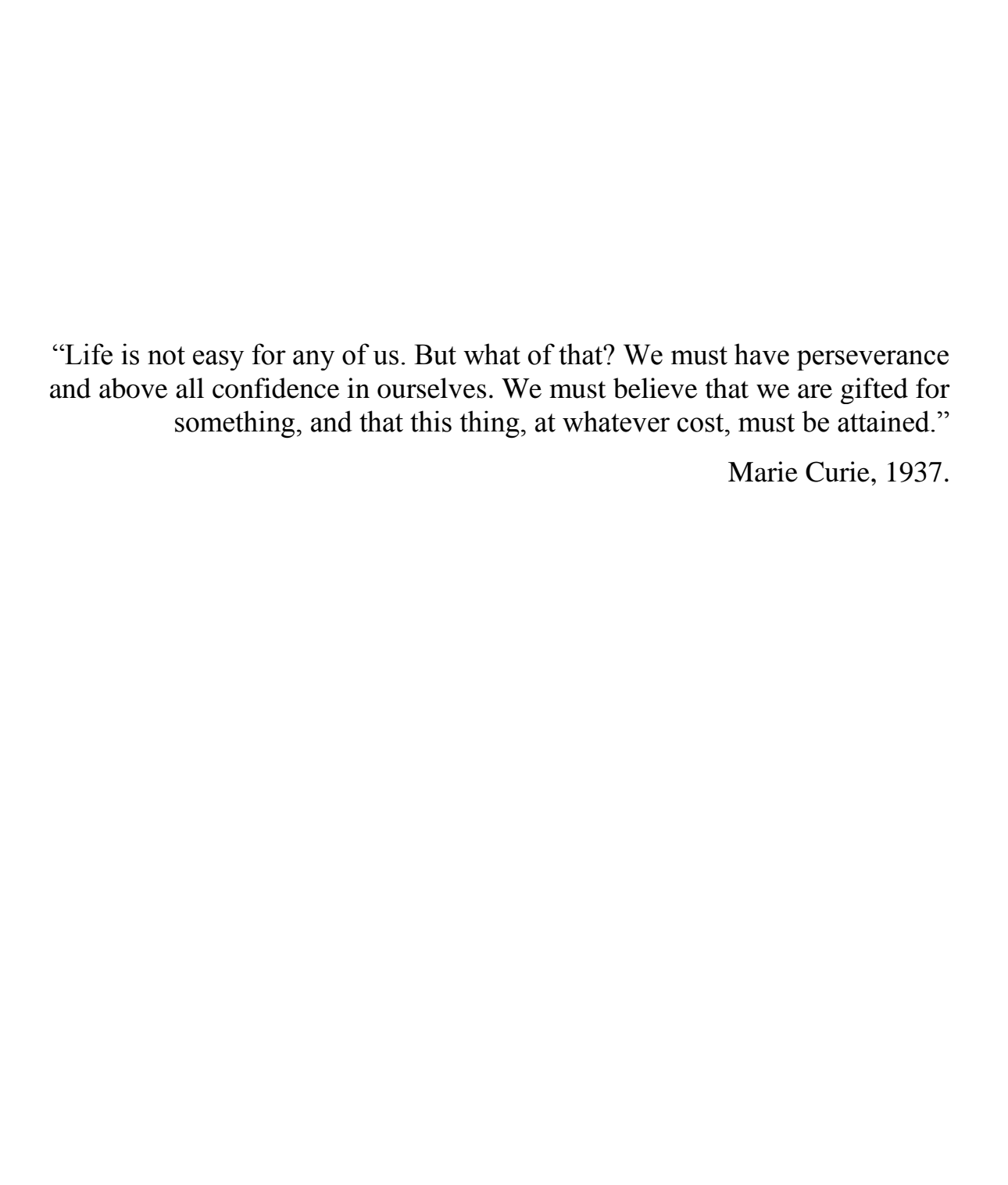
Ana Elizabeth Ochoa Sánchez, autora del trabajo de titulación "Unraveling evapotranspiration dynamics and processes in tropical Andean tussock grasslands", certifico que todas las ideas, opiniones y contenidos expuestos en la presente investigación son de exclusiva responsabilidad de su autoraa.

Cuenca, 15 de octubre del 2019

Ana Elizabeth Ochoa Sánchez

Anticobello

C.I: 0104162243



Acknowledgements

During the almost four years that it took to complete this Doctoral Programme, I gained considerable knowledge on mountain hydrological processes and acquired experiences and skills that made this journey, one of the most important achievements in my life. This definitely happened with the help and support of many people to whom I am deeply grateful.

I am grateful to my *alma máter*, the University of Cuenca, for the awarding of a scholarship that allowed me to enrol and complete the Doctoral Programme and the funding of the project whereof this study was part.

I want to thank the Jury of this PhD thesis: Prof. Jan Feyen, Prof. Luis Timbe and Prof. Bradford Wilcox for their thoughtful comments and efforts towards improving this document.

I want to thank my advisors for their important contribution to this success. They have always been willing to help and answer to the numerous things a PhD student faces, from research to personal challenges. Particular thanks are due to Rolando for being comprehensive, respectful and encouraging. I am sure that I am one of the few women that coincided with a supervisor that is open to talk and take actions for gender equality in a workplace. Rolando, as the head of the Department, has led the path of many scientists. I think of him as one of my dearest mentors and I will always look at him with respect and admiration. I also would like to thank Patricio for being my mentor since I was 17 years old. I chose civil engineering because I looked up to him. He codirected my undergrad thesis, he encouraged me to go to Belgium for doing my Masters, he was my support during very difficult moments in my life, he coauthored my first research article, he is the co-advisor of this thesis and he definitely will be pushing me to the limit forever.

Although Esteban Samaniego was not my thesis advisor, I consider him my mentor for introducing me to the scientific method. I worked with him after I came back from my Masters in Belgium and before I started my PhD. I acknowledge him for the unique way he passes knowledge to his mentees by asking deep questions and philosophizing about the thoughts of great scientists. I thank him for giving me freedom to do research in my own terms and times.

The Department of Water Resources and Environmental Sciences (iDRHICA) is an outstanding group in Ecuador and it is the perfect environment for doing research. I would like to express my gratitude to all its members, especially to those who collaborated directly

and indirectly to this project: Prof. Jan Feyen, Galo Carrillo, Adrián Sucozhañay, Mario Córdova, Franklin Marín, Patricio Lazo, Juan Pesántez, Pablo Mosquera and Johanna Orellana.

I would like to thank the Ecuadorian Network of Women in Science (REMCI, by its initials in Spanish), whose members have been crucial in increasing my confidence and motivation. I especially thank Daniela Ballari, Ximena Palomeque, Johanna Orellana, Verónica Pinos, Gina Berrones, Gabriela Álava, Lourdes Illescas, Lorena Sigüenza, Jennifer Yépez and Victoria Abril. I consider them great scientists, my friends and allies.

My high school friends Paola, Picky, Tatty y Lore are also part of this achievement. They are strong intelligent women who I looked up to. We have grown up together and shown the world what women are capable of.

I want to thank my family, especially my parents, who made me believe that I can achieve everything. My dad Marcelo and my mom Elvia Rosa have always been my support and my safe place. I want to thank my aunt Magaly, my uncle Patricio, my cousin and friend Irene, my grandfather Manuel, my mother-, father- and sister-in-law. I especially thank my partner and friend Edisson, who has listened to my thoughts, projects and complains and who has dealt with my ups and downs during these years. He is an incredible and committed parent of our twins, Ariana and Camila, who are of course my inspiration, my motivation and my major challenge in life.



Chapter 1 Introduction

1.1 Importance of the study

Mountain research on hydrology and climatology are of outmost importance for developed and developing countries towards achieving several of the seventeen goals of the 2030 Agenda for Sustainable Development (UN, 2018); especially goal 6 (clean water and sanitation) and goal 13 (climate action). Regarding goal 6, water availability requires correct measurement and estimation of the water cycle. Important variables that need understanding and measurement are precipitation, evapotranspiration and discharge. With respect to goal 13, climate action needs correct estimation of the climate change impacts on mountain regions, in order to assess their vulnerability and create mitigation plans accordingly.

In South America, one of the most important mountain environments, for its ecosystem services, is the páramo. The páramo occupies 36,000 km² and is located above 3300 m. a.s.l., mainly in Ecuador and Colombia, but also in Costa Rica, Venezuela and Peru (Figure 1.1). Water from the páramo is used by many cities in Ecuador and Colombia for drinking water, agriculture, hydropower generation and for sustaining aquatic ecosystems. In addition, the páramo is inhabited by indigenous communities that live and develop at this region. The intrinsic complexity of mountain terrains demands further assessment of their hydrological processes. The complex orography makes it difficult to measure or estimate correctly the large spatial and temporal variability of hydrological variables. Major efforts towards the closing of the water balance at the páramo led to an increase of the monitoring of precipitation and discharge in the last decade (Ochoa-Tocachi et al., 2018). However, the monitoring of evapotranspiration received considerably less attention.

The correct measurement or estimation of evapotranspiration enables the closure of the water balance and the energy budget. Evapotranspiration is a key variable since it explains the exchange of water and energy between the soil, vegetation and the atmosphere. It has regulating effects over precipitation and soil moisture (Ren et al., 2018). It links ecosystem functioning, carbon and climate feedbacks, agricultural management, and water resources (Fisher et al., 2017). Insights on the evapotranspiration process are of major importance for solving current and future science questions about the terrestrial biosphere.

An important step towards the understanding of the evapotranspiration process and the links between hydrologic and ecologic systems, is the quantification of the evapotranspiration (ETa) components (Good, Noone, & Bowen, 2015; Savenije, 2004). The components of ETa include soil and intercepted water evaporation and transpiration. Seasonal variation of ETa and the contribution of its components depend on how vegetation processes energy and water (Saleska, 2003). This variation and partitioning are important and yet unclear at some sites in the Tropics.

Evapotranspiration in grasslands at high altitudes have been rarely measured (Coners et al., 2016; Gu et al., 2008; Knowles, Burns, Blanken, & Monson, 2015; van den Bergh, Inauen, Hiltbrunner, & Körner, 2013). At the páramo, evapotranspiration was estimated calculating the reference evapotranspiration using either the Penman-Monteith equation (Córdova, Carrillo-Rojas, Crespo, Wilcox, & Célleri, 2015) or the Hargreaves equation (Maffei, 2012). The installation of the eddy-covariance tower at the páramo in 2016 led to the first measurement of actual evapotranspiration (Carrillo-Rojas, Silva, Rollenbeck, Célleri, & Bendix, 2019). This was a major step towards accuracy, although this method presents its own difficulties (e.g. complex installation, operation, maintenance and data processing). Actually, the available measurements of evapotranspiration open the opportunity for finding alternative methods that might be suitable for different applications.

In addition, the adequate understanding of evapotranspiration includes the assessment of its drivers. The páramo ecosystem is probably vulnerable to climate change impacts due to their dependence on surface and sub-surface water. If temperature and precipitation change, evapotranspiration will change as well. Unveiling the controls on evapotranspiration leads to a better understanding on the dependency among variables.

In summary, the quantification of evapotranspiration and its components requires the availability of accurate and reliable methods for estimating evapotranspiration and the unveiling of the controls on evapotranspiration; all of these in order to advance towards a better understanding of the hydrological processes at one of the most important mountain ecosystems.

1.2 Objectives

In order to contribute to the understanding of the hydrological processes of the páramo, the main aim of the doctoral project was to unravel the dynamics and processes of

evapotranspiration that enables proper closing of the water balance of the páramo biome. Doing so, will improve the hydrological modelling and further analysis of the impact of climate and land use change at this important biome. The specific objectives can be summarized as:

- (1) quantification of the interception and transpiration and investigation of their contribution to evapotranspiration,
- (2) measuring and estimation of evapotranspiration using different methods with the intention to compare them and analyse their potential for different applications, and
- (3) understanding of the evapotranspiration process by investigating its controls.



Figure 1.1. The páramo biome located above the 3300 m a.s.l. This map was elaborated by T. Distler and provided by C. Ulloa, Missouri Botanical Garden.

1.3 Outline of the doctoral thesis

The outline of the thesis is depicted in Figure 1.2. The first chapter highlights the importance of the study by reviewing past studies, identifying the knowledge gaps and the objectives. In addition, this chapter provides a detailed outline of the study are in support of the multiple studies in the following chapters.

The second and third chapters quantify the major components of evapotranspiration at the páramo site: interception is described and discussed in Chapter 2 and transpiration in Chapter 3. The amount of data enabled define the drivers of interception and a mathematical model for estimation of the interception. The availability of actual evapotranspiration measurements enabled to understand the contribution of evaporation and transpiration to the evapotranspiration process as discussed in Chapter 3.

Thereafter, Chapter 4 presents several methods to measure and estimate evapotranspiration. Each method's advantages and disadvantages are discussed to give the reader the possibility to select the best method conform the application.

Finally, the main and secondary controls on evapotranspiration are presented in Chapter 5. The relate discussion focussed on comparing the páramo site to other tropical sites with similar characteristics to close the knowledge gap on mountain hydrology in the Tropics.

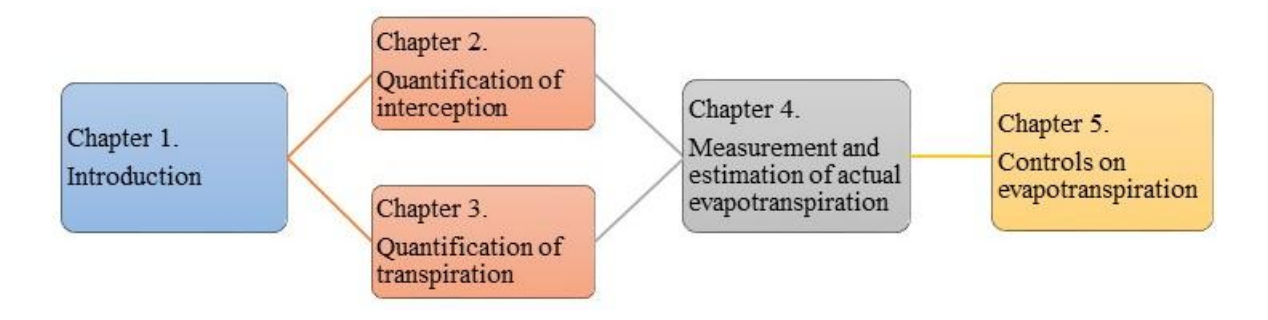


Figure 1.2. Outline of the doctoral thesis

1.4 Study area

The study site is located at the headwater of the Zhurucay Ecohydrological Observatory, which has a drainage area of 7.36 Km². Zhurucay is located in a wet páramo ecosystem on the Pacific side of the western Andean cordillera (Figure 1.3) and it is an open-field laboratory where hydrological, micrometeorological and ecological research is conducted. Elevations range from 3500 to 3900 m a.s.l. The study site is representative of the wet páramo ecosystem based on its location, vegetation, climate, and soil characteristics. Climate

is influenced by the west Pacific regime and the air masses from the Amazon (Córdova, Carrillo-Rojas, & Célleri, 2013). Mean annual precipitation is approximately 1300 mm. Intraannual precipitation is highly uniform (very low seasonality) with a slightly higher precipitation from January to June. Precipitation is frequent and characterized by its low intensity and high occurrence of drizzle which is present 80 % of the rainy days and accounts for 30 % the annual rainfall depth (Padrón, Wilcox, Crespo, & Célleri, 2015). Only 20 % of the days are completely dry and even in the drier months there are only few consecutive days with no rain (Padrón et al., 2015). Furthermore, Padrón et al. (2015) reports that during rainy days, precipitation is less than 1 mm/day in 20 % of the days in a year and only 10 % of the days record a precipitation higher than 10 mm. Rainfall intensity is less than 2 mm/h (for a 30-min duration) during 90 % of the time. During dry days and even during rainy days, there are sunny hours with high solar radiation, enhancing evaporation. Solar radiation can reach instantaneous values of 1.4 kW/m2 due to the latitude and elevation of the area. Mean air temperature is 6°C and mean relative humidity 90 %, and mean wind velocity 3.6 m/s.

The study area is mainly covered (>80 %) by tussock grasses (*Calamagrostis Intermedia* (J. Presl) Steud. sp., commonly known as "*pajonal*"), which are perennial plants, approximately 30 cm tall, that grow in bunches leaving no bare soil at the study site. At the Soils correspond mainly to Andosols with a minority of Histosols (24 %) (FAO/ISRIC/ISSS, 1998). Andosols are black loamy soils with a high organic matter content and moderately granular.

Precipitation and discharge are continuously monitored at several stations within Zhurucay. For this study, five rain gauges (Figure 1.3, P1 – P5) and three weirs (Figure 1.3, M1 – M3) were used for closing the water balance of three microcatchments (M1, M2 and M3). Characteristics of these three microcatchments are detailed in Table 1.1. In addition, a supersite exists at Zhurucay (Figure 1.3), located at 3765 m a.s.l. equipped with micrometeorological sensors such as an eddy-covariance tower, a meteorological station, energy fluxes sensors, precipitation sensors (rain gauges and a laser disdrometer), as well as a hillslope equipped with a set of 38 water content reflectometers (WCRs).

Table 1.1. M1, M2 and M3 microcatchment characteristics. Soil type correspond to Andosol (AN), Histosol (HN) and Leptosol (LP). Vegetation coverage correspond to tussock grass (TG), cushion plants (CP), Polylepis forest (QF) and pine forest (PF). Soil and vegetation characteristics were calculated from the corresponding microcatchments in Mosquera et al. (2015). However, names M1, M2 and M3 differ from Mosquera et al. (2015).

Catchment	Area (km²)	Altitude (m a.s.l.)	Slope (%)	Soil type distribution (%)		Vegetation coverage (%)				Annual precipitation	Runoff coefficient	
				AN	HS	LP	TG	CP	QF	PF	(mm)	cocificient
M1	0.38	3770 - 3900	24	83	15	2	87	13	0	0	1063	0.43
M2	1.6	3680 - 3900	17	82	16	2	82	16	0	2	1042	0.48
M3	4.31	3676 - 3900	18	77	19	4	77	20	2	1	1019	0.42

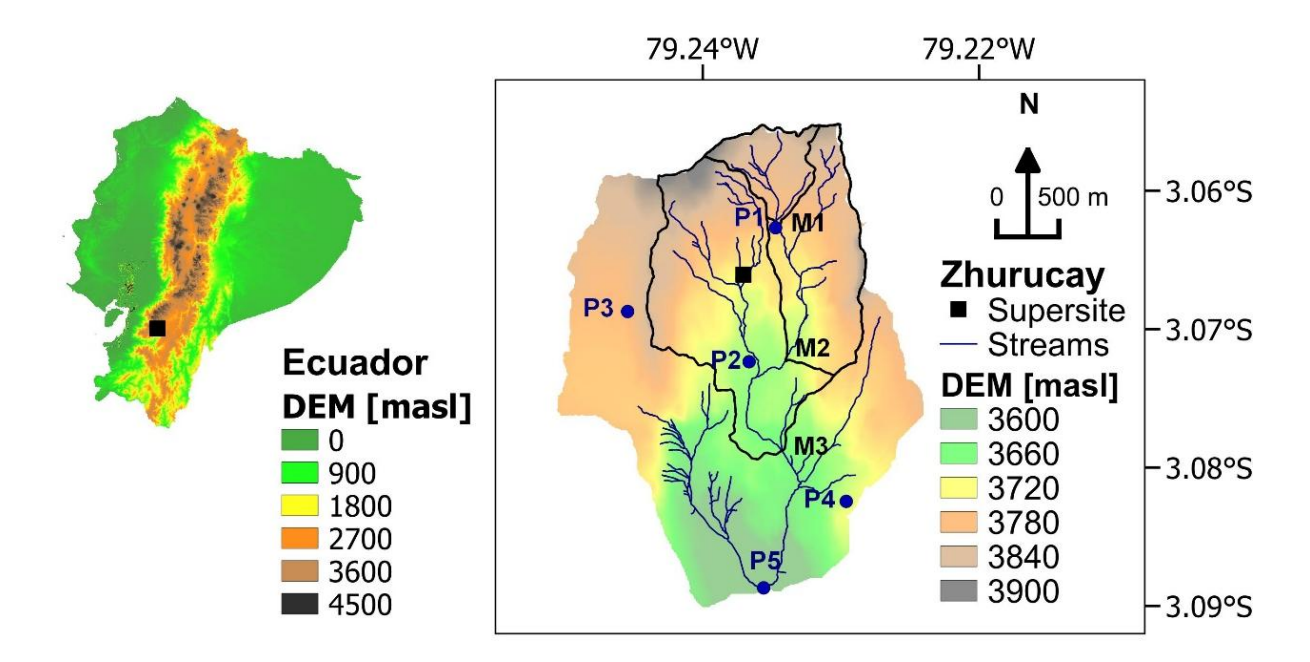


Figure 1.3. Zhurucay Ecohydrological Observatory located in Southern Ecuador. Three main microcatchments within the Zhurucay Observatory are numbered from M1 to M3 and five raingauges are numbered from P1 to P5.

Chapter 2

Quantification of rainfall interception

Páramo ecosystem provide most of the water for the tropical Andean highlands in South America. While the comprehension of this environment has increased lately, there remains an urgent need to quantify the processes involved in the hydrological cycle. Interception loss (IL) is one of the least studied processes in the páramo, and more generally, in grasslands globally. The main objective of this study was to quantify IL at event scale by estimating it indirectly from precipitation (P) and effective rainfall (ER). Furthermore, the following questions were assessed: (1) how much of the P becomes ER; (2) what is the impact on IL calculations of using a raingauge instead of a disdrometer?; (3) which meteorological variables are related to the IL process?; and (4) is it possible to estimate IL from meteorological variables?. High percentages of IL in relation to P were found (10 - 100 %). The maximum canopy storage capacity of tussock grasses was approximately 2 mm. The disdrometer observations led to more accurate results than the raingauge observations since only the disdrometer registers light precipitation, horizontal precipitation, and drizzle which increases the amount of P, ER, and IL estimates. Also, we found that IL is more strongly correlated with P; and IL can be estimated with a multiple linear regression (R²=0.9) from P and relative humidity for events where 1.7 < P < 8.5 mm. These findings show the important role of IL in the páramo and provide a stepping stone to the modelling of water resources.

Related publication

Ochoa-Sánchez, A., Crespo, P., & Célleri, R. (2018). Quantification of rainfall interception in the high Andean tussock grasslands. *Ecohydrology*, 11(3), e1946. https://doi.org/10.1002/eco.1946

2.1 Introduction

Research on mountain hydrology presents several difficulties such as data scarcity, complex orography, and harsh environmental conditions that limit field work. In the Andean region, hydrometeorological variables (e.g. precipitation) have strong spatial variability, which intensifies the need for more detailed information from field studies. These, in combination with the remoteness of study sites, have hindered ecohydrological research in the Andean region and limit the capacity for science-based management of most of its water ecosystem services (provisioning, supporting, and regulating services). The páramo ecosystem (generally above 3000 m a.s.l.), characterized by a large presence of tussock grasses (Hofstede, Segarra, & Mena, 2003), provides most of the water for the Andean highlands of Venezuela, Colombia, and Ecuador, extensive parts of the adjacent lowlands, and even some of the arid coastal plains in Northern Peru (Buytaert, Iñiguez, et al., 2006). Furthermore, considering that the increasing demand of human activities, land use and climate change will produce a severe impact on the hydrological services of the high Andes (Beniston, 2003; Buytaert, Célleri, et al., 2006; Foster, 2001), it is of outmost importance to understand and estimate the hydrological cycle components in order to preserve the ecosystems and develop adequate strategies for the sustainable management of the regional water resources.

Evapotranspiration (ETa) is a very important component of the hydrological cycle and its knowledge improves the understanding of the water and energy exchange processes between land and atmosphere. The term evapotranspiration encompasses the different evaporative processes; and should be partitioned in order to conceptualize each process: evaporation from the soil and canopy interception, and transpiration (Savenije, 2004). Interception loss (IL) from the canopy (the proportion of rainwater retained and evaporated by vegetation) can constitute a considerable fraction of evaporation and it is an important hydrological process as it determines the amount of water reaching the soil as effective rainfall. Interception is certainly not small in rough surface canopies (Beven, 2001) but it is commonly disregarded or underestimated in many models (e.g. THALES, DBSIM, Topkapi, QPBRRM, and InHM models), hindering the proper closing of the water balance. Indeed, no previous research exists on the interception loss in Andean páramos where most studies have focussed on other processes or components of the hydrological cycle such as precipitation (Muñoz, Célleri, & Feyen, 2016; Padrón et al., 2015), soil water movement (Buytaert, De Bièvre, Wyseure, & Deckers, 2005; Buytaert et al., 2002), percolation and erosion (Harden, 2001; Harden & Scruggs, 2003; Poulenard, Podwojewski, Janeau, & Collinet, 2001; Zehetner & Miller, 2006),

runoff sources (Correa et al., 2016, 2017), and rainfall-runoff processes (Braud, Fernandez, & Bouraoui, 1999; Crespo et al., 2011; Mosquera et al., 2015; Perrin, Bouvier, Janeau, Ménez, & Cruz, 2001). Grasslands, in general, intercept less water than forest or high vegetation (Nisbet, 2005) and perhaps because of that, grass interception has not received proper attention. Indeed, when rainfall intensity is high IL in general is small (Q Xiao, McPherson, Ustin, & Grismer, 2000) since most of the water drips fast from the vegetation and falls to the ground. However, low rainfall intensity and the lack of climate stationarity, typical in the páramo, easily results into more interception despite the short stature of the vegetation. Not surprisingly that IL in the páramo, depending from the conditions, can play an important role in the water cycle.

In order to quantify interception, the water balance of the vegetation canopy should be closed, i.e. precipitation (P) minus effective rainfall (ER) equals IL. For forests, ER is divided into SF (stemflow that goes to the ground via branches and stem) and TF (throughfall of raindrops to the ground either by dripping from the vegetation or contactless). P is measured by raingauges usually located at a nearby open-field, SF is commonly measured by wrapping collectors in a spiral or ring around tree trunks, and TF is measured by placing raingauges and similar devices below the tree canopy (Chen & Li, 2016; Pereira et al., 2009; Sun, Onda, Kato, Gomi, & Komatsu, 2015; Qingfu Xiao, McPherson, Xiao, & McPherson, 2011; and others). However, these measurements are not feasible in pastures and tussock grasses since the vegetation is not tall enough to place collectors on the stems and to collect water under the canopy.

For short vegetation, former studies indirectly measured interception in the laboratory and in the field. Lab experiments were performed by creating a device that contains aerial biomass above a wire-mesh screen of the same diameter as the sample which was installed over a funnel and then the water collected was compared to the water applied as simulated rain (Ataroff & Naranjo, 2009; O. Clark, 1940). The main problem with lab experiments is that rainfall intensity cannot be properly reproduced with sprinklers; and therefore, IL measurements are prone to inaccurate assumptions since they do not take into account the meteorological factors that may influence IL. Field experiments have been performed by positioning plastic trays near or on the ground to collect rainfall transmitted through the plants (Brye, Norman, Bundy, & Gower, 2000), by using pit gauges and canals at the soil surface to collect effective rainfall (Rincón, Ataroff, & Rada, 2005) and by using lysimeters (Campbell & Murray, 1990; Rowley, 1970). Most of these experiments cannot be

Chapter 2

implemented in páramo where high vegetation coverage impedes the installation of trays or canals below the canopy. In summary, field experiments are preferable over lab experiments to account for all the environment conditions, as long as their techniques are suited to the study site.

Therefore, our study pursued the quantification of interception loss in the tussock grasses of páramo with a field experiment that consists in closing the vegetation water balance during rain events by measuring soil water storage (measured with water content reflectometers) representing ER, and precipitation (measured with laser disdrometer) representing P. With IL (P – ER) depending on the measurement of two variables, two limitations of this method are evident. First, the requirement of precise precipitation measurements is challenging since the páramo rainfall occurs primarily as drizzle (Padrón et al., 2015). As shown by Padrón et al. (2015) precipitation volume was 15 % higher when recorded with a disdrometer than when recorded with a classical raingauge, affecting of course the closing of the water balance. However, the most common instruments available in our region are raingauges. Therefore, a comparison of disdrometer versus raingauge measurements is required, also to identify if similar studies can be reproduced at other sites. Second, ER errors arise from the measurement of the soil water storage and also the selection of the particular event period which involves the analysis of the precipitation records. Hence, in addition, a description of ER measurements is needed. Besides, ER measurements also enable the calculation of the canopy storage capacity: a vegetation parameter that is used in hydrological modelling. On the other hand, a clear advantage of using the presented field method is the possibility to understand the influence of meteorological variables on IL. In other regions, this influence included fast evaporation from the canopy due to wind velocity, limited evaporation due to high air humidity, higher interception with lighter rainfall, and positive correlations of interception with gross rainfall, duration, and wind speed (Baloutsos, Baltas, & Bourletsikas, 2009; Fan et al., 2015; Koichiro, Yuri, Nobuaki, & Isamu, 2001; Q Xiao et al., 2000). In fact, in several studies IL has been estimated from meteorological variables alone (Baloutsos et al., 2009; Genxu, Guangsheng, & Chunjie, 2012).

In conclusion, the present study mainly focusses on interception loss estimation, addressing simultaneously the following questions: (1) how much of the precipitation in the páramo becomes effective rainfall; (2) is it possible to derive similar ER values and therefore IL estimates, when using a raingauge (0.1 mm resolution) instead of the laser disdrometer (0.01

mm resolution)?; (3) which meteorological variables are related to the interception loss process?; and (4) is it possible to estimate IL from meteorological variables?

2.2 Materials and methods

2.2.1 Data

Four-year time series of precipitation, meteorological variables, and soil water content were available at 5-minute temporal resolution. Precipitation was recorded with a raingauge and a disdrometer. Texas Electronics tipping-bucket TE525MM rainfall sensor's resolution is 0.1 mm. Disdrometer (Thies Clima Laser Precipitation Monitor 5.4110.00.000V2.4x STD (LPM)) measures the size and falling velocity of drops, from which rainfall amounts are derived with a resolution of 0.01 mm (evaluation of the Thies disdrometer can be found at (Frasson, da Cunha, & Krajewski, 2011). Meteorological variables such as solar radiation, long and short wave net radiation, wind velocity and direction, atmospheric pressure, air temperature and relative humidity were recorded respectively with the instruments Campbell Scientific CS300 Apogee pyranometer, CNR2 – Kipp and Zonen, Met-One 034B Windset anemometer, and Campbell Scientific CS-2150 combined probe with radiation shield. Soil water content was measured with two CS616 water content reflectometers (WCRs) installed nearby the weather station at 10 cm soil depth, in a flat area, four meters apart from each other; thus there will be absence of events given the absence of lateral flow between both measuring points. WCRs accuracy is 2.5 % with standard calibration, while resolution and precision are better than 0.1 % (Campbell Scientific, 2012). Volumetric water content was calculated with the calibration curve depicted in equation 1.2 which was derived in the laboratory with the following procedure:

- a) Three unaltered soil samples were extracted from the study site in large PVC cylinders (20 cm diameter and 35 cm length) and transported to the laboratory.
- b) The samples were placed in buckets with water up to 30 cm and left for about a week in order to achieve soil saturation by capillarity. After saturation, samples were taken out of the water.
- c) The CS616 sensor was introduced in one of the soil samples and then connected to a CR800 datalogger and a PS100 power supply. The sensor output period (P) was recorded.
- d) Two small cylindrical samples of 2 cm diameter and 10 cm length were extracted from the large cylinders to obtain the soil volumetric water content (VWC) with equation 1.1.

$$VWC = \theta_g * \rho_{bulk} \tag{1.1}$$

where,

$$\theta_g = \frac{m_{wet} - m_{dry}}{m_{dry}}$$
 and

$$\rho_{bulk} = \frac{m_{dry}}{volume_{cylinder}}$$

where, m_{wet} and m_{dry} correspond to the wet and dry mass of the soil samples, respectively; and the volume_{cylinder} corresponds to $\frac{\pi 2^2}{4} \times 10 \text{ cm}^3$.

- e) The three large cylinders were placed in the oven at 30 °C.
- f) Every 24 hours the samples were taken out of the oven to record P from the sensor and to extract two small samples to calculate VWC until a value of 0.4 VWC was reached. This value corresponds to the wilting point determined before in a laboratory test, for the same soil at the same site.
- g) At the end, the VWC from the two soil samples were averaged and plotted against P, as depicted in Figure 2.1. The best calibration curve was a second-degree polynomial. The 95 % confidence interval of the polynomial regression was calculated to present the uncertainty in the measurement of soil water content.

The calibration curve depicted in equation 1.2 can be used in Andosols to measure volumetric water content (VWC) in m³/m³ with the CS616 WCR output period (P) in microseconds.

$$VWC = 0.0037 P^2 - 0.1949P + 2.9257$$
 (1.2)

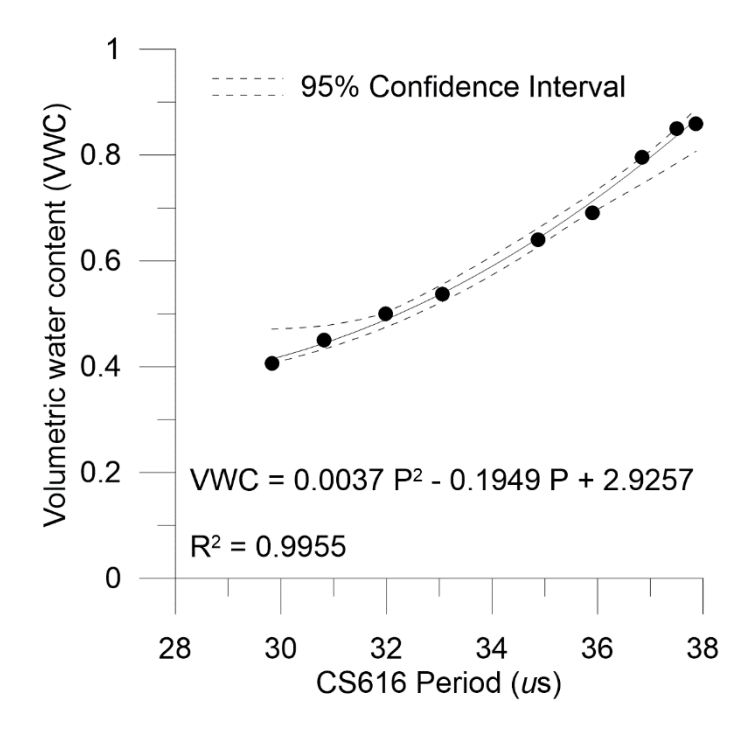


Figure 2.1. CS616 WCR calibration curve and its 95 % confidence interval

2.2.2 Interception loss calculation

Interception loss was quantified by closure of the vegetation water balance during a precipitation event (equation 1.3) where IL is the interception loss, P precipitation and ER effective rainfall, all recorded during an event:

$$IL = P - ER \tag{1.3}$$

Effective rainfall was estimated first as the change in soil water storage during an event. The change in soil water storage corresponds to the change in the volumetric water content, recorded by the average of two WCRs, multiplied by the installation depth of the sensor (100 mm). Selected events that fulfil the conditions explained in 2.2.1 were used as input in a script in R x64 3.3.2 to calculate ER and IL for each event.

2.2.2.1 Events selection

In this study, as suggested by Rutter, Kershaw, Robins, & Morton (1971) and Gash (1979), an event starts when the first drop of precipitation falls on dry grass leaves and lasts until the grass is dry again. Thus, the event length is the sum of the duration of the precipitation event plus the time that it takes the tussock grasslands to dry. By using net radiation records, and given the high radiation present in the environment, we selected the events in which at least

four hours of sunshine occurred prior and after the event, assuming this time is enough for the tussock grassland leaves to get dry.

Also, only events that did not reach soil saturation were selected. Saturation was avoided since runoff might occur and it cannot be included as effective rainfall, as this would prevent closure of the vegetation water balance. Therefore, a pF curve was determined in the field and only events with soil water content below 85 % were selected. Similarly, precipitation events up to 8.5 mm are used for this study to avoid soil saturation.

2.2.3 Effective rainfall and interception loss calculated with a disdrometer vs. a raingauge

Rainfall was assessed using both a raingauge and a laser disdrometer to identify whether the more widely available and low cost raingauge can be used reliably to quantify effective rainfall and therefore interception loss in the páramo. Events selection, ER, and IL calculations were performed with the disdrometer and with the raingauge records separately. Effective rainfall versus cumulative precipitation events were plotted together with their respective linear regression for each instrument. Alongside, the canopy storage capacity (S = the maximum amount of water that can be retained by the canopy before dripping occurs) was calculated as in Rutter et al. (1971) by constraining the regression slope to one, and then the intercept equals S. Comparison between the linear regressions was performed by visual means together with the linear equation coefficients, their coefficient of correlation, and their respective calculation of S. The duration of events was plotted against P from the raingauge and from the disdrometer records. Finally, to compare the effect of the instruments on the calculation of ER and IL, box plots of each variable were plotted together.

2.2.4 Relationship between interception loss and meteorological variables

The meteorological variables described in Table 2.1 were averaged per event and the variables P, Temp, RH, Rn, u₂, WI, MI, and ETo were calculated for 6, 12, 18, and 24 hours prior to the event, resulting in a total number of 48 independent variables. The dependent variable (IL) and the independent variables are continuous and the relationships might be linear or not and involve complex interactions. Although principal component analysis is usually a convenient means of selecting variables from a large group, it does not allow determination of dependent variables in the system. Regression trees (RTs) have the advantage of enabling the selection of the dependent variable while finding its relationship

with the independent variables. On the other hand, random forest (RF) allows determination of the importance of the variables; consequently, a reduced number of them are used in the construction of the tree. RF and RTs have been widely used in ecological studies for their ability to handle missing values, outliers, complex interactions between explanatory variables, and their ease of implementation and interpretation (De'ath & Fabricius, 2000; Moisen, 2008). They have already been used for hydrological purposes as well (J. Jones, 1987; J. Jones & Connelly, 2002; Scherrer & Naef, 2003; Uchida, Tromp-van Meerveld, & McDonnell, 2005; Wilson & Smart, 1984).

Random forest (RF) and regression trees (RTs) techniques were used in this study, as follows. Random Forests can help to reduce the number of variables included in the building of a tree. RF is a combination of trees that is created independently (Breiman & Leo, 2001). The meteorological variables that define the split of the trees are randomly chosen. Then, a subsample of variables is determined in order to find the optimum split. As a consequence, RF rates the importance of each meteorological variable with the mean square error (MSE) and the node impurity percentage decreases when taking into account the variable. In this way, the most important meteorological variables that are related with IL can be chosen. After this, a RT is built. A regression tree repeatedly splits events into more homogeneous groups, using combinations of meteorological variables. Each group is characterized by a typical IL value, the number of observations, and the values of the meteorological variables that define the group. The resulting tree could have too many splits with only a few observations per group, making interpretation cumbersome. Pruning (Moisen, 2008) is therefore applied to reduce the size of the tree to its optimum and to prevent overfitting. Evaluation of the tree, after the pruning, is performed by looking at its correlation coefficient for each split quantity. In this way, a sufficiently short tree can be selected. Finally, the tree is formed with the variables and thresholds that have a relationship with the interception loss process; thus, we can conceptualize the relations of the variables to IL with the interpretation of the tree. RF and RTs were coded in R x64 3.3.2 software using the "randomForest" and "rpart" packages.

Table 2.1. Meteorological variables included in this chapter

Abbreviation	Variable description	Unit
P	Accumulated precipitation during the event	(mm)
D	Duration of rainfall event	(min)
Temp	Mean temperature	(°C)
Tmax	Maximum temperature	(°C)
Tmin	Minimum temperature	(°C)
RH	Relative humidity	(%)
SR	Solar radiation	(W/m2)
SWnet	Shortwave net radiation	(W/m2)
LWnet	Longwave net radiation	(W/m2)
Rn	Net radiation	(W/m2)
\mathbf{u}_2	Wind speed	(m/s)
WI	Weighted mean intensity (Baloutsos et al., 2009)	(mm/h)
WS	Weighted wind speed (Baloutsos et al., 2009)	(m/s)
WC	Initial water content	(%)
MI	Maximum intensity	(mm/h)
ЕТо	Potential evapotranspiration	(mm)
ETo/P	Relative potential evapotranspiration	(-)

2.2.5 Estimation of interception loss from meteorological variables

Finally, to estimate interception loss from the variables that influence its process, a multiple linear regression was conducted along with the verification of the normal distribution of the residuals and the homogeneity of the variance. The coefficient of determination and residual square error from the regression give an idea of the goodness of fit of the regression; while the verifications of normality and variance homogeneity assure that the regression is applicable to the data. However, to verify whether the model is likely to be generalizable to other datasets, k-fold cross validation was applied (Cramer, Bunce, Patterson, & Frank, 1988; Krstajic, Buturovic, Leahy, & Thomas, 2014). It was chosen over the common split-sample validation method (where all events would have been split in 70 % for fitting of the model and 30 % for validation) in order to make use of all the events during the fitting of the

regression. As recommended in Hastie, Tibshirani, & Friedman (2010), k should be equal to 10; and therefore, a 10-fold cross validation was selected. It consists in partitioning of all the events into 10 mutually disjoint groups chosen randomly that leave aside N/10 events (where N is the total number of events). Then, the multiple linear fit is applied to nine groups and predicted values are computed for the 10th group. After repeating this for 10 times, each event has an IL prediction value. Then a coefficient of determination is calculated from predicted and observed values giving an idea of how well the model will perform on an independent data-set. This was coded in R software with the stats and bootstrap package.

2.3 Results and discussion

2.3.1 Effective rainfall and interception loss calculated with a disdrometer vs. a raingauge

Events were chosen from the disdrometer records (as depicted in 2.2.1) leading to 311 events over a period of around four years. The results corresponding to the effective rainfall and cumulative precipitation are presented in Figure 2.2. There is a clear division of linear trends in the observations since small events (P < 1.7 mm) have an almost flat slope and larger events have an 87 % slope. This bilinear model has been found in the literature too (Klaassen, Bosveld, & de Water, 1998; Leyton, Reynold, & Thompson, 1967; Rutter et al., 1971). According to our observations, the canopy storage capacity (S) of the tussock grass is 2 mm, which is higher than previous reports on other short vegetation types (Table 2.2). Vegetation types discussed in Table 2.2 include tussock grasses and shrubs; however, S depends on several factors like canopy leaves surface area and roughness, which might be different for the *calamagrostis instermedia* tussock grass than for the *stipa tenacissima* tussock grass studied by Domingo, Sánchez, Moro, Brenner, & Puigdefábregas (1998), the snow tussock grass studied by Campbell & Murray (1990), and definitely different for grasses studied in Crouse, Corbett, & Seegrist (1966). During small events effective rainfall is almost negligible (Figure 2.2a).

For the raingauge data, 1000 events were selected and their duration (3 vs 9 hours on average), effective rainfall quantities (0.6 vs 0.9 mm on average) and P volume (1.4 vs 2.2 mm on average) were different from those selected with the disdrometer. Many more events were selected with the raingauge than with the disdrometer, due to its inability to capture horizontal precipitation and drizzle between events; therefore, more dry periods are assumed

Chapter 2

and thus more events chosen as independent. ER versus P calculated from a raingauge shows no separation from small and large events (Figure 2.2b). The regression line with all events where effective rainfall occurred has a 68 % slope and an intercept of -0.5 mm which is different from the regression found with the disdrometer records. Consequently, S calculated with these events was different too (1.65 mm). Although both regressions show a coefficient of determination of 0.8, the residual sum of squares (RSS) reveals more dispersion on the events calculated from the raingauge records. Additionally, when the event starts and/or ends with drizzle (P equal or less than 0.1 mm, typical for the páramo) only the disdrometer counts them as part of the event, making it longer; this also enables the tussock leaves to get dry during the event. As a consequence, several disdrometer events lasted more than raingauge events and the cumulative precipitation was higher (Figure 2.2c).

Figure 2.2d shows P, ER, and IL boxplots in which it is evident that the disdrometer records on average reveal: (i) more precipitation by taking into account drizzle, as stated in Padrón et al. (2015); (ii) more effective rainfall by taking into account a higher soil water storage when events last longer; and consequently (iii) more interception loss. In fact, the mean P, ER, and IL calculated from the disdrometer are 57 %, 52 %, and 60 % higher than the mean P, ER, and IL derived from the raingauge data.

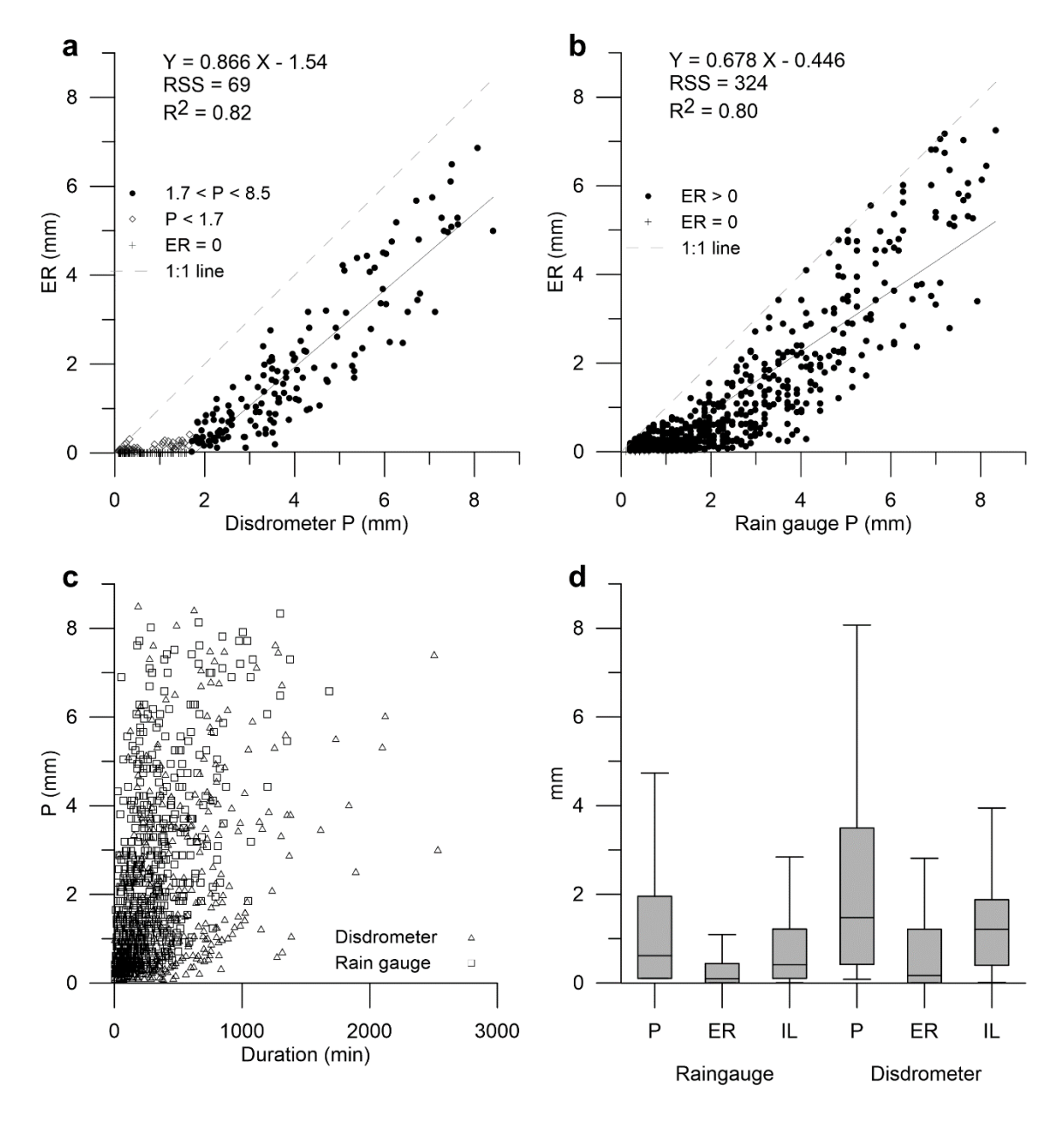


Figure 2.2. Effective rainfall (ER) vs. cumulative precipitation (P) calculated from: a) the disdrometer and b) the raingauge; where RSS corresponds to the residual sum of squares and R² to the coefficient of determination. c) Event duration vs. cumulative precipitation from events selected with the disdrometer and raingauge. d) P, ER and interception loss (IL) box plots calculated from the disdrometer and raingauge records.

In conclusion, evidence is presented that a disdrometer, using the methodology suggested in this study, enables a more accurate calculation of effective rainfall and interception loss.

2.3.2 Quantification of interception loss

Interception loss calculated for each event selected from the disdrometer records is plotted in Figure 2.3a as a percentage of the cumulative precipitation. Dispersion of the events is

obvious at first sight and clearer than in the ER-P graph shown in Figure 2.2a. The pattern and dispersion of the relative IL described in this study has been found in the literature for forest (Bruijnzeel, 2000; Llorens, Poch, Latron, & Gallart, 1997; Q Xiao et al., 2000) as well as for grasslands (Table 2.2 reference numbers 2, 4 and 6). Dispersion is partly attributed to the measurement errors of the instruments. Uncertainty from the precipitation and soil water storage measurements can be considered small. Lanzinger, Theel, & Windolph (2006) and Padrón et al. (2015) have shown very good performance of the disdrometer for low rainfall intensities as at our site; and the WCR sensors have been calibrated for the Andosols at the study site, decreasing their uncertainty measurement (Figure 2.1).

In small events (empty circles in Figure 2.3a), vegetation intercepts more than 80 % of the total precipitation. Small events have cumulative precipitation less than the canopy storage capacity (2 mm), which can be entirely retained by tussock grasslands; thus canopy drip is limited and evaporation follows. In total, around 80 events were fully intercepted (black crosses in Figure 2.3a). On larger events (filled circles in Figure 2.3a), the canopy only captures a small proportion of rainfall; consequently, the percentage of interception decreases from 100 to 10% as the amount of precipitation increases. Relative IL values for tussock grasses were found equal to values found by Campbell & Murray (1990) for snow tussock grasses and higher than other estimations for short vegetation sites (Table 2.2). Most of those studies found percentages of IL up to 40 % and as low as 5 %. Reasons for this discrepancy include vegetation characteristics and site climatic conditions (e.g. precipitation intensity). Most of the study sites have shorter stature grasses, partial coverage with bare soil, and are located at low altitudes, all of which contrast sharply with the conditions at our site. Indeed, in our study area, rainfall characteristics (low cumulative precipitation, low intensity, and low duration) favours interception loss. Hence the importance of calculating this variable for the páramo.

2.3.3 Relationship between interception loss and meteorological variables

Random forest algorithm results show that the six most important variables affecting the IL process are, in order of importance: the cumulative precipitation during the event, the maximum intensity during the event, the mean arithmetic intensity eighteen hours prior to the event, the cumulative precipitation of the eighteen hours prior to the event, the mean wind speed during the event, and the mean arithmetic intensity during the event (Figure 2.4). Importance is rated in accordance to the mean square error and the node impurity percentage

decrease when taking into account the variable noted. The rest of the variables not shown in Figure 2.4 had values of MSE and node impurity reductions of almost zero.

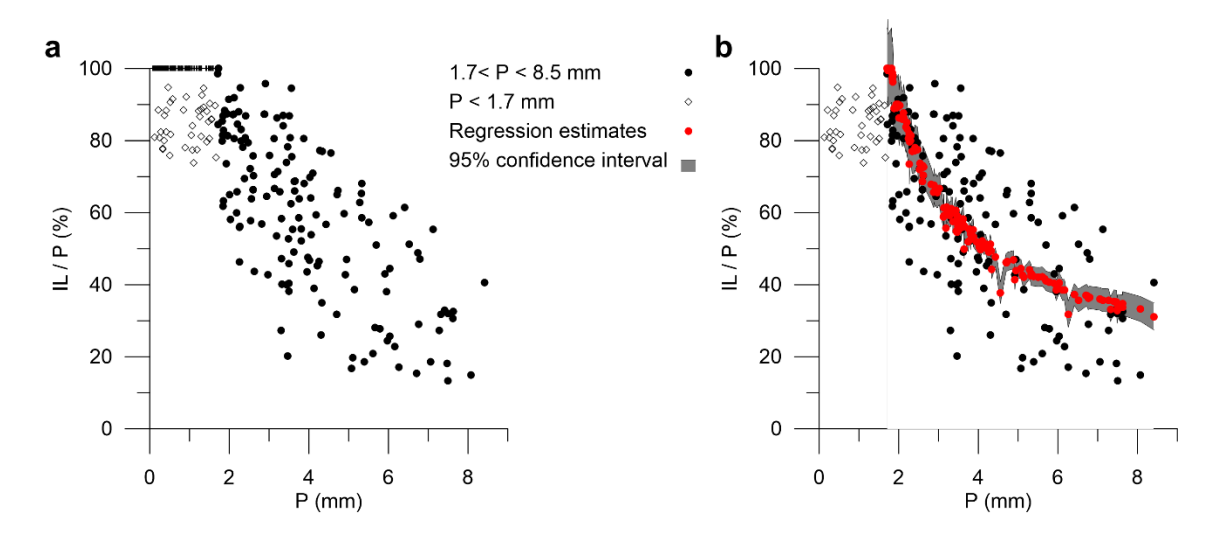


Figure 2.3. a) Interception loss relative to cumulative precipitation (IL/P) calculated from the disdrometer and WCRs observations and b) IL/P estimated from the multiple linear regression expressed in equation 1.4 (red dots).

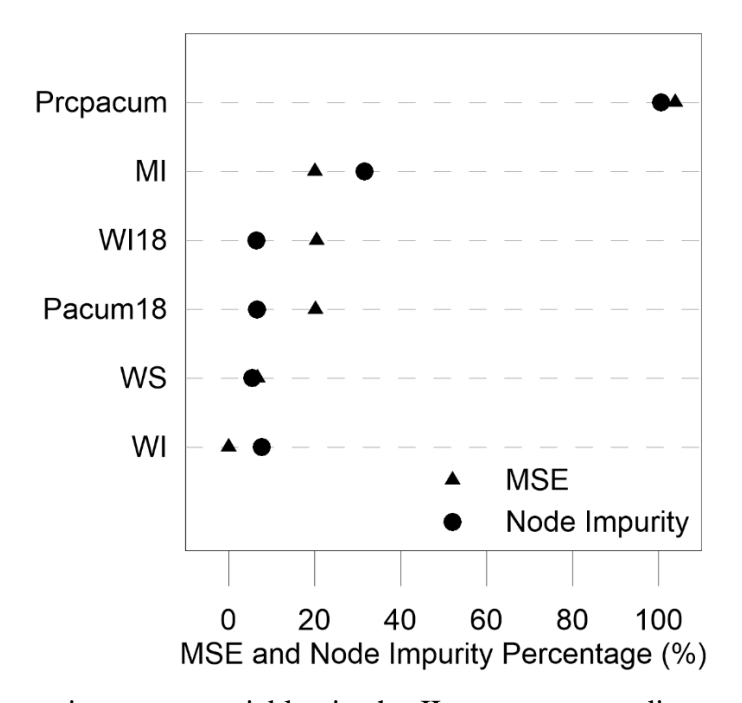


Figure 2.4. The most important variables in the IL process according to the RF algorithm have the highest reduction in the mean square error (MSE) and the highest reduction in the node impurity presented as percentages. The variables are cumulative precipitation (Prcpacum), maximum rainfall intensity (MI), mean rainfall intensity in the eighteen hours before the event (WI18), cumulative precipitation eighteen hours before the event (Pacum18), weighted wind speed (WS), and weighted mean rainfall intensity (WI).

A regression tree was built and pruned afterwards. The splits were formed only with the following variables: the cumulative precipitation during rain events, the cumulative precipitation of the eighteen hours prior to the events, and the maximum intensity during the events (Figure 2.5). The r-square error of the tree with five splits is 0.8 and with four splits is 0.7; therefore, a tree with five splits was preferred. The first split is coherent with Figure 2.2a and Figure 2.3a, where there is a clear difference between small and large events. The second split to the left divides the small events in two groups by their cumulative precipitation. While it is not as evident as the previous split, a careful examination of Figure 2.2a shows that almost all the events below the P = 0.6 mm threshold have zero effective rainfall. The third split is formed by the cumulative precipitation variable with a threshold of 3 mm. In Figure 2.2a, there is less dispersion of the events when P is less than 3 mm; thus, probably the tree is separating the events up to 3 mm that have a more linear relationship between IL and P. From the fourth split on, IL is related with other variables rather than P. The fourth split divides the events according to the cumulative precipitation of the eighteen hours before the event. The right side in which that variable is lower than 25 mm has a higher IL mean. This suggests that when there is less precipitation eighteen hours before the event, interception loss is higher. The last split includes the maximum rainfall intensity (MI) suggesting that there is more interception loss when maximum intensity is lower, which is explicable since lower intensity allows more canopy interception, less dripping, and therefore higher IL. This statement is based on a split that results in eight events on the left branch which represents only 3 % of the total events since paramo is a region characterized by low rainfall intensities. Therefore, at our site MI is not influencing IL for common rainfall intensities. However, Domingo et al. (1998) found this relationship between IL and MI to be strong in their tussock grasses and shrubs site under a precipitation regime with higher rainfall intensities (2-16 m/h). In summary, it is no surprise that IL is mainly related with P; but it is interesting that other meteorological variables are not influencing this process.

2.3.4 Estimation of interception loss

Multiple linear regression was performed for estimating interception loss with all the available variables described in section 1.2.4 but only for precipitation events between 1.7 and 8.5 mm. This decision was made after demonstrating that P is the variable that relates best to IL (section 3.3) and the evident linearity of ER vs. P when 1.7 < P < 8.5 mm as shown in Figure 2.2a. We found that the linear regression with the least residual standard error (RSE

= 0.67 mm) and the highest coefficient of determination ($R^2 = 0.9$) was a function of cumulative precipitation and relative humidity (RH) (equation 1.4).

$$IL = 0.410P + 0.016RH \tag{1.4}$$

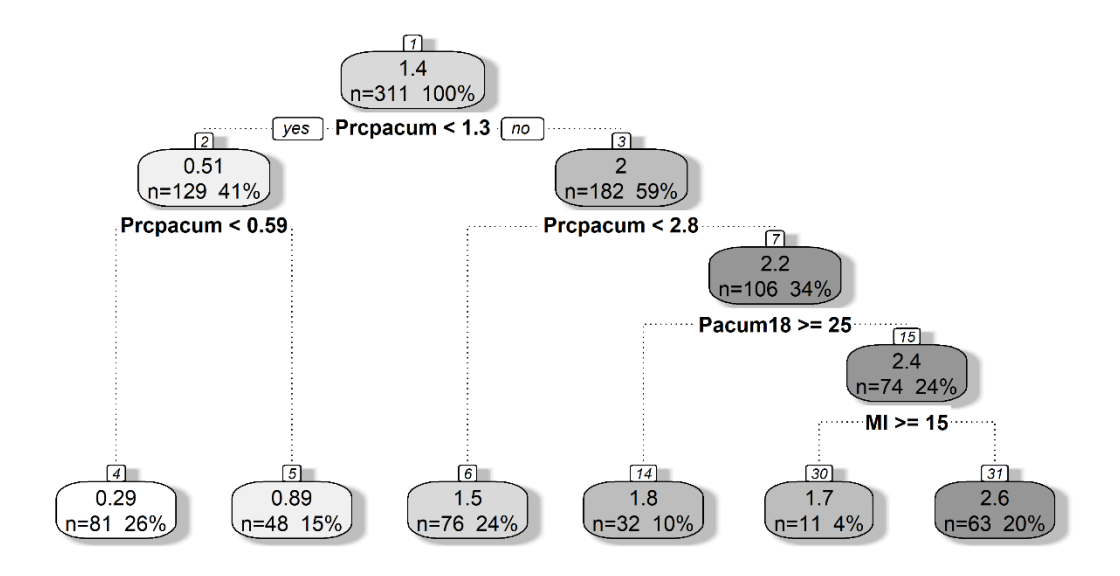


Figure 2.5. Regression tree for interception loss. In each node: IL mean, number of items in the node, and percentage of data included in the node. Each split is determined by a variable with its threshold.

The second best multiple linear regression was a function of P and Ws (wind speed) but the R² dropped to 0.85 and the RSE increased 35 %; thus the first regression was preferred. Regression residuals were checked for normal distribution and homogeneity of the variance. Interception loss variance is explained in 90 % by the cumulative precipitation (P) and the relative humidity (RH). Although, RH only explains 10 % of the variance, if it had not been taken into account, the coefficient of determination would have dropped to 0.8 and the RSE increased 40 %. To test the multiple linear regression model in terms of its generality, a 10-fold cross validation was performed obtaining a correlation coefficient of 0.99 meaning that the model can definitely be used with other datasets.

It is important to note that RH comes as a new variable for estimating IL in the multiple linear regression. However, when running the RF and the RTs, RH was not present (see section 3.3). The RF was found with all events while the multiple linear regression was performed only with events where 1.7 < P < 8.5 mm. To verify if this is the only reason for the discrepancy, a RF with the large events was performed, and RH appeared in the first six

Chapter 2

variables according to its importance. However, it was preferred to take into account all the events when performing RF and RTs for a review of the non-linear relations of the variables with IL.

IL estimates from the regression calculated as a percentage of P were plotted together with IL estimates from field measurements in Figure 2.3b. As mentioned, values were estimated when the cumulative precipitation was higher than 1.7 mm. For values of P below this threshold, interception can be estimated as 90 % of P. The 95 % confidence interval of the regression model is shown in Figure 2.3b, meaning that 95 % of the time IL mean will fall inside the plotted grey range. Also, it is relevant to note that power functions have been used to estimate relative IL (Genxu et al., 2012) with success ($R^2 = 0.9$) for grasslands; however, for this study such functions only had a coefficient of determination smaller than 0.5.

Table 2.2. Bibliographical revision of studies reporting interception loss estimations for short vegetation around the world: Interception loss relative to cumulative precipitation (IL / P), canopy storage capacity (S), and positive (+) or negative (-) relations between interception loss and meteorological variables. "No cor" corresponds to no correlation of the variable to IL.

Reference	IL/P (%)	S (mm)	P (mm)	RH (%)	D (h)	Ws (m/s)	WI (mm/h)	Vegetation coverage (%)
1.(Ochoa-Sánchez, Crespo, & Célleri, 2018)	10-100	2	+	+	No cor	No cor	No cor	
2. (Genxu et al., 2012)	5-20		+		+		+	+
3. (Baloutsos et al., 2009)	26-40		+		+	+	No cor	
4. (Domingo et al., 1998)	20-40	0.25-0.75	+					
5. (Lockwood & Sellers, 1982)						No cor		+
6. (Campbell & Murray, 1990)	10-100	0.6-0.7	+					
7. (Crouse et al., 1966)	30	0.127	+					+
8. (Beard, 1956)	10		+				-	

Table 2.2 shows a bibliographic review of studies conducted on short vegetation (most of them on grasslands), in which relationships were derived between interception loss and other variables, similar as those included in this study. Most of them include a positive relationship with cumulative precipitation, as in our study. Some studies found that when the percentage of vegetation coverage increases, more water is lost by interception (in this study vegetation

coverage was 100 % since no bare soil was found in the study site). Furthermore, our investigation showed that relative humidity was linearly related to IL. Duration has been found important in some studies mentioned in Table 2.2, but when this variable was included with P in the multiple linear regression in our study, the coefficient of determination did not increase, even though the variable was highly significant. For our events, similar values of precipitation were indistinctly accumulated during short and long events (Figure 2.2d). Wind speed has been found important in grasses and forests (Lockwood & Sellers, 1982; Q Xiao et al., 2000), although it is clearly more important for tall vegetation and for sites where wind velocities exceed 5 m/s (Lockwood & Sellers, 1982), which is not the case in our study where wind speed can be up to 4.5 m/s but the average is around 3.6 m/s.

2.4 Conclusions

For the first time, this study quantified in paramo the rainfall interception loss using a fouryear time series of experimental field data. The main results of the IL study can be summarized as follows:

- 1. Events selection from the disdrometer and from the raingauge led to ER versus P plots which allowed to conclude that drizzle in paramo ought to be taken into account to quantify precipitation, and therefore interception loss more accurately. Also, the disdrometer-based plot enabled to determine the canopy storage capacity of tussock grasslands (S = 2 mm).
- 2. Interception loss expressed as a percentage of the cumulative precipitation per event (relative interception) was clearly different for small and large events. For small events, relative interception was always higher than 80 % of P, and even 100 % for the two-thirds of those events. For larger events relative interception decreased to 10 % of P.
- 3. Although low cumulative precipitation, low intensity, and low duration favour interception loss in the páramo, no clear relationships with meteorological variables were found when using random forests and regression trees. For all the events, only cumulative precipitation was found to be important. However, a multiple linear regression equation $(R^2 = 0.9)$ was identified to estimate IL as a function of P and relative humidity, which is valid for events when 1.7 < P < 8.5 mm.
- 4. In the first study of IL in páramo, high percentages of IL related to P were found, showing that this process plays an important role. These findings are a stepping stone

Chapter 2

towards modelling of the water resources since the variables and parameters used by the majority of hydrological models were quantified in this study.

Chapter 3

Quantification of transpiration

The amount of water consumed through transpiration and lost through evaporation differs from one ecosystem to another. Transpiration is usually associated with plant growth and it affects land-atmosphere patterns. Its quantification and contribution to the evapotranspiration process of páramo were investigated in this chapter. Transpiration rates of tussock grasslands were on average 1.5 mm/day (range 0.7 - 2.7 mm/day) and it was found that interception contributes more to evapotranspiration than transpiration. This finding sets a precedent towards a better understanding of the evapotranspiration process of the páramo and will ultimately lead to a better hydrological and climate modelling.

Related publication

Ochoa-Sánchez, A., Crespo, P., Carrillo-Rojas, G., Marín, F., & Célleri, R. (2019). Controls on Andean grasslands evapotranspiration and quantification of transpiration at event scale. *Hydrological Processes, in review*.

3.1 Introduction

An important step towards the understanding on the ETa process is the quantification of each of its components (Savenije, 2004). The components of ETa include evaporation from soil, evaporation from water intercepted by vegetation, and transpiration. The contribution of its components is important, depend on how vegetation processes energy and water (Saleska, 2003), and yet unclear at some sites around the world.

In agriculture practices, transpiration is usually associated with plant growth while evaporation is seen as an undesirable component, since water lost to the atmosphere does not directly contribute to production (Agam et al., 2012; Kool et al., 2014; Van Halsema & Vincent, 2012). For climate change concerns, the influence of the evapotranspiration components on land-atmosphere patterns are important to investigate since they affect global climate simulations (Lawrence, Thornton, Oleson, & Bonan, 2007). Transpiration has been linked with increased carbon uptake and with variation of the temperature and moisture in the atmosphere. Studies have recorded a cooling of the atmosphere with increasing transpiration; while others claim that higher transpiration reduces soil moisture and albedo which increases surface temperature (Kool et al., 2014; Penuelas, Rutishauser, & Filella, 2009).

Transpiration accounts for about 64% of global terrestrial ET according to Good, Noone, & Bowen (2015). The amount of water consumed through transpiration and lost through evaporation differs from one ecosystem to another; hence, more knowledge is needed on the soil, vegetation and microclimate characteristics in order to determine transpiration and evaporation rates at regional and local scales.

Regarding the ETa components of natural páramos, interception loss was quantified in Chapter 2 and soil evaporation can be neglected due to scarce bare soil conditions. Transpiration, the remaining component of ETa, has not been quantified before and, thus no information exists regarding its contribution to the evapotranspiration process. This chapter contributes to the quantification of transpiration and offers insight on the contribution of transpiration to the evapotranspiration process.

3.2 Materials and methods

3.2.1 Data

Three-year time series of precipitation and soil water content were available at 5-minute temporal resolution. Precipitation was recorded with a disdrometer of the brand Thies Clima Laser Precipitation Monitor 5.4110.00.000V2.4x STD (LPM), measuring the size and falling velocity of drops, from which rainfall amounts are derived with a resolution of 0.01 mm (evaluation of the Thies disdrometer can be found at Frasson et al. (2011)). Soil water content was measured with two CS616 water content reflectometers (WCRs) installed nearby the weather station at 10 cm soil depth, in a flat area, four meters apart from each other. Records by both reflectometers are independent in the absence of lateral flow. WCRs accuracy is 2.5 % with standard calibration, while resolution and precision are better than 0.1 % (Campbell Scientific, 2012). The volumetric water content was calculated with the calibration curve depicted in equation 1.2.

3.2.2 Quantification of transpiration

During dry events, the soil volumetric water content (VWC) was used to quantify the amount of water transpired by vegetation. The VWC was obtained by averaging two WCRs time series located at the head of the hillslope of the monitoring supersite at Zhurucay (Figure 1.3) to avoid the effect downslope flow, if any. WCRs were located at a soil depth of 10 cm to capture root water uptake. The root system at the supersite was carefully characterized in ten soil pits along the hillslope, finding root depths up to 15 cm. The deeper WCRs available are located at 25 cm depth; however, their signal did not change during the events, and therefore it is assumed that the WCRs signal located at 10 cm depth are appropriate for the measurement of transpiration. Figure 3.1 shows clear steps in the VWC signal (10 cm depth) for a 6-days dry event. The VWC signal does not change during the night, therefore, no percolation, downslope or lateral flow occurs while during the day the VWC drops due to transpiration.

The three-year precipitation time series (disdrometer observations) was used to find dry events in which the steps in the VWC signal were visible for at least one day. The amount of transpiration (in mm/event) corresponded to the daily change in VWC multiplied by the soil depth at which the WCRs were placed (100 mm). In some days, a slight increase in the VWC during early morning hours was visible (Figure 3.1). Since this water input was not detected

by the disdrometer it might correspond to dew and/or fog. Nevertheless, this small increase was considered in the computation of transpiration. Events with dew presence were marked when hourly air temperature was lower than dew temperature. Dew temperature was calculated using equation 2.1 (Jensen, Burmann, & Allen, 1990).

$$T_{dew} = \frac{116.91 + 237.3 \times \ln\left(\frac{e_a}{10}\right)}{16.78 - \ln\left(\frac{e_a}{10}\right)}$$
(2.1)

where e_a corresponds to the actual vapour pressure (equation 2.2) and Temp to air temperature.

$$e_a = 0.0611 \times RH \times exp\left(\frac{17.27 \times Temp}{Temp + 237.3}\right) \tag{2.2}$$

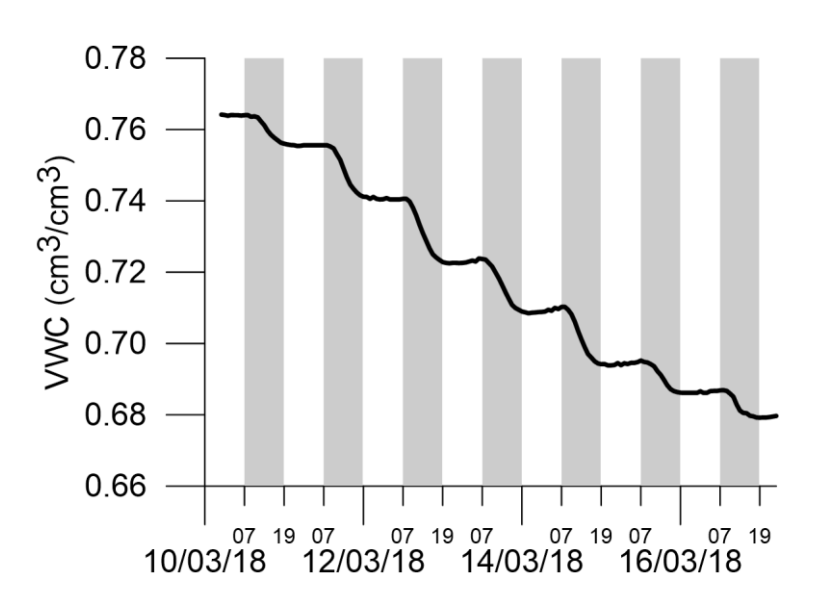


Figure 3.1. Example of the soil volumetric water content signal (VWC) during a 6-day dry event. Daylight hours are coloured in grey.

3.3 Results and discussion

Forty dry events, with zero-precipitation for more than one day, were used to quantify tussock grasslands transpiration. They are plotted against averaged observations of ETa for each event in Figure 3.2. Transpiration ranged from 0.7 to 2.7 mm/day with a mean of 1.5 mm/day. Mean ETa was higher than the mean transpiration for the entire event. Events in which dew occurred (hourly air temperature was lower than dew temperature) are coloured in blue in Figure 3.2. Dew for different events lasted over a large range from 2 to 15 hours and occurred mainly during daylight hours (9 am - 5 pm). Figure 3.3 shows a dry event

commonly used to quantify transpiration. During dry periods, tussock grasslands transpired around 9 hours at daylight from 9 a.m. to 6 p.m. (VWC signal in Figure 3.3).

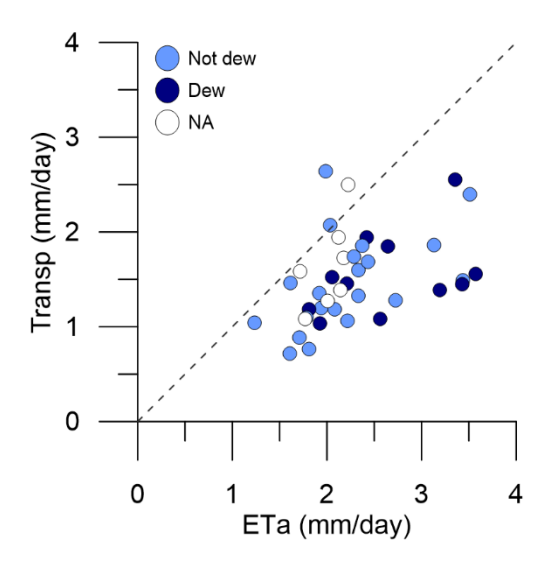


Figure 3.2. Transpiration (Transp) against actual evapotranspiration (ETa) for zero-precipitation events. Blue dots are events with dew, light blue dots are events without dew and white dots are events where dew temperature could not be calculated due to missing data.

Similar tussock grasslands have shown comparable transpiration rates to the values found in this study. Campbell & Murray (1990) found rates between 0.55 and 3.32 mm/day in New Zealand and lower transpiration rates between 0.35 and 0.51 mm/day in Spain with wet soil conditions but lower Rn (Ramírez, Bellot, Domingo, & Blasco, 2007). ETa values remained almost always higher than transpiration values during the dry events of this study (Figure 3.2). The probable causes are fog and/or dew retained in the canopy that eventually evaporate and that can be as high as 2 mm (Ochoa-Sánchez et al., 2018). Fog regimes influence canopy interception, foliar water uptake and evapotranspiration (Aparecido et al., 2018). On one hand, fog in combination with cloud cover and high relative humidity can inhibit transpiration (Buytaert, Cuesta-Camacho, & Tobon, 2011), but on the other hand, fog can be intercepted by vegetation and eventually evaporated, contributing to ETa. In addition, dew might also be contributing to evaporation. If dew reached the soil, it was taken into account in the calculation of transpiration, but the amount of dew captured by the canopy was recorded by the eddy-covariance tower but not recorded by the disdrometer. This situation is plausible at the páramo where fog and dew are common and long zero-precipitation periods rarely occur (Padrón et al., 2015). Furthermore, during dry periods, net radiation increased and evaporation of dew and fog was heightened. Quantification of fog is needed to provide a better understanding of the ETa process. It is common that in an event, like the one in Figure

3.3, the drop in the VWC signal lasts less hours than the increase in the ETa signal. As a consequence, transpiration lasts less hours than evapotranspiration. Thus, the aforementioned evaporation of fog and dew might be taking place, especially at the first hours of the morning. This highlights the more important contribution of evaporation to the ETa process, in comparison with the impact of transpiration.

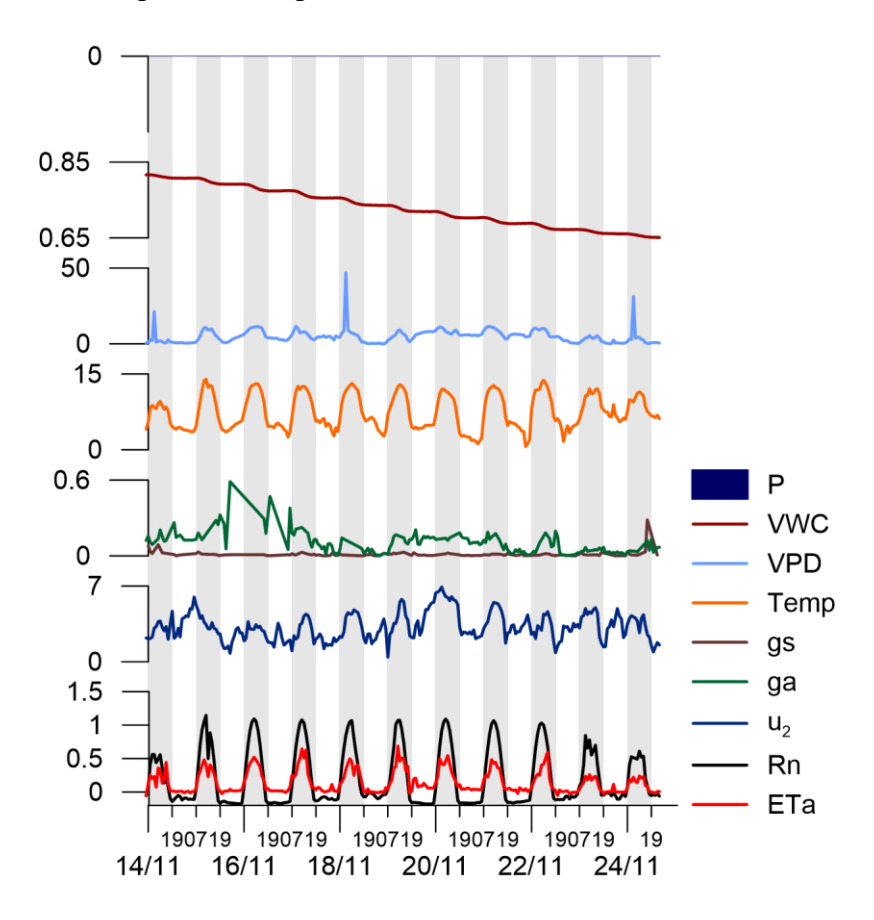


Figure 3.3. Dry event including the following variables: precipitation (P), soil volumetric water content (VWC), vapour pressure deficit (VPD), temperature (Temp), surface conductance (g_s) , aerodynamic conductance (g_a) , wind speed (u_2) , net radiation (Rn) and actual evapotranspiration (ETa). Shadow bars show daylight hours from 7 am to 7 pm.

3.4 Conclusions

Transpiration was quantified for the first time at the paramo. The contribution of transpiration and evaporation, separately, clarified questions that that were formulated in the first studies of this important biome, back in the nineties.

This study found that transpiration rates of tussock grasslands were on average 1.5 mm/day (range 0.7 - 2.7 mm/day). During dry periods, it was expected that only transpiration occurs. However, during days without precipitation, dew or fog was present, primarily as a consequence of páramos humid climate. In consequence, vegetation retains the dew or fog

which evaporated afterwards. This evaporation, in addition to the higher evaporation after wet periods, explains the higher contribution of evaporation to the evapotranspiration process, rather than transpiration.

Although more data is required in order to find the controls on the transpiration process, this study sets a precedent towards a better understanding of the hydrological processes at the páramo and, in consequence, improvements on hydrological and climate modelling.

Chapter 4

Quantification of actual evapotranspiration: comparison of measurement and estimation methods

Actual evapotranspiration (ETa) explains the exchange of water and energy between soil, land surface and atmosphere, a continuous numerical variable difficult to measure directly. The objective of this study was to compare measurements and estimations of ETa in a mountain grassland ecosystem using different approaches. The study was conducted in the Zhurucay Ecohydrological Observatory, located in the high Andes of Ecuador between 3500 and 3900 m a.s.l. The study area is a representative site of the páramo ecosystem, in which the vegetation mainly consists of tussock grass. ETa was measured or estimated using the following methods: eddy-covariance (EC), volumetric lysimeters (Lys), water balance (WB), energy balance (EB), the calibrated Penman-Monteith equation (PMCal), and two hydrological models (the Probability Distribution Model (PDM) and the Hydrologiska Byråns Vattenbalansavdelning model (HBV-light)). During the 1-year of analysis, precipitation (P) accumulated to 1094 mm while ETa (measured with EC) accumulated to 622 mm (with ETa/P = 0.57). On a daily basis, the EC method measured average ETa rates of 1.7 mm/day. The best daily estimates according to percentage bias (pbias), normalized root mean square error (nRMSE), Pearson's correlation coefficient (r) and the volumetric coefficient (ve) came from the HBV-light model, followed by the PMCal and the PDM (pbias: -2 to -20 %, nRMSE: 12–15 %, r: 0.7–0.9, and ve: 0.7–0.8). On the other hand, the WB, EB, and Lys estimates showed a poor performance (pbias: -10 to -19 %, nRMSE: 25–93 %, r: -0.4 to 0.5, and ve: -0.5 to 0.7). As the methods used in this study are of different types (hydrological, micrometeorological and analytical), their suitability and applications are discussed in terms of their costs, temporal resolution and accuracy. This study identifies lowcost and easy-to-implement alternatives to EC measurements, such as hydrological models and the calibrated Penman-Monteith equation. It is evident that a correct assessment of the actual evapotranspiration will result in a more accurate analysis of the water balance of tussock grassland.

Related publication

Ochoa-Sánchez, A., Crespo, P., Carrillo-Rojas, G., Sucozhañay, A., & Célleri, R. (2019). Actual Evapotranspiration in the High Andean Grasslands: A Comparison of Measurement and Estimation Methods. *Frontiers in Earth Science*, 7(55). https://doi.org/10.3389/feart.2019.00055

4.1 Introduction

Actual evapotranspiration (ETa) is a major component of the hydrological cycle and one of the most important physical processes in natural ecosystems. It explains the exchange of water and energy between the soil, land surface and the atmosphere. An improved characterization of ETa is especially important for: (1) the modelling and management of water resources and related ecosystem services, which include provisioning, supporting, and regulating services; and (2) the assessment of the effect of global climate change. Climate change affects ETa rates, therefore soil moisture, vegetation productivity, the carbon cycle and water budgets might also be affected (Gu et al., 2008). Natural grasslands cover around 26 % of the Earth's ice-free land surface (Foley et al., 2011). They represent a widespread ecosystem that requires special attention, as processes such as interception or transpiration have traditionally been assumed to be low or even negligible while they could in fact constitute an important loss of water to the atmosphere (Ochoa-Sánchez et al., 2018).

The most important ecosystem in the Andean region for water resources supply is the páramo and it is primarily covered by tussock grasslands (locally referred to as pajonal) (Hofstede et al., 2014). The Andean páramo extends from the North of Colombia (11°N) to the North of Peru (8°39'S), occupying around 36,000 km². The páramo geomorphology includes wide valleys covered by wetlands that act as natural reservoirs. The flora of the páramo has attracted the attention of scientists owing to the high number of endemic species. The fauna is also important for its emblematic species (e.g. condor, spectacled bear, mountain tapir and puma). In addition, the sociological importance of the páramo lies in the millenary interaction between this ecosystem and its inhabitants. This lengthy occupation and the constant use of the páramo by nearby communities qualifies it as a socio-ecosystem (Hofstede et al., 2014). The ethnic diversity of the páramo highlands promotes a lively culture that is still in development. The páramo itself is especially important as it serves as a sponge that captures precipitation and releases water gradually to the surrounding areas (Llambí et al., 2012). This characteristic is vital during dry periods or extreme summers, when water that was retained during the wet periods in the highlands is gradually delivered to lowlands through runoff. The páramo is the primary water source for communities located nearby this ecosystem, which include major cities in Colombia, Ecuador, and Peru. This environment provides water that is intensively used for agriculture, rural and urban drinking water systems, hydro-power production, and for sustaining aquatic ecosystems. Consequently, the accurate closure of the

water balance is essential. While precipitation and discharge have been increasingly monitored in the páramo (Ochoa-Tocachi et al., 2018), the monitoring of ETa received considerably less attention and requires further assessment.

Few studies have measured evapotranspiration in grasslands at high altitudes (Coners et al., 2016; Gu et al., 2008; Knowles et al., 2015; van den Bergh et al., 2013). In the páramo, ETa has been recently measured using the eddy-covariance (EC) method (Carrillo-Rojas et al., 2019). Although the EC method has proven to be a reliable technique, it is costly and still rarely available around the world. To our knowledge, twelve eddy-covariance towers are located in South America, among which only one is located in the páramo (Carrillo-Rojas et al., 2019; Fisher et al., 2009). This highlights the importance of finding alternative methods to quantify ETa. Weighing lysimeters have always been considered as a viable tool for measuring ETa, and as a possible alternative to the EC measurements (Coners et al., 2016). However, most of the studies focus on the use of weighing lysimeters (e.g. Rana & Katerji (2000) and Coners et al. (2016)) whose construction and operation is still costly. For that matter, some authors have constructed volumetric lysimeters as a low-cost alternative (e.g., Khan, Mainuddin, & Molla (1993) and Poss et al. (2004)).

The estimation of ETa can represent an important alternative for agricultural or hydrological studies, for example when no measurement techniques are available due to their high cost, complex installation and/or intensive maintenance. ETa has therefore been estimated through several different methods, such as using the water balance, the energy balance, the Penman-Monteith equation and hydrological models. Globally, the water balance has been used as a reference method to estimate ETa. However, the closure of the water balance involves the measurement of not only precipitation and discharge, but in some cases the measurement of other variables that are not easy to quantify, such as the change in soil moisture and groundwater recharge. The energy balance has been used to estimate ETa in the paramo, although those estimations were validated using estimations from the water balance (Carrillo-Rojas, Silva, Córdova, Célleri, & Bendix, 2016). The potential evapotranspiration (ETo) was estimated in the páramo through the use of the Penman-Monteith equation (Córdova et al., 2013, 2015), a simple method to estimate ETa using only meteorological data. However, these estimations have not yet been validated with ETa measurements. Finally, hydrological models are a valuable estimation tool, as they are usually feasible to implement. The Probability Distribution Model (PDM) and the Hydrologiska Byråns Vattenbalansavdelning model (HBV-light) were calibrated for páramo and have proven to be valid for runoff

estimation (Iniguez, Morales, Cisneros, Bauwens, & Wyseure, 2016; Sucozhañay & Célleri, 2018). Although several efforts have led to ETa estimations, they seldom have been compared with actual measurements.

Currently, little is known regarding which methods are suitable for accurately measuring or estimating ETa at high altitudes and, in a wider sense, studies have not compared ETa by simultaneously implementing several methods at the same site. This study therefore compared the EC measurements with low-cost volumetric lysimeters and hydrological, micrometeorological and analytical methods that estimate ETa (i.e. water and energy balance methods, the calibrated Penman-Monteith equation and two hydrological models: PDM and HBV-light). Furthermore, the study aimed to provide insights into the performance of the methods and information on the suitability of each method for similar grassland ecosystems around the globe.

4.2 Materials and methods

4.2.1 Methods for measuring and estimating actual evapotranspiration

Rose & Sharma (1984) suggested that methods should be grouped as those that measure ETa and those that estimate ETa. In addition, methods may be classified as experimental and physically-based. Each method has been developed based on certain assumptions and to fulfil a different objective, therefore each depends on concepts from hydrology or micrometeorology. Among the methods used in this study, eddy-covariance and lysimeters measure ETa, while the water balance method, energy balance method, the hydrological models and the calibrated evapotranspiration equation estimate ETa. Volumetric lysimeters and the water balance method depend on hydrological concepts, while the energy balance and micrometeorological eddy-covariance methods are approaches. The calibrated evapotranspiration equation and the estimation through hydrological models can be grouped as analytical approaches.

All methods have a different time and spatial resolution, as summarized in Table 4.1. In this study all methods were compared on a daily timescale over a period of one year (05/05/2017–30/04/2018), which included comprehensive field campaigns, especially for the implementation of the eddy-covariance tower and the lysimeters

Table 4.1. Spatial and temporal resolution of the actual evapotranspiration measurement and estimation methods used in this study.

Method	Time resolution	Spatial resolution
Eddy-covariance	30-min	100 – 130 m
Volumetric lysimeter	7 days	Group of plants
Water balance	Daily	Micro-catchment
Energy balance	Hourly	Uniform area
Hydrological models	Daily	Micro-catchment
Calibrated evapotranspiration equation	Daily	Uniform area

4.2.1.1 Eddy-covariance method (ETa $_{EC}$)

Water vapour and energy fluxes were measured by an EC tower from May 2017 to April 2018. The EC site is a FLUXNET observatory (ID: EC-Apr). A photograph of the EC tower is shown in Figure 4.1. A LI-7200 enclosed-path infrared gas analyser (LI-COR, Lincoln, NE, USA) measured ETa fluxes at a sampling rate of 20 Hz, and the analyser used an insulated heated tube to avoid water condensation during sampling. Wind components and the sensible heat flux were measured using a three-dimensional sonic anemometer (Gill New WindMaster 3D, Gill Instruments, Hampshire, UK). Additional micrometeorological measurements were taken with slow sensors (with a 1 min sampling frequency) collecting net radiation data (Kipp & Zonen CNR4, Delft, Netherlands), air temperature and relative humidity levels (Vaisala HMP155, Helsinki, Finland), and soil heat fluxes (3 × Hukseflux HFP01, Delft, Netherlands; buried at 8 cm in the soil). The array of instruments was set up at a 3.6 m elevation, surveying the grassland fetch up to approximately 100-130 meters in the prevailing upwind direction of the flux source (northeast). The ET flux contributions developed from a homogeneous cover of tussock grassland with low orographic affectation (<10°). Detailed characteristics of this pioneering high Andean EC experiment have been described in Carrillo-Rojas et al. (2019).

High-frequency sampling data (ETa and sensible heat) were 30-min block averaged using the EddyPro software (version 6.2.0, LI-COR, Lincoln, NE, USA). The raw data processing contemplated diagnostic flags, plausibility limits and spike removal. In addition, data quality assurance and quality control were performed, along with corrections for density fluctuations, time lags, wind planar fit, and high- and low-frequency spectral losses, following the recommendations of Mauder et al. (2013).



Figure 4.1. Eddy-covariance tower at the supersite in Zhurucay (3765 m a.s.l.). Photograph: Galo Carrillo-Rojas.

Footprint assessment, based on the methodology of Kljun, Calanca, Rotach, & Schmid (2015), excluded less than 2 % of flux data related to unimportant sources in the area, and the EC energy balance closure amounted to 99 %. This outstanding closure of the energy balance is attributed to the smooth and homogeneous canopy of the native vegetation, the constant moist conditions and the particular location of our site (tropical latitude with low seasonality). Other tropical sites with high moisture environments have shown similar energy balance closures (Cabral, da Rocha, Gash, Freitas, & Ligo, 2015; Cabral et al., 2010). Advectionaffected fluxes were removed through the detection of data with low friction velocity (u*). This was performed using the Moving Point Test for the u* threshold detection (Papale et al., 2006). Missing ET fluxes (scarce temporal gaps of <1 day), due to the u* filtering, power or instrumental failures, and low quality data amounted to 23 % of the total amount of 30-min data. This represents a good level of EC temporal coverage according to Falge et al. (2001). These data gaps were filled using the standard method used in FLUXNET, i.e. Marginal Distribution Sampling (MDS) (Reichstein et al., 2005). We selected such an approach due to its wide application at other EC sites and to maintain consistency with former and future studies. The MDS algorithm infilled the missing values with solar radiation, air temperature and vapour pressure as input variables. The uncertainty error induced by gap filling was assessed using a bootstrapping approach (resampling with replacement). A dataset of pseudoreplicates was created. Here, the difference between the high (95 % quantile) and low (5 % quantile) threshold estimates of the bootstrapped uncertainty distribution corresponded to the

uncertainty level. A detailed description of the EC data processing and specific corrections can be found in Carrillo-Rojas et al. (2019).

4.2.1.2 Lysimeters installation and methodology

Four volumetric lysimeters were installed at the top of the hillslope at the supersite, as depicted in Figure 4.2a. Actual evapotranspiration (ETa_{Lys}) was calculated by closing the water balance for each lysimeter as shown in equation 3.1:

$$ETa_{Lvs} = P - D \pm \Delta S \tag{3.1}$$

where P corresponds to precipitation (in mm/7days), D corresponds to drainage (in mm/7days), and ΔS is the change in soil water storage (in mm/7days). The lysimeter illustration depicted in Figure 4.2b indicates the design and instrumentation used for the closure of the water balance. Lysimeters contain only the organic horizon and the bedrock is located immediately below the instruments. Precipitation was recorded with a laser disdrometer (Thies Clima Laser Precipitation Monitor 5.4110.00.000 V2.4× STD, with 0.01 mm resolution). Changes in soil water storage were calculated from the difference between two water content reflectometers (WCRs) installed inside the lysimeters (CS655 Campbell Scientific WCRs). Changes in soil water tension and soil water potential were continuously checked with tensiometers (T8-UMS) and dielectric water potential sensors (MPS-2 Decagon). Drainage was obtained by placing fiberglass wicks at the bottom of the lysimeters. The wicks acted as a hanging water column, drawing water from the undisturbed field soil without external application of suction (Boll, Steenhuis, & Selker, 1992). Lysimeters were sealed laterally and at the bottom, leaving only a central output in the base (2 cm in diameter) evacuating the drainage water in the wick sampler, located at the bottom of the volumetric lysimeter, via a flexible tube to a rain gauge (TE525MM, Texas, with 0.1 mm resolution). Tips recorded by the rain gauge were corrected for the real collection area, which corresponded to the lysimeter circular area. The daily water balance of the lysimeters frequently gave negative values of ETa. Values were therefore aggregated and a 7-day water balance was found to be sufficient to obtain only positive values of ETa. A weekly closure of the lysimeters' water balance was therefore selected for this study.



Figure 4.2. a) Lysimeters installed at the study site before they were covered by soil and vegetation. Sensors shown are T8 tensiometers. b) Illustration of the lysimeter instrumentation (WCR = water content reflectometers, DWP = dielectric water potential sensors, T8 = tensiometers). Dimensions are shown in centimetres. Photograph: Galo Carrillo-Rojas. Illustration: Juan Pablo Córdova.

4.2.1.3 Water balance method

The water balance was closed for each of three microcatchments M1, M2 and M3 (Figure 1.3) as outlined in equation 3.2:

$$ETa_{WB} = P - Q \pm \Delta S \tag{3.2}$$

where P is precipitation (in mm/day), Q is discharge (in mm/day), and ΔS is the change in soil water storage (in mm/day). Precipitation for each microcatchment (M1 to M3) was calculated with Thiessen polygons (Jones & Hulme, 1996) from five rain gauges (4 ONSET and one Texas TE525MM). Discharge was registered by using V-notch weirs installed at the outlet of the microcatchments. The change in soil water storage was estimated via the daily difference in the storage calculated with soil moisture data from ten water content reflectometers (CS616 Campbell Scientific WCRs) located at five depths (10, 25, 35, 60 and 70 cm) on the supersite hillslope (Figure 1.3). Daily storage was calculated by integrating the storage of the mineral and organic soil depths located at five hillslope topographic positions classified in Table 4.2. The total area for each catchment corresponds to only tussock grasslands vegetation coverage (87 % for M1, 82 % for M2, and 77 % for M3, see also Table 1.1). The daily storage of catchment M1 at the toe slope position, for example, corresponds to 1.87 % (calculated as: area percentage of the toe slope position \times [(400 \times VWC) (i.e. the organic soil depth x the soil volumetric water content (VWC), which is here the average of the WCRs located at the toe slope position and at the organic soil depth) + (300 x VWC) (i.e. the mineral soil depth × soil volumetric water content (VWC), which is here the average of

the WCRs located at the toe slope position and at the mineral soil depth)]. All hillslope topographic positions were calculated in this manner and summarized, giving the daily storage of the M1 area. Microcatchments M1 to M3 differ mainly by their size.

Table 4.2. Zhurucay microcatchments soil characteristics where vegetation cover corresponds to tussock grasslands.

Hillslope topographic position	Slope (%)	Organic soil depth (mm)	Mineral soil depth (mm)	M1 area (%)	M2 area (%)	M3 area (%)
Toe slope	5–15	400	300	1.99	3.26	31.18
Lower slope	15–32	300	300	1.87	1.49	0.16
Middle slope	32–40	350	300	27.61	24.27	24.15
Upper slope	40–56	380	200	46.92	41.72	21.33
	>56	380	200	5.2	7.02	0.13
Summit	1–5	335	310	3.41	4.26	0.04

4.2.1.4 Energy balance method

Actual evapotranspiration is equivalent to the latent heat flux variable (LE, in mm/hour), which is used in the Earth's surface energy budget (Monson & Baldocchi, 2014). It is defined as the amount of energy necessary to transform liquid water into vapour, and corresponds to the amount of water that is evaporated or transpired from the Earth's surface. Thus, actual evapotranspiration (ETa_{EB}) can be calculated with the energy balance presented in equation 3.3:

$$ETa_{EB} = LE = Rn - G - H \tag{3.3}$$

where Rn is the net radiation (in mm/hour), G is the ground heat flux (in mm/hour) and H is the sensible heat flux (in mm/hour).

Rn was measured immediately above the vegetation height at around 0.6 m, by averaging two net radiometers (CNR4 Kipp & Zonen) located on the hillslope of the Zhurucay supersite. In order to calculate G, two pairs of soil heat flux plates (HFP01SC Campbell Scientific) were located at 8 cm depth from the soil surface (one pair below each net radiometer). G was calculated as the average of the soil heat flux plates plus the heat storage estimation of (Mayocchi & Bristow, 1995). Therefore, each plate was installed together with a water content reflectometer (CS616 Campbell Scientific) and soil temperature probes (TCAV). H was estimated with the flux variance method detailed in Wesson, Katul, & Lai (2001), in

order to calculate it from available meteorological variables without including any complex or uncommon methods such as the eddy-covariance method. The flux variance method calculates H with the following input variables measured by the meteorological station: mean air temperature T (CS-2150 Campbell Scientific), mean wind speed u₂ (Met-One 034B Windset anemometer), and net radiation Rn (CNR4 Kipp & Zonen). Since the flux variance method uses different equations for calculating H during day-time and night-time hours, we chose an hourly timestep for the energy balance method.

4.2.1.5 Potential evapotranspiration equation calibrated with eddy-covariance measurements

The American Society of Civil Engineers (ASCE) through its Water Resources Institute Technical Committee (ASCE-ET) selected the alfalfa-basis model ASCE Penman-Monteith equation (ASCE-PM) for standardization of the potential evapotranspiration estimation (Walter et al., 2000). Equation 3.4 presents the ASCE-PM equation in its reduced form, including C_n and C_d, which represent the numerator and denominator parameters that change with vegetation reference type and calculation time-step. These parameters were calibrated in this study for the páramo vegetation at a daily timescale. The calibration procedure compared two-year daily data (01/05/2016-30/04/2018) from the eddy-covariance measurements with the corresponding values of actual evapotranspiration estimated with the ASCE-PM calibrated equation (ETa_{PMCal}). The parameters C_n and C_d vary over the ranges 0–1000 and 0.25–1, respectively. The best values of the parameters were found by randomly creating 5000 values for each parameter inside the given ranges. The values with the lowest bias, the lowest normalized root mean square error (nRMSE) and the highest Pearson's correlation coefficient (r) were then selected. The 10-fold cross-validation method was then used to prove whether the equation could be used with a different dataset. The method was implemented by partitioning the total number of ETa values (368) into ten groups. As 368 divided by 10 does not give an integer result, nine groups had 36 values and the last group had 44 values. The function (equation 3.4) was then applied ten times and one group was left out for fitting at each iteration. The fitted values were compared with the observed values using the coefficient of determination (\mathbb{R}^2) .

When equation 3.4 is used with $C_n = 900$ and $C_d = 0.34$, the result gives the Penman-Monteith potential evapotranspiration (ETo), which was also calculated for the period of this

study in order to provide the estimates of evapotranspiration when plenty of water is available in the soil:

$$ETa_{pMCal} = \frac{0.408 \Delta (R_n - G) + \gamma \frac{C_n}{T + 278} u_2 (e_s - e_a)}{\Delta + \gamma (1 + C_d u_2)}$$
(3.4)

where Rn is the net radiation (in MJ/m²/day), G is the soil heat flux density (in MJ/m²/day) (which tends to be zero after 24 hours), T is the mean air temperature at 2 m elevation (in °C), τ is the psychrometric constant (in kPa/°C), u_2 is the mean wind speed at 2 m elevation (in m/s), e_s is the saturation vapour pressure at 2 m elevation (in kPa), e_a is the mean actual vapour pressure at 2 m elevation (in kPa), and Δ is the slope of the saturation vapour pressure-temperature curve (in kPa/°C).

4.2.1.6 Hydrological models

The hydrological models PDM and HBV-light were run for the M1 microcatchment (Figure 1.3). The M1 microcatchment is the most similar to the EC footprint compared to the M2 or M3 microcatchments, in terms of the altitude, soil type distribution and vegetation coverage. The following input variables were measured at the Zhurucay meteorological station: daily precipitation P (calculated with Thiessen polygons from five rain gauges: 4 ONSET and one Texas TE525MM, Figure 1.3), daily potential evapotranspiration ETo (see section 4.2.1.5), and daily mean air temperature T (CS-2150 Campbell Scientific).

The probability distribution model (PDM) (Moore, 1985; Moore & Clarke, 1981) was calibrated at a nearby catchment (approx. 2 km from the Zhurucay supersite) and proved to work well for estimating slow flows and evapotranspiration. Thus, the parameters calibrated and validated by Iniguez et al. (2016) were used to estimate actual evapotranspiration during the period of this study. The PDM model was implemented within a MATLAB toolbox using the options of calculating the actual evapotranspiration ETa_{PDM} as a function of the potential evaporation and the soil moisture deficit (S_{max} -S(t)) by Wagener et al. (2001), as in equation 3.5:

$$ETa_{PDM} = \left\{1 - \left[\frac{S_{max} - S(t)}{S_{max}}\right]\right\} \times ETo \tag{3.5}$$

The Hydrologiska Byråns Vattenbalansavdelning model, in its HBV-light version, is a semi-distributed model (Bergström, 1976), which was calibrated and validated at Zhurucay (Sucozhañay & Célleri, 2018). The HBV-light was run at the M1 microcatchment with the

same parameterization. Actual evapotranspiration from the soil box equals the potential evaporation if the current soil water storage (S(t)) over the maximum soil water storage (S_{max}) is above the parameter threshold for reduction of evaporation (P_{LP}) multiplied by the S_{max} , while a linear reduction is used when S(t) over S_{max} is below this value (Seibert & Vis, 2012) (equation 3.6):

$$ETa_{HBV} = ETo \times min\left(\frac{S(t)}{S_{max} \times P_{LP}}, 1\right)$$
(3.6)

4.2.2 Comparison of actual evapotranspiration measurements and estimates

Eddy-covariance and lysimeters both measure actual evapotranspiration. They were therefore considered as the references to which the estimation methods should be compared. However, the volumetric lysimeters used in this study have a lower temporal resolution than the eddy-covariance method (7-days compared to 30 min), and the eddy-covariance measurements were therefore preferred for the comparison in order to analyse all the methods on a daily basis. To analyse the lysimeter performance, the EC measurements were aggregated to 7 days.

First, daily averages of ETa_{EC} for each month were examined together with precipitation data in order to characterize ETa seasonally. The daily comparison between methodologies was assessed by accumulating the measurements and estimates during one year, then plotting daily ETa boxplots of the measurements and estimates, and calculating daily statistics such as the bias percentage (pbias), the normalized root mean square error (nRMSE), Pearson's correlation coefficient (r), the volumetric efficiency (ve), and the coefficient of determination (R²). Finally, daily differences between the different methods and the EC measurements were plotted.

The bias percentage (equation 3.7) measures the average tendency of the daily ETa estimations (sim) to be larger or smaller than the daily EC measurements (obs). It should be taken with caution as it compensates over-estimations with under-estimations at the end of the year. RMSE is commonly used for model performance applications to calculate positive errors. However, the RMSE is sensitive to outliers and extreme values as deviations are squared. The nRMSE (equation 3.8) was therefore used instead. The Pearson's correlation coefficient (equation 3.9) was calculated to measure the linear correlation between estimates and measurements, however it is sensitive to outliers. To overcome the problem with the compensation of over- and under- estimations and the sensitivity to outliers and extreme

values, the ve was also selected (equation 3.10). The ve has been proposed as an alternative to the Nash-Sutcliffe Efficiency and has been suggested to be complementary to other metrics, with the advantage that it eliminates the squaring of the deviations (Criss & Winston, 2008). The values of ve range from 0 to 1 and represent the fraction of water delivered at the proper time. In addition, the coefficient of determination R² (equation 3.11) was chosen to estimate the proportion of the variance in the ETa measurements that can be predicted from the ETa estimates. All metrics were computed with the hydroGOF package of R, version 3.5.1:

$$pbias = 100 \frac{\sum_{i=1}^{n} sim_{i} - obs_{i}}{\sum_{i=1}^{n} obs_{i}}$$
(3.7)

$$nRMSE = 100 \frac{\sqrt{\frac{1}{n} \sum_{i=1}^{n} (sim_i - obs_i)^2}}{obs_{max} - obs_{min}}$$
(3.8)

$$r = \frac{cov(sim,obs)}{\sigma_{sim}\sigma_{obs}} \tag{3.9}$$

$$ve = 1 - \frac{\sum_{i=1}^{n} |sim_i - obs_i|}{\sum_{i=1}^{n} obs_i}$$
 (3.10)

$$R^{2} = \frac{\sum_{i=1}^{n} (sim_{i} - \overline{obs})^{2}}{\sum_{i=1}^{n} (obs_{i} - \overline{obs})^{2}}$$
(3.11)

where n is the total number of daily ETa values, sim is the corresponding daily ETa estimate from each method, obs is the ETa_{EC} measurement, obs_{max} is the maximum ETa_{EC} value, obs_{min} is the minimum ETa_{EC} value, cov is the covariance between daily ETa measurements and estimates, and σ is the variance.

Furthermore, in order to discuss the performance of each method, the following approaches were taken:

- Lysimeters: the cumulative ETa for each lysimeter was plotted together with the change in storage;
- Water balance: ETa_{WB} for each catchment (M1 to M3), with and without the Δ S term, were compared with EC measurements;
- Energy balance: each term of the balance equation was compared with the terms measured by the eddy-covariance method;

 Hydrological models: the soil water storage calculated by each model was compared with WCRs observations at the Zhurucay supersite, in terms of the variations throughout the year.

4.3 Results

4.3.1 Measuring daily actual evapotranspiration with the eddy-covariance method

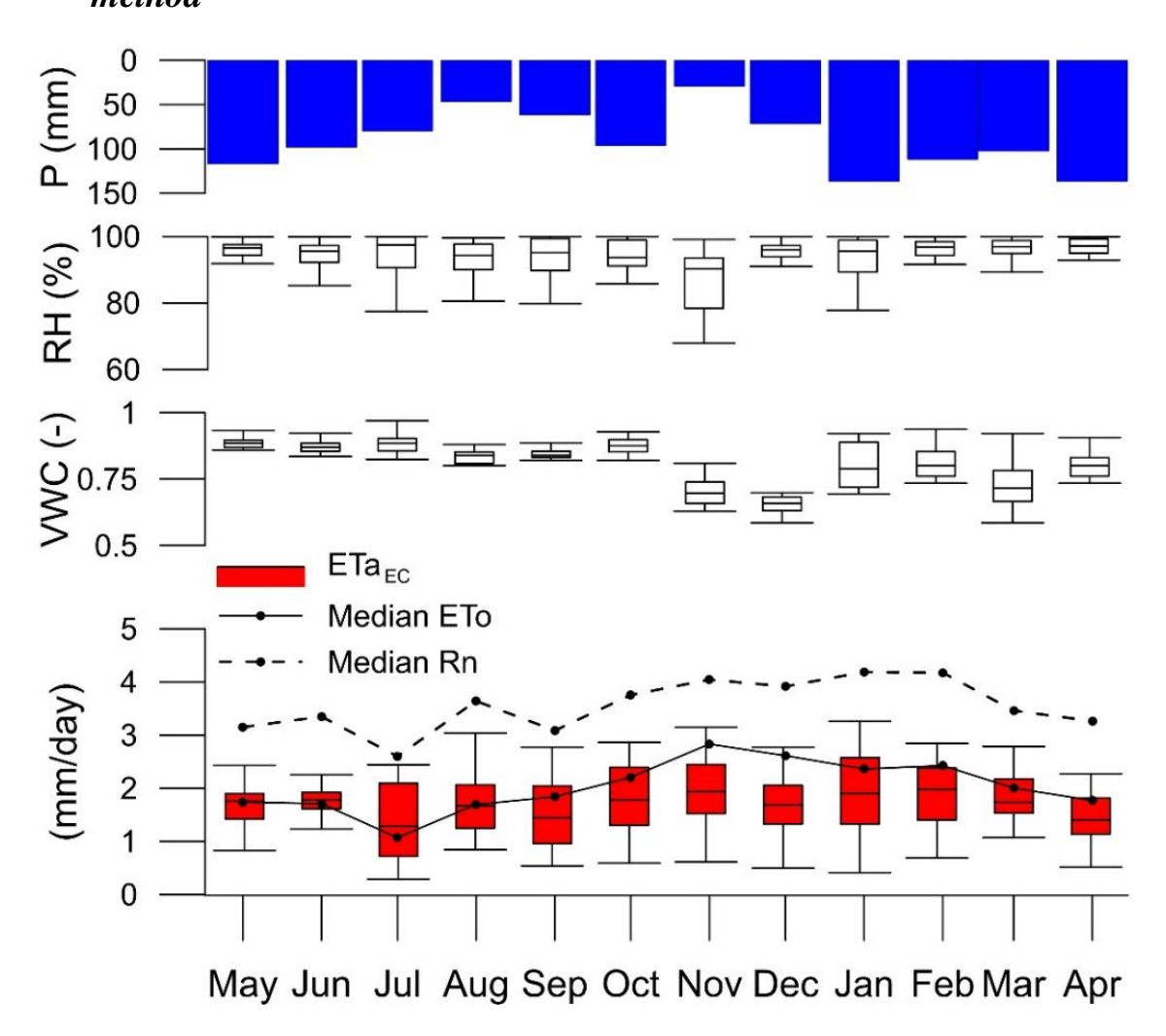


Figure 4.3. Daily actual evapotranspiration measured with the eddy-covariance method (ETa_{EC} in mm/day) shown for every month together with the median potential evapotranspiration (ETo in mm/day) estimated with the Penman-Monteith equation and median net radiation (Rn in mm/day). Additionally, monthly precipitation (P in mm/month), soil volumetric water content (VWC), and relative humidity (RH in percentage) are shown.

Eddy-covariance measurements of daily actual evapotranspiration are shown for every month from May 2017 to April 2018 in Figure 4.3. The daily ETa varied little throughout the year,

with a minimum median of 1.3 mm/day in July and a maximum median of 2.0 mm/day in February. The minimum ETa value was 0.3 mm/day and the maximum value was 4.0 mm/day. The mean ETa for the entire year was 1.7 mm/day. ETa_{EC} boxplots, in Figure 4.3, show a higher variance for July, September, October, November, January and February. Variables that are important for the evapotranspiration process, such as net radiation, precipitation, volumetric soil water content, potential evapotranspiration and relative humidity, are also shown in Figure 4.3. The ETa distribution, median ETo and median Rn were plotted together, showing a similar variability throughout the year. The ETa was on average 13 % lower than the daily ETo.

4.3.2 Comparison of methods for the estimation and measurement of actual evapotranspiration

Cumulative values of daily actual evapotranspiration (for every method), daily potential evapotranspiration and daily precipitation are shown in Figure 4.4. The ETa_{EC} measurements amounted to 622 mm at the end of one year, while cumulative precipitation was 1094 mm. In general, all methods except the calibrated evapotranspiration equation underestimated ETa throughout the year. At the end of the year, the calibrated evapotranspiration equation, water balance, and lysimeters were the most accurate in estimating annual ETa (with a 3-10 % underestimation), while the other methods underestimated annual ETa by around 20 %. The EC and the PMCal methods found an ETa/P value equal to 0.57, while the other methods found an ETa/P value equal to 0.5. This indicates that a little more than a half of the precipitation returns to the atmosphere by evaporation and transpiration. Similarly, the EC and PMCal methods found that the ETa/Rn evaporative fraction was equal to 0.48, while the other methods underestimated this value (the lysimeters and water balance method found ETa/Rn = 0.44, while the hydrological models and the energy balance method found ETa/Rn = 0.40). This indicates that almost half of the energy available at the surface was used for evaporation and transpiration.

Daily measurements of actual evapotranspiration by the EC method are shown in Figure 4.5 as a boxplot for the entire year. Boxplots of daily ETa estimates from the hydrological models (HBV-light and PDM), water and energy balance methods, and the PMCal equation are also shown. The hydrological models and the PMCal were the most similar to the EC measurements distribution. The energy balance estimates had a very similar median to the EC measurements but the variance was much higher. The water balance estimates were the least

similar to the EC measurements out of all methods, with a lower median and a very different distribution. These results were corroborated with the bias percentage (pbias), the normalized root mean square error (nRMSE), the Pearson's correlation coefficient (r), the volumetric efficiency (ve), and the coefficient of determination (R^2), which are shown for all methods in Table 4.3. The bias percentage of all the methods in comparison with the EC measurements were, from lowest to highest: -3 % for the calibrated evapotranspiration equation (PMCal), -10 % for the lysimeters, -10 % for the water balance method, -18 % for the PDM model, -19 % for the energy balance, and -20 % for the HBV-light model. Regarding error and correlation, the hydrological models and the PMCal presented, on a daily basis, the best performance with the lowest error (12–15 %), the highest correlation (r = 0.7–0.9 and $R^2 = 0.5$ –0.8), and the highest efficiency in estimating the water volume (ve = 0.8).

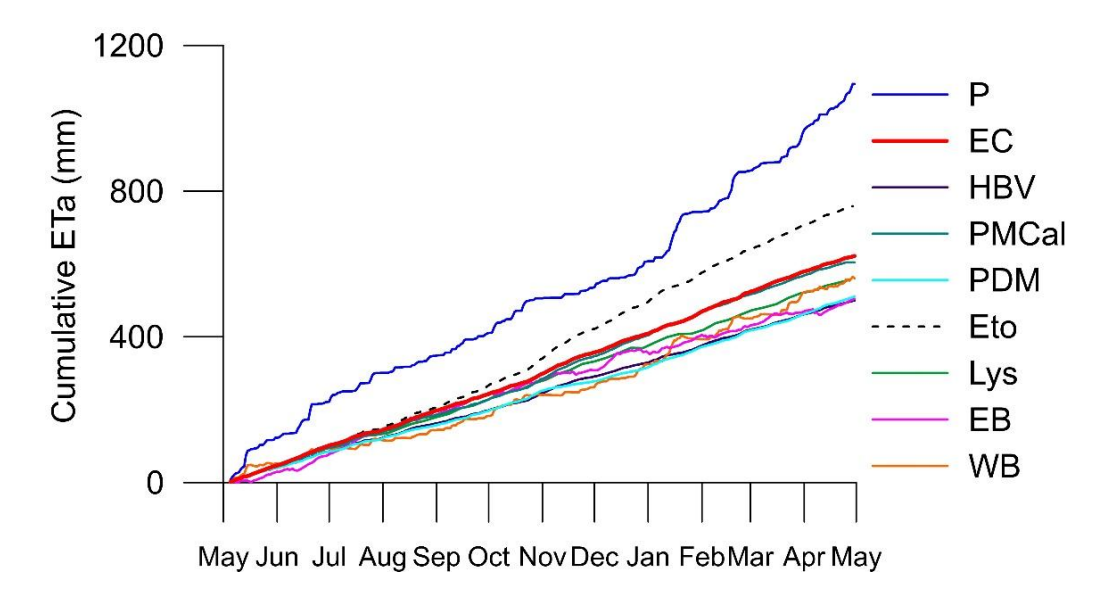


Figure 4.4. Cumulative daily actual evapotranspiration measured by the eddy-covariance (EC) and lysimeters and estimated by the PDM and HBV-light hydrological models, the water balance (WB) and energy balance (EB) methods, the calibrated evapotranspiration equation (PMCal), and the potential evapotranspiration (ETo). Cumulative precipitation (P) is also shown.

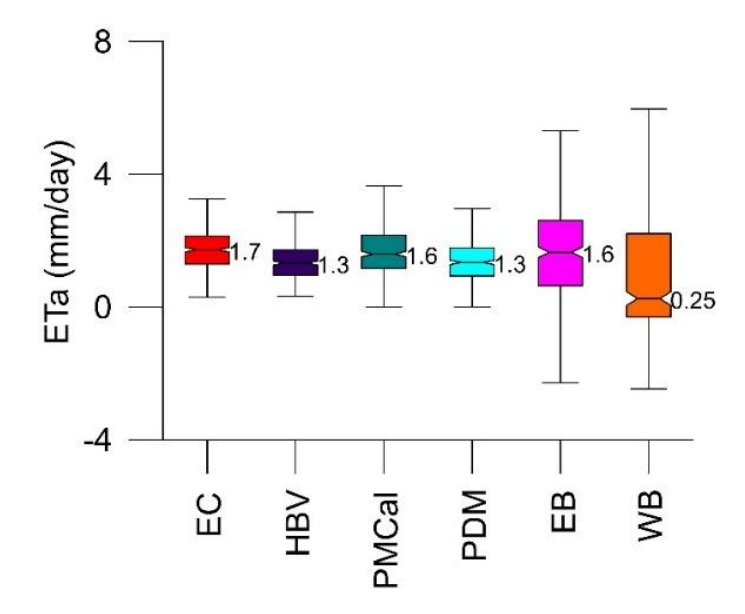


Figure 4.5. Daily actual evapotranspiration measured by the eddy-covariance method (EC) and estimated by the HBV-light and PDM models, the calibrated evapotranspiration equation (PMCal), the energy balance (EB) and the water balance methods (WB).

Table 4.3. Bias percentage (pbias), normalized root mean square error (nRMSE), Pearson's correlation coefficient (r), volumetric efficiency (ve), and coefficient of determination (R²) for the actual evapotranspiration estimated with the HBV-light and PDM models, the calibrated evapotranspiration equation (PMCal), the lysimeters (Lys), the energy balance (EB), and water balance (WB) methods against the eddy-covariance measurements.

Method	pbias (%)	nRMSE (%)	r (-)	ve (-)	$\mathbf{R}^2(-)$
HBV-light	-19.70	12.00	0.88	0.78	0.77
PMCal	-2.40	14.90	0.66	0.78	0.45
PDM	-17.90	14.80	0.72	0.75	0.52
Lys*	-10.00	24.60	0.45	0.72	0.20
EB	-18.90	53.80	0.25	0.18	0.06
WB	-9.90	92.50	-0.41	-0.54	0.17

^{*}Lysimeters statistics were calculated for every 7 days

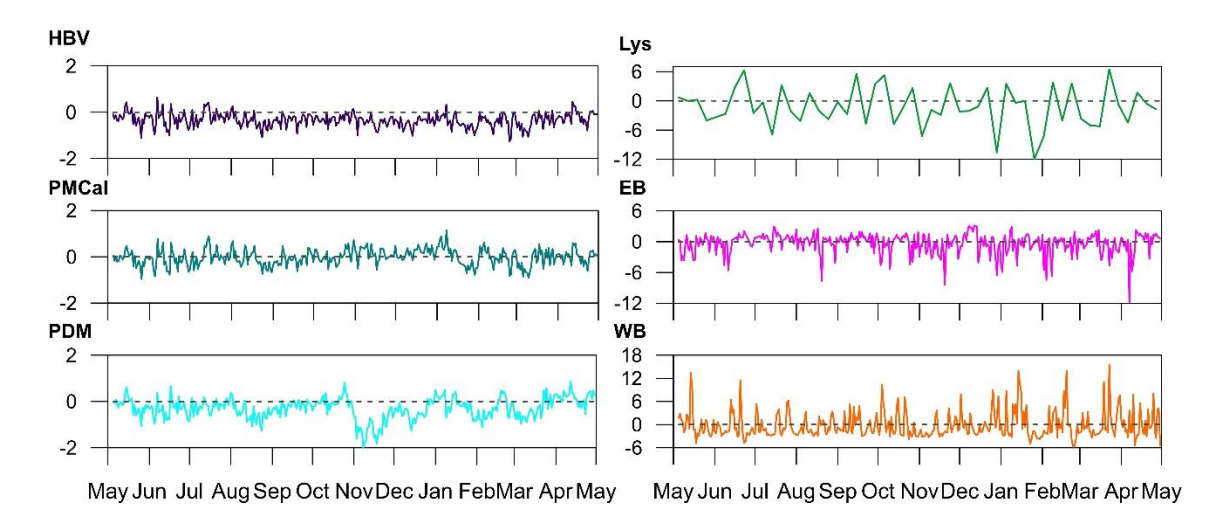


Figure 4.6. Daily differences in evapotranspiration between the methods and the eddy-covariance. Methods include: PDM and HBV-light hydrological models, lysimeters (Lys), energy balance (EB), water balance (WB), and the calibrated evapotranspiration equation (PMCal).

Figure 4.6 shows the daily differences between the methods and the EC measurements. The hydrological models and the calibrated evapotranspiration equation were biased from the EC measurements over a range -2 to 2 mm/day, the energy balance method was biased over a range -12 to 4 mm/day, the lysimeters were biased over a range -12 to 6 mm/day, and the water balance method was biased over a range -6 to 14 mm/day. Remarkably, the HBV-light outperformed the rest of the models while the water balance method was the one that presented major differences in comparison with the EC measurements. Although the water balance and lysimeters had the second lowest bias percentage throughout the year (Table 4.3), the differences shown in Figure 4.5 and Figure 4.6 suggest that this value is the result of the compensation of the considerable over- and under-estimation of daily differences. Thus, these methods estimate ETa better than other methods at the end of the year, but fail at estimating ETa on a daily or weekly basis.

Overall, these results indicate that the hydrological models and the calibrated evapotranspiration equation are the most efficient methods for estimating daily ETa when compared with the EC measurements.

4.4 Discussion

4.4.1 Actual evapotranspiration and its environmental controls

Actual evapotranspiration in the páramo was 1.7 mm/day on average (ranging from 0.3 to 4.0 mm/day) according to the EC measurements. ETa has rarely been measured or estimated in the páramo or at high altitudes, such as at 3765 m a.s.l. where the EC tower and the lysimeters are located. At a nearby location, Iniguez et al. (2016) modelled ETa with the PDM and found slightly lower daily averages of 1.47 mm/day (ranging from 0.19 to 3.33 mm/day). At 3250 m in the Tibetan meadows, Gu et al. (2008) measured ETa with the EC method and found daily values of 4 mm (ranging from 1.9 to 6 mm) for 30 cm herbaceous vegetation with almost no bare soil (90 % vegetation coverage). Coners et al. (2016) measured at the same site a daily ETa range of 1.9 to 2.2 mm/day with EC and lysimeters. Nevertheless, the ETa/P ratio found in this study (0.57) is similar to the studies mentioned previously (0.6–0.7) and is slightly lower than the mean terrestrial ratio (0.66) (Oki & Kanae, 2006). Also, at New Zealand sites Campbell & Murray (1990) and Holdsworth & Mark (1990) registered an ETa/P ratio between 0.2 and 0.5, where the tussock grasslands are very similar to our site despite a lower altitude of around 1000 m (a.s.l.). In Peru, similar daily ETa values were found for puna grasslands (ranging from 1.5 to 2.3 mm/day). However, given the high precipitation at that site, the annual ETa/P ratio was 0.2 (K. Clark et al., 2014). Finally, Fisher et al. (2009) found ETa values of 1096 mm/year from eddy-covariance towers located in the Amazonian rainforest in the tropics.

The ETa amount depends mainly on the water and energy availability. As precipitation (P) and the soil volumetric water content (VWC) are high at the study site (Figure 4.3), high rates of drizzle have been measured (Padrón et al., 2015) and high interception rates during low intensity events quantified (Ochoa-Sánchez et al., 2018), sufficient water is available for evaporation and transpiration almost all year long. Regarding the available energy, Figure 4.3 shows that the variability of ETa is the same as that of ETo and Rn. On average, ETa was found 13 % lower than ETo. The evaporative fraction was 0.48. Moreover, an important characteristic of our site is the high relative humidity present in the páramo that keeps the air saturated or almost saturated, thus no additional vapour is allowed in the atmosphere (Figure 4.3). This is corroborated by the high differences in ETa/P between wet and dry months (0.46 and 0.95 on average, respectively). During dry months (less than 100 mm/month), although

less water is available for evapotranspiration, lower cloudy conditions allow higher radiation (Figure 4.3), and consequently more evaporation. The opposite occurs during wet months.

In summary, the constant rainfall balances ETa loss and drainage. A similar water balance was also found for native tussock grassland catchments in New Zealand (Bowden, Fahey, Ekanayake, & Murray, 2001). There is practically no time in the year where the soil volumetric water content (VWC) drops below 0.7 (field capacity), except during drier months when values of 0.6 were recorded. However, these values are not below the wilting point (0.45).

4.4.2 Sources of uncertainty in the ETa estimation methods

In general, the ETa was underestimated by all methods except the PMCal equation (Table 4.3, Figure 4.4). Volumetric lysimeters were the most accurate in closing the water balance at the vegetation scale, as they used disdrometer observations to measure P and also took into account the change in soil water storage (ΔS). However, disdrometer measurements were only available at the supersite, therefore the water balance and the hydrological models used rain gauge measurements for quantifying P. In addition, the water balance did not include the ΔS term. Here, we showed that the water balance and lysimeters are good at estimating ETa by the end of the year while hydrological models were the most correlated with EC measurements, although they underestimated ETa by the end of the year. During the time period of the comparison, the daily disdrometer measurements recorded 4 % more rainfall than rain gauge measurements and they showed a difference of 10 % in absolute daily values. If we assume homogeneity between the supersite and microcatchments inside Zhurucay, disdrometer measurements of P could improve the water balance estimation of annual ETa.

Due to the similarities between the ETa and ETo during the first months of this comparison period (May–August), as ETa seems to be limited by the energy availability and not by water availability, the energy balance was very close to the cumulative values of EC measurements (Figure 4.4). In addition, the outstanding performance of the PMCal (Table 4.3) is due to the calibration with the EC measurements that served as a bias correction for ETo.

In the following sections, the sources of uncertainties from each method are discussed.

4.4.2.1 The eddy-covariance technique

The eddy-covariance method applied to non-ideal surfaces, such as steep terrain, and harsh environments can present uncertainties (Baldocchi, 2003). The main sources of biases are

related to night-time advection (mostly related to carbon dioxide and methane fluxes, rather than ETa) (Novick, Brantley, Miniat, Walker, & Vose, 2014) and to the energy exchange that is affected by the underlying sloped surface (Serrano-Ortiz et al., 2016). Such uncertainties cannot be accounted for in the present study, due to the need for additional sensors. However, the uncertainties induced by the data gap-filling process have been calculated via a bootstrapping technique, and amounted to 0.002 ± 0.008 mm/h (1.3 %) of the hourly ETa mean for the gap-filled data values exclusively (~20 % of the total dataset).

4.4.2.2 Lysimeters

Four volumetric lysimeters measured ETa over a period of one year by closing the water balance every seven days. The variables involved in the water balance are precipitation, drainage, and storage. Precipitation measured with the disdrometer (with a resolution of 0.01 mm) includes observations of light-rain and drizzle, commonly present in the páramo. However, the cumulative drainage differed greatly between lysimeters (up to 165 mm) by the end of the year. Consequently, the ETa measured with each lysimeter differed in a similar manner. This difference represented 38 % of the total cumulative ETa. The uncertainty between lysimeters is large in comparison with other studies, for example Gebler et al. (2015) found a difference of 40 mm that represents 7.7 % of the total ETa. In addition, the change in soil water storage values calculated with the WCRs were small but appear important for closing the water balance. In summary, the uncertainty in measuring ETa with volumetric lysimeters might be due to differences in vegetation, root density, soil pore space and soil heterogeneity at each lysimeter. These differences at such a small scale could have caused variability in interception loss, transpiration, and consequently drainage. Furthermore, errors made by measurement instruments such as water content reflectometers should also be considered. Figure 4.7 shows the cumulative ETa for every lysimeter. The uncertainty between these instruments is the result of two lysimeters in particular. While lysimeters Lys2 and Lys4 measured very similar ETa values, Lys3 and Lys1 strongly over- and underestimated ETa, respectively. Drainage from lysimeter Lys3 was minimal in comparison with the others, while drainage from lysimeter Lys1 was very high. Nevertheless, the average ETa measured with lysimeters Lys1 and Lys3 was similar to the ETa measured with lysimeters Lys2 and Lys4. This indicates that these values underestimated ETa when compared to the EC measurements. However, these over- and under-estimations were compensated for when they were aggregated over a monthly timescale. A higher correlation was found at a monthly timescale (r = 0.5, $R^2 = 0.4$, and ve = 0.8).

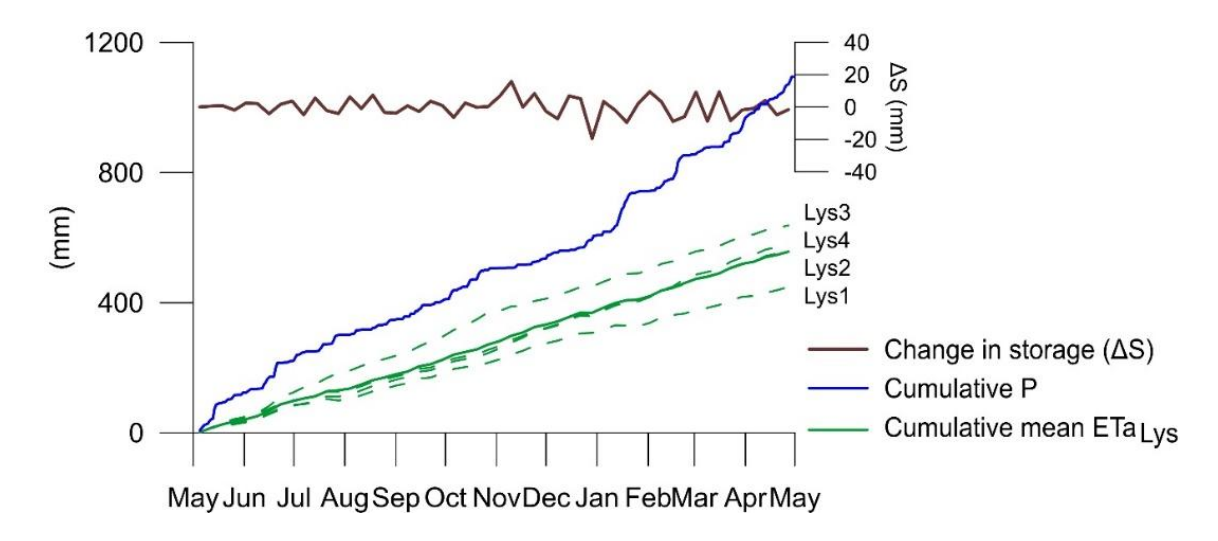


Figure 4.7. Cumulative evapotranspiration measured with the four lysimeters every 7 days, cumulative precipitation, and the change in soil water storage (ΔS).

4.4.2.3 Water balance

The water balance method has been extensively used to validate ETa estimates from diverse sources (e.g. remote sensing, hydrologic models) and the water balance of three well monitored microcatchments, different in size, was assessed in this study with the objective to define ETa_{WB}. The found values of ETa_{WB} did not prove to be very accurate or to correlate with the EC measurements on a daily timescale. Figure 4.8 shows the mean performance of the three microcatchments depicted in Figure 1.3. Microcatchments M1 to M3 are different in size and relatively similar in terms of vegetation coverage, soil and hydrological properties. The M1 microcatchment is the most similar to the EC footprint. Table 4.4 shows the differences between each microcatchment when comparing their estimates with the EC measurements. The estimates were very similar among microcatchments and only the bias percentage was different. The average was therefore sufficient to give a representation of the performance of the water balance method. However, these estimates did not take into account the change in the soil water storage (ΔS). Figure 4.8 shows the difference between ETa_{WB} and ETa_{EC} estimates when the ΔS term was included, respectively excluded. Inclusion of the ΔS term in the water balance equation on the basis of the WCRs measurements resulted in an increase of the daily ETa estimates. In addition, Table 4.4 shows the mean estimates of ETa when the term ΔS was considered, confirming its lower performance. This occurred because the WCRs were only located on the supersite hillslope and no other soil VWC measurements were available at Zhurucay. It is noteworthy that the daily over- and under-estimations did not balance one another when they were aggregated weekly or monthly and large differences with EC measurements were still found. However, by the end of the year, the water balance

was as accurate as lysimeters in estimating ETa, and was better than the other methods, except PMCal. The concept of closure of the water balance to estimate ETa is the same as the lysimeters' water balance, and when their terms were compared differences arose in the ΔS term. The daily water balance estimates were aggregated to weekly and monthly data, and were found to be far from as good as the lysimeter measurements. At a daily timescale, it is difficult to close the water balance as the precipitation that drains a day after or even later cannot be included. In addition, the poor performance of the water balance could be attributed to the poor estimation of ΔS . This term is important at daily and monthly timescales in order to estimate ETa properly. After one year though, the soil water storage is negligible. Studies with long-term data (e.g. Marc & Robinson (2007); Moehrlen, Kiely, & Pahlow (1999); Wilcox, Dowhower, Teague, & Thurow (2006)) or with accurate measurements of ΔS (e.g. Wan et al. (2015)), have therefore found high accuracy in water balance estimates. However, such studies are uncommon at remote sites (e.g. high altitude sites). Finally, a better measurement of precipitation, which includes hidden precipitation such as drizzle and fog, could close the water balance, and thus ETa could be better estimated.

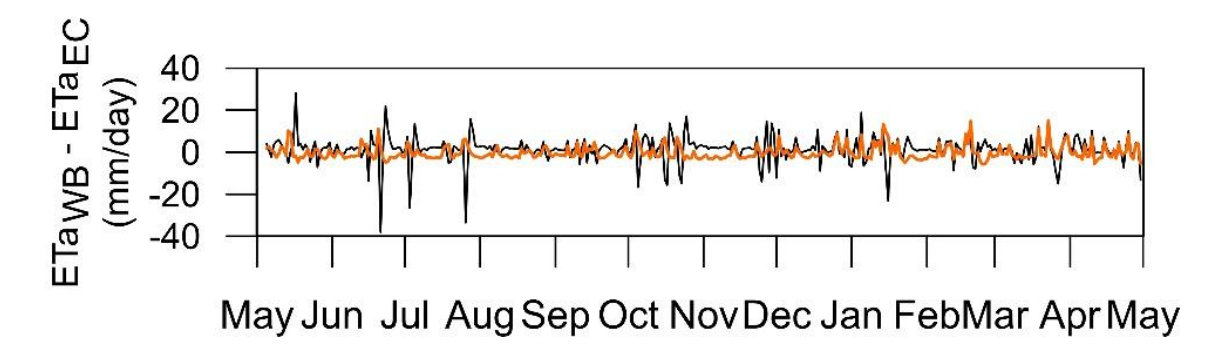


Figure 4.8. Differences between the mean water balance estimates (without the change in storage term) with EC measurements (orange line) and the differences between the mean water balance estimates (including the change in storage term) and the EC measurements (black line).

Table 4.4. Bias percentage (pbias), normalized root mean square error (nRMSE), Pearson's correlation coefficient (r), volumetric efficiency (ve), and coefficient of determination (R²)

for the ETa estimates from the water balance closure in three catchments against the eddy-covariance measurements.

Microcatchment	pbias (%)	nRMSE (%)	r (-)	ve (-)	R^2 (-)
WB1	-12.80	99.70	-0.40	-0.63	0.16
WB2	-12.10	93.50	-0.40	-0.55	0.16
WB3	-4.70	89.40	-0.40	-0.47	0.16
Mean WB with ΔS	-16.20	167.10	0.07	-1.20	0.00

4.4.2.4 Energy balance

The variables involved in the energy balance were aggregated monthly together with the eddy-covariance measurements in Figure 4.9, showing their seasonal variance. The net radiation from the eddy-covariance was expected to be smaller than the net radiation from the energy balance, as the measurement elevations differ (3.6 m and 0.6 m, respectively). The ground heat flux was very small and similar between methods. The difference between the ETa estimations with the energy balance and with the EC measurements is therefore attributed to the estimates of the sensible heat flux. The flux variance method overestimated the sensible heat flux when compared with the EC measurements (Figure 4.9), therefore the EB method underestimated ETa (Figure 4.6). The flux variance method is preferred for estimating the sensible heat flux rather than the latent heat flux (Hsieh, Lai, Hsia, & Chang, 2008; Katul et al., 1995), however studies corroborate that H was overestimated (e.g. Katul et al. (1995)). Although the flux variance estimates of H depend on air temperature, wind speed and net radiation (Wesson et al., 2001), we found that for the study site that the variation of the estimates is mainly influenced by the air temperature variance (σT), as shown in Figure 4.9 where the variability between H and σT is the same throughout the year. In the páramo, hourly variations in temperature might be higher than at other sites ($\sigma = 4.5$ °C/hour), therefore high fluctuations of the H values occur. The energy balance method presented in this study is relatively simple to implement, especially taking into account that G is negligible, and turned out to be more accurate than the water balance method. A more widely used and easy-to-implement method that estimates H or LE is the Bowen ratio-energy balance (BREB) (Fritschen & Simpson, 1989). This method involves differential measurements of temperature and relative humidity, and although it is an indirect measurement of the energy fluxes, it is recommended for future implementation to increase the accuracy of the estimations of ETa with the energy balance methodology.

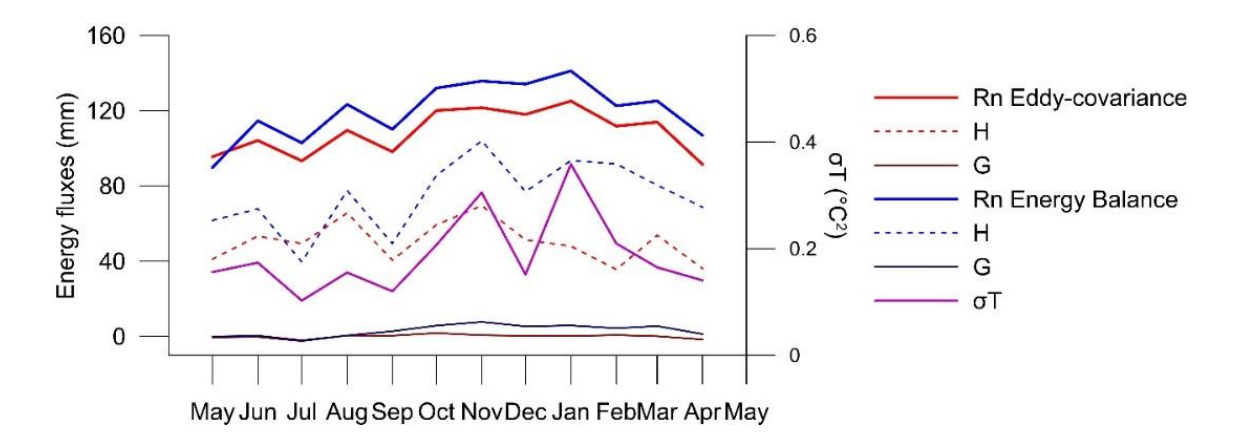


Figure 4.9. Energy fluxes measured with the eddy-covariance method vs. energy fluxes estimated with the energy balance method. Energy balance method is highly dependent on the variance of the temperature (σT) .

4.4.2.5 The calibrated evapotranspiration equation

After calibration with EC measurements, the coefficients for the ASCE-PM equation were C_n = 550 and $C_d = 0.4$. They differed from the Penman-Monteith coefficients that estimate ETo $(C_n = 900 \text{ and } C_d = 0.34 \text{ for short grass and } C_n = 1200 \text{ and } C_d = 0.38 \text{ for tall grass (Allen,}$ Clemmens, Burt, Solomon, & O'Halloran, 2005)). Indeed, the ETo and ETa provide different insights, as ETo explains the evapotranspiration when there is no water stress while ETa explains the actual evapotranspiration of the system. In addition, the difference between standard values and the ones found in this study, are due to the vegetation properties. Tussock grasslands differ from short and tall ideal grasses, especially in the high amount of dead leaves that lowers transpiration. The calibration purpose was therefore to find ETa estimates as a function of widely available measurements on a daily scale. The cross-validation of the calibrated evapotranspiration equation proved that results are independent from the dataset $(R^2 = 0.9)$. The PMCal method is the least biased method (-2 %) as EC measurements were used as input for the calibration procedure. Calibration causes a bias correction of the potential evapotranspiration to fit the EC measurements. At our site, this was useful as ETa varies similarly to ETo, as noted in section 4.4.1. The differences between PMCal and EC measurements were therefore minimal (Figure 4.6). Results of the calibrated evapotranspiration equation are accurate and useful at several sites as meteorological stations are widely available. We encourage the use of the calibrated coefficients at páramo sites where only meteorological stations are available to estimate ETa, as we have shown here that the common use of ETo to represent evapotranspiration overestimates this important variable by 13 %.

4.4.2.6 The hydrological models

The PDM estimates ETa as a function of soil water storage and ETo. In general, model performance was good when compared with the EC measurements (Table 4.3). The few important differences occurred during November and March (Figure 4.6). During these months, there was less water available and the PDM underestimated ETa, while the EC measurements showed a relatively high ETa as there was low relative humidity and high ETo that allowed more transpiration (Figure 4.3). Figure 4.10 shows the differences between observed field values of volumetric soil water content (VWC) and the storage modelled with the PDM (PDM S), which cannot be compared in magnitude but should have the same variability throughout the year. However, it appears that there is no correlation, especially during November and March. Most importantly, the variability was not the same between VWC and PMD S.

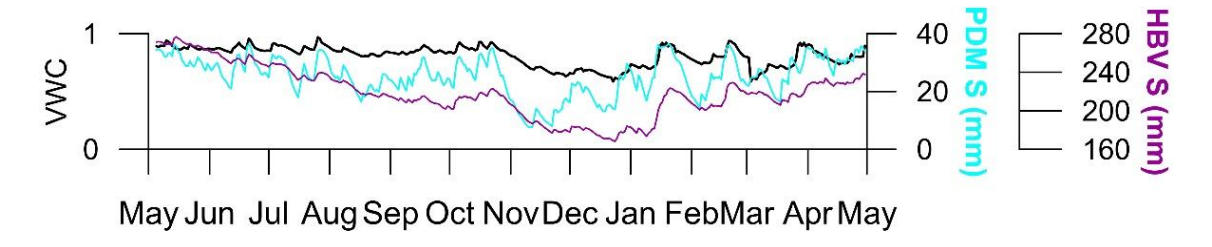


Figure 4.10. Soil volumetric water content observed with a water content reflectometer (VWC), soil water storage modelled with the PDM (PDM S), and soil water storage modelled with the HBV-light model (HBV S).

The HBV-light model outperformed all methods, evidenced by its high correlation with the EC measurements (0.8–0.9), despite underestimating ETa at the end of the year with a bias of -20 %. The bias percentage of the model is higher than other methods, as the over- and underestimations of the other methods are compensated by the end of the year. HBV-light residuals are small (ranging from -1 to 1) and mostly negative, therefore these underestimations are not compensated, which explains the large negative bias. The volumetric efficiency, on the other hand, analyses absolute errors, and shows a high performance of the model (ve = 0.8). HBV-light ETa estimates are a function of the same variables as in other hydrological models (e.g. PDM). Nevertheless, it appears that the factors multiplying ETo and the soil moisture variables, plus the corrections for temperature anomalies and an estimation of rainfall interception separately from soil evaporation and transpiration (Seibert & Vis, 2012), gave better estimates of ETa. Figure 4.10 shows the high correlation between VWC and the soil water storage of the HBV-light (HBV S).

It is challenging to represent the change in soil water storage in a model. Even though hydrological models are not very accurate at estimating storage, they take into account this term and this is one important reason why they are well correlated with daily ETa. Additionally, ETa remains as the only variable that the model needs in order to estimate ETa, as deep percolation and groundwater recharge are negligible at the site. At similar sites where EC or other methods are not available, hydrological models present a solid alternative.

4.5 Summary and conclusions

For the first time, we compared actual evapotranspiration measurements with estimations from several methods in the páramo ecosystem. This study contributes to the advances on the assessment of ETa, which is part of the main challenges for earth sciences (Fisher et al., 2017). The mean daily actual evapotranspiration was found to be equal to 1.7 mm/day, and in a range from 0.3 to 4 mm/day. Over one year, ETa amounted to 622 mm and the ratio of ETa to the total precipitation was 0.57. Furthermore, we have discussed in detail the drivers that led the methods to over- or under-estimate ETa when compared with the EC method. Here we present a brief summary of the suitability of the methods with the main conclusions found in this study.

The main advantages and disadvantages documented for the measurement and estimation of actual evapotranspiration have been summarized in Table 4.5. In conclusion, the most accurate method with the best temporal resolution is the EC method. However, building the tower includes costly sensors and data corrections that require specific knowledge. A more affordable technique that still gives a complete understanding of the functioning of the environment in terms of the water exchange between the vegetation and the atmosphere, consists in installing a volumetric lysimeter. However, these proved to be effective only when monthly timescales are necessary and when precipitation is accurately measured, taking into account that horizontal precipitation, drizzle and fog are commonly present in the páramo and a disdrometer is preferred over rain gauge measurements (Padrón et al., 2015). The energy balance method also gives a complete understanding of the energy exchange but the sensible heat flux could not be properly estimated in this study and requires further attention.

Although the water balance has been widely used as a validation method for numerous approaches, we showed here that for relatively small ETa values, the measurement of the change in soil water content plays a crucial role in estimating daily ETa. Even with several water content reflectometers available at our site and information on the soil hydrophysical

properties, it was difficult to estimate this term accurately, and at other sites where other variables might be important the accuracy might be even more difficult to improve. Therefore, the water balance is only useful when ETa values are relatively large and other variables are correctly measured or negligible. Furthermore, lysimeters and the water balance method were the least biased in estimating annual ETa, as at the páramo site no other variable appears to be crucial for closing the water balance on that timescale.

When daily estimates and few details on the energy fluxes are needed, the hydrological models (PDM and HBV-light) have proved to be robust for estimating ETa during wet and dry periods. Furthermore, these methods can properly assess the hydrology of the site, are freely available, require only few data as inputs and are easy to implement. They correlate very well with EC measurements and the use of better observations of P (e.g. thorough disdrometers) might improve their accuracy even more.

Finally, it is possible that a meteorological station is available at a páramo site but complete or high-quality data for catchment characterization is not available, and therefore, a model cannot be run. However, the calibration of the Penman-Monteith equation presented here could serve for the estimation of ETa with great accuracy. Moreover, at sites where ETa is not limited by water, the ETo would give very similar results as the ETa. The use of the PM equation is therefore highly advised.

This study presented and analysed alternatives to the ETa_{EC} measurements in páramo grasslands. Further work on this environment is needed to attain higher spatial and temporal resolution. In the future, long-term monitoring studies are required to capture ETa variability under extreme conditions. In addition, partitioning of this variable in the páramo will improve ETa assessment and water resources modelling, important requirements worldwide (Fisher et al., 2017).

Table 4.5. General advantages and disadvantages of the actual evapotranspiration measurement and estimation methods.

Method	Relative advantages	Relative disadvantages	
Eddy-covariance	Precise measuring technique	Expensive sensors	
	via high-frequency optical		

Method	Relative advantages	Relative disadvantages				
	detection					
	High time resolution data	Medium to difficult installation				
	Useful to understand the energy and water exchange	Medium difficulty for data acquisition				
Volumetric lysimeter	Measuring technique	Medium difficulty for installation				
	Easy data acquisition	Low time resolution data				
	Medium to low cost					
	Useful to understand the water exchange					
Water balance	Easy to implement and to calculate	Estimation technique				
	Low cost	Difficult to estimate accurately where groundwater or other variables are important				
	World-wide used for ETa estimation	Only viable for extensive areas and over large periods				
Energy balance	Medium to low cost	Estimation technique				
	High time resolution data	Difficult to estimate latent heat flux				
	Easy to calculate					
Hydrological models	Low cost	Estimation technique				
	Easy to implement	Demand a proper calibration and validation				
Calibrated evapotranspiration	Only meteorological variables are needed	Estimation technique				
equation	Easy to calculate	Demand a proper calibration and validation				
	Low cost					

Controls on actual evapotranspiration

The study of the controls and components of the evapotranspiration leads to a better understanding of the actual evapotranspiration (ETa) process that links the functioning of the soil, water and atmosphere. It also improves local, regional and global ETa modelling. At the Tropics, few studies so far focussed on the controls and components of ETa, especially at remote highland areas such as the tussock grassland. In this chapter, the controls on ETa were unveiled, finding that the wet páramo is an energy-limited region and net radiation (Rn) is the main controller on ETa. The monthly average evaporative fraction (ETa/Rn) was 0.47 and it remained similar for wet and dry periods. The secondary controls on ETa were wind speed, aerodynamic resistance and surface resistance that appeared more important for dry periods, where significantly higher ETa rates were found (20 % increase). Knowledge on the ETa process will lead to improving the process understanding and modelling of the land-atmosphere fluxes in the Tropics.

Related publication

Ochoa-Sánchez, A., Crespo, P., Carrillo-Rojas, G., Marín, F., & Célleri, R. (2019). Controls on Andean grasslands evapotranspiration and quantification of transpiration at event scale. *Hydrological Processes*, *in review*.

5.1 Introduction

An important challenge in ecohydrology is to understand the controls of the surface water balance, especially the partitioning of precipitation (P) into actual evapotranspiration (ETa) and runoff (Q) (Williams et al., 2012). From these components, ETa represents the key variable in linking ecosystem functioning, carbon and climate feedbacks, agricultural management, and water resources (Fisher et al., 2017). Insights on the ETa magnitude and controls is of importance for current science questions about the terrestrial biosphere. Furthermore, revealing ETa controls will improve local, regional and global modelling of the soil-vegetation-atmosphere gas and energy exchange. ETa modelling at the Tropics remains a challenge since models are site-specific and their validation is problematic due to low measurement accuracy, a lack of long term monitoring and low spatial and temporal resolution (Fisher et al., 2009, 2017).

The páramo environment, mainly covered by tussock grasslands (> 80 %), is an important ecosystem of the Andean region for its endemic fauna, flora and especially for its water resources (Llambí et al., 2012). It is located above 3300 m. a.s.l. and it provides drinking water to cities and communities along Colombia, Ecuador and Peru. Its water is also used for agriculture, hydro-power production and for sustaining aquatic ecosystems. Studies about this ecosystem increased lately; however, due to its remoteness, information on the soil-vegetation-atmosphere exchange processes is still limited (Pepin et al., 2015).

Studies on the controls of evapotranspiration at the Tropics focussed mainly on the Amazon rainforest, for its important contribution to global land surface evapotranspiration, and on some eddy-covariance sites in South-East Asia, Africa and Oceania (Costa et al., 2010; Fisher et al., 2009; Hasler & Avissar, 2007). At the páramo, actual evapotranspiration seasonality has been briefly discussed before using one or two years of measurements (Carrillo-Rojas et al., 2019; Ochoa-Sánchez, Crespo, Carrillo-Rojas, Sucozhañay, & Célleri, 2019); however, identifying the controls on ETa was not the purpose of those studies; and therefore, they were not assessed. Additionally, differences in the controls on ETa for wet and dry periods have not been studied, mainly due to the low seasonality of precipitation at the páramo (Ochoa-Sánchez et al., 2019).

As a consequence, the aim of this chapter is to find the biotic and abiotic controls on ETa and whether these controls remain the same for wet and dry periods. Such an analysis will improve the understanding of the evapotranspiration process at one of the most important environments in the Andean region.

5.2 Methods

5.2.1 Data

The site equipment used in this study corresponds to a laser disdrometer, a meteorological station, an eddy-covariance tower and 38 water content reflectometers along the hillslope, located at the monitoring supersite of Zhurucay (Figure 1.3). Since the eddy-covariance tower was placed in March 2016, three years of micrometeorological and soil moisture hourly-average time series were available (01/03/2016 - 28/02/2019). Table 5.1 specifies the variables used in this study, together with their acronyms, mean, maximum and minimum values and the sensors or equations used for their measurement or estimation.

The eddy-covariance tower is part of the FLUXNET (EC-APr). The energy balance was closed at the study site by measuring the turbulent components of latent heat (LE) and sensible heat (H) with an enclosed-path infrared gas analyser (LI-COR 7200) and a three-dimensional sonic anemometer (Gill New WindMaster) respectively, both working at a sampling frequency of 20 Hz. On the other hand, the net radiation (Rn) and soil heat flux (G) components of the EB were measured with a 4-component net radiometer (CNR4 Kipp Zonen) and three soil heat flux plates (Hukseflux HFP01). High-frequency raw data from turbulent fluxes were processed with the EddyPro software, version 6.2.0 (LI-COR) and averaged to a 30-min blocks. Data quality assurance and quality control (QA/QC) with diagnostic flags, plausibility limits and spikes removal were mandatory to remove unreliable data. In addition, site-specific corrections were applied for time lags between measurements, humidity-dependent spectral losses and wind planar fit of the flux contributions. More detail of the aforementioned corrections is provided in Carrillo-Rojas et al. (2019). The energy balance closure (Rn - G = H + LE) for the 3-year dataset amounted to 99% and a correlation value of $R^2 = 0.9$.

5.2.2 Evapotranspiration and meteorological variables seasonality and their difference between wet and dry periods

The M1 Zhurucay microcatchment (Figure 1.3) was used to give a first insight on the hydrological cycle components at the supersite. M1 is the nearest monitored microcatchment to the supersite and it has the most similar vegetation, soil and climate characteristics than the other monitored microcatchments within Zhurucay. Precipitation was estimated with a disdrometer and actual evapotranspiration was measured with the eddy-covariance method, both installed at the supersite. Discharge was measured with a V-notch weir placed at the outlet of the M1 Zhurucay microcatchment.

The meteorological variables P, ETa, Temp, VPD, g_a, g_s and Rn were averaged monthly to show their seasonality. The páramo is a wet tropical ecosystem with low precipitation seasonality; although less wet months were recorded from June to December (P < 100 mm/month). The Budyko plot (ETa/P vs. ETo/P) was therefore used as criterion for dividing wet and dry periods. Usually Budyko plots are applied in an annual timescale; however, given the limited length of the time series in the study, 3-month periods were used (Mar-May, Jun-Aug, Sep-Nov and Dec-Feb). The meteorological variables mentioned were averaged for wet and dry periods. Additionally, a t-test on the daily values of each meteorological variable (except P) was applied to verify if there was a difference between wet and dry periods, at the 0.05 significance level.

Table 5.1. Variables used in this study. Sensors or equations used for each variable. Mean, maximum and minimum daily values for the three-years study period (03/2016 - 02/2019).

Variable	Sensor	Mean	Max	Min	Unit
Precipitation (P)	Laser disdrometer: Thies Clima Laser Precipitation Monitor 5.4110.00.000 V2.4× STD		34.03	0.00	mm/day
r recipitation (r)			34.03	0.00	IIIII/day
Discharge (Q)	V-notch weir	2.01	0.05	26.84	mm/day
Actual evapotranspiration (ETa)	LI-7200 enclosed path infrared gas analyser (IRGA), LI-COR.	1.70	5.24	0.24	mm/day
Sensible heat flux (H)	LI-7200 enclosed path infrared gas analyser (IRGA), LI-COR.	5.02	16.24	-0.72	MJ/m²/day
Net radiation (Rn)	Net radiometer: Kipp & Zonen CNR4 at 3.6m height	8.88	18.48	-0.43	MJ/m²/day
Relative humidity (RH)	Thermometer/Hygrometer: Vaisala HMP155 + Radiation Shield at 3m height	92.52	100.00	11.30	%
Air temperature (Temp)	Thermometer/Hygrometer: Vaisala HMP155 + Radiation Shield at 3m height	6.50	10.14	2.29	°C
Soil volumetric water content (VWC)	Water content reflectometer: Campbell Scientific CS616	0.81	0.99	0.49	cm ³ /cm ³
Pressure (Pa)	Barometer: Vaisala PTB110 at 1m height	64.95	64.95	64.95	kPa
Wind speed (u ₂)	3D Sonic Anemometer: GILL-WM Gill New WindMaster at 3.6m height		8.20	1.50	m/s
Friction velocity (u*)	3D Sonic Anemometer: GILL-WM Gill New WindMaster at 3.6m height	0.42	0.86	0.16	m/s
	Implemented in R version 3.3.2 package plantecophys. (H. Jones, 2013)				
Vapour pressure deficit (VPD)	$(1.0007 + 3.46x10^{-5}Pa) \times 6.1121 \times exp\left(\frac{(18.678 - (Temp/234.5)) \times Temp}{257.14 + Temp}\right) - e_a$ (1)	10.95	93.73	-87.94	hPa
	where, $\epsilon_a = 0.0611 \times RH \times exp\left(\frac{17.27 \times Temp}{Temp + 237.3}\right)$				
Aerodynamic conductance (ga)	$\frac{u_x^2}{u_2}$ (2) Brutsaert (1982)	0.048	0.383	0.014	m/s
	The inverted Penman-Monteith equation was implemented in R version 3.3.2. package bigleaf.				
Surface conductance (g _s)	$\left[\frac{\rho_{\alpha}c_{p}VPD}{\gamma_{LE}} - \frac{1}{\rho_{\alpha}}\left(1 - \frac{\Delta H}{\gamma_{LE}}\right)\right]^{-1} (3)$	0.031	0.430	0.003	m/s
	where, c_p is the specific heat of air at constant pressure (in J/kg/°C), LE and H (in W/m²), γ is the psychometric constant (in hPa/°C) and Δ is the slope of the saturation vapour pressure curve (in hPa/°C).				
Dew temperature (Tdew)	$T_{\text{diew}} = \frac{116.91 + 237.3 \times \ln \left(\frac{p_{\text{st}}}{16.0}\right)}{16.78 - \ln \left(\frac{p_{\text{st}}}{10}\right)} $ (4) (Jensen et al., 1990)	4.87	8.41	-25.29	°C

5.2.3 Controls on evapotranspiration

According to Costa et al. (2010), evapotranspiration in the tropics is influenced by four main variables: net radiation available at the surface (Rn), the vapour pressure deficit between the evaporating surface and the atmosphere (VPD), the conductance of the water vapour flow known as aerodynamic conductance (ga), and surface/stomatal conductance (gs). Rn, VPD and ga are the abiotic environmental controls on ETa, while gs is the biotic control. However, all available variables were considered in this study. In total, the following variables were intended as predictors of ETa: net radiation (in mm/day), relative humidity (in %), temperature (in °C), wind speed (in m/s), vapour pressure deficit (in hPa), precipitation (in mm/day), soil volumetric water content (in cm³/cm³), mean soil volumetric water content (VWC in cm³/cm³), soil volumetric water content at the start of an event (VWC_{ini} in cm³/cm³), aerodynamic conductance (in m/s), surface conductance (in m/s) and dew temperature (in °C). These variables were measured or calculated as detailed in Table 5.1 at an hourly timescale and averaged for each event (see section 5.2.3.1 for the definition of an event). The multiple linear regression (MLR) was implemented on R version 3.3.2, with the following steps:

- 1. The MLR model was calibrated with 80 % of the dataset and the remaining 20 % was used for validation.
- 2. The least number of predictors was chosen with the stepwise method (Venables & Ripley, 2002), in which the initial model does not have any predictor but the constant term. From this, all possible models are generated with one of the available variables. The variable that improves the model is selected. The following variables are included one by one. After each variable is included, an extraction test is made in which a predictor is deleted when it is not useful for the MLR. Each variable was used or discarded with the Akaike (AIC) criterion (Akaike, 1974).
- 3. Predictors were tested for independency with correlation plots and correlation coefficients.
- 4. The linear relationship between ETa and the predictors was confirmed with dispersion plots between the model residuals and each predictor. Residuals should be randomly distributed around zero and they should vary constantly along the x-axis.
- 5. Residuals normal distribution was checked graphically with a q-q plot and statistically with the Shapiro-Wilk test (Royston, 1982).

- 6. Homoscedasticity of the residuals was checked with dispersion plots between the model residuals and the fitted values (estimations) of ETa. Residuals should be randomly distributed around zero and they should vary constantly along the x-axis. Additionally, the studentized Breusch-Pagan test was used to check for homoscedasticity (Breusch & Pagan, 1979).
- 7. The validation set of observations was compared with estimations finding the Pearson's correlation coefficient (r) and the bias percentage (pbias).
- 8. The 10-fold cross validation method was performed to test the MLR in terms of generality, to know if the MLR could be used with a different dataset. The method was implemented by partitioning the total number of ETa events into ten groups. The MLR was then applied ten times and one group was left out for fitting at each iteration. After finding all the fitted values, they were compared with the observed values using the Pearson's correlation coefficient (r). The cross-validation method was implemented through the bootstrap package in R version 3.3.2.

5.2.3.1 Events selection

Event timescale was selected for finding controls on ETa. Daily and even hourly timescale were available for all variables; however, time lag exists between some meteorological variables (Zhang, Manzoni, Katul, Porporato, & Yang, 2014). The closure of the water balance at vegetation scale, therefore, was chosen as a better approach for understanding controls on ETa. For closing the vegetation water balance, an event starts with the first drop of precipitation falling in dry grass leaves and it lasts until the grass is dry again and a new event starts. Thus, the total length of an event is the sum of the following: (1) the duration of the precipitation event, (2) one day that allows the grass leaves to dry and that avoid short events with night-only observations (where ETa is minimal), and (3) the dry hours until another event starts; to include the 3-year available time series. The disdrometer precipitation measurements were used to define the event separation dates.

5.3 Results

5.3.1 Evapotranspiration seasonality

Annual precipitation, evapotranspiration and discharge, measured for the period March 2016 – February 2019 at M1 microcatchment (Figure 1.3) were on average 1267 mm/year, 610 mm/year and 726 mm/year. The annual evapotranspiration ratio (ETa/P) is on average 0.49,

the annual evaporative fraction (ETa/Rn) 0.47, and the annual ratio of actual to potential evapotranspiration (ETa/ETo) 0.99.

Seasonality of actual evapotranspiration and meteorological variables related to the process are plotted in Figure 5.1. All variables exhibited a seasonal variation. Daily temperature decreases slightly with 1.3 $^{\circ}$ C on average from June to September. P, Rn and VPD vary similar to ETa, while g_s varies in the opposite direction to ETa and g_a does not vary as ETa.

Since ETa variability is linked with precipitation, wet and dry periods were divided with the Budyko criterion. The evapotranspiration ratio as a function of the dryness index, plotted in Figure 5.2, shows that most of the 3-month periods lie on the energy limit line. Three periods were and they were chosen as dry periods: September, October and November of the years 2016, 2017 and 2018, labelled in Figure 5.2 as D1, D2 and D3. D1 is limited by water (ETo/P >1) and it might be that water input was not fully measured since ETa/P exceeds 1. Fog and dew might be important components additional to precipitation which cannot be measured by the disdrometer. D2 was chosen also as a dry period since it is apart from other points and very close to ETo/P = 1. D3 is clearly a dry period (ETo/P >1).

P, ETa, Rn, VPD, g_a and g_s were averaged on an annual basis for wet and dry periods, and a t-test was performed to prove if significant differences occur between the mentioned periods at the 5 % significance level (Table 5.2). Precipitation changed during wet periods from 4.5 mm/day to 2 mm/day during dry periods. ETa had a significant increase of 19 % during dry periods in which Rn, VPD and Temp also increased significantly (22 %, 178 % and 8 %); while g_s decreased significantly in 30 %. The only variable that did not change significantly between wet and dry periods was the aerodynamic conductance.

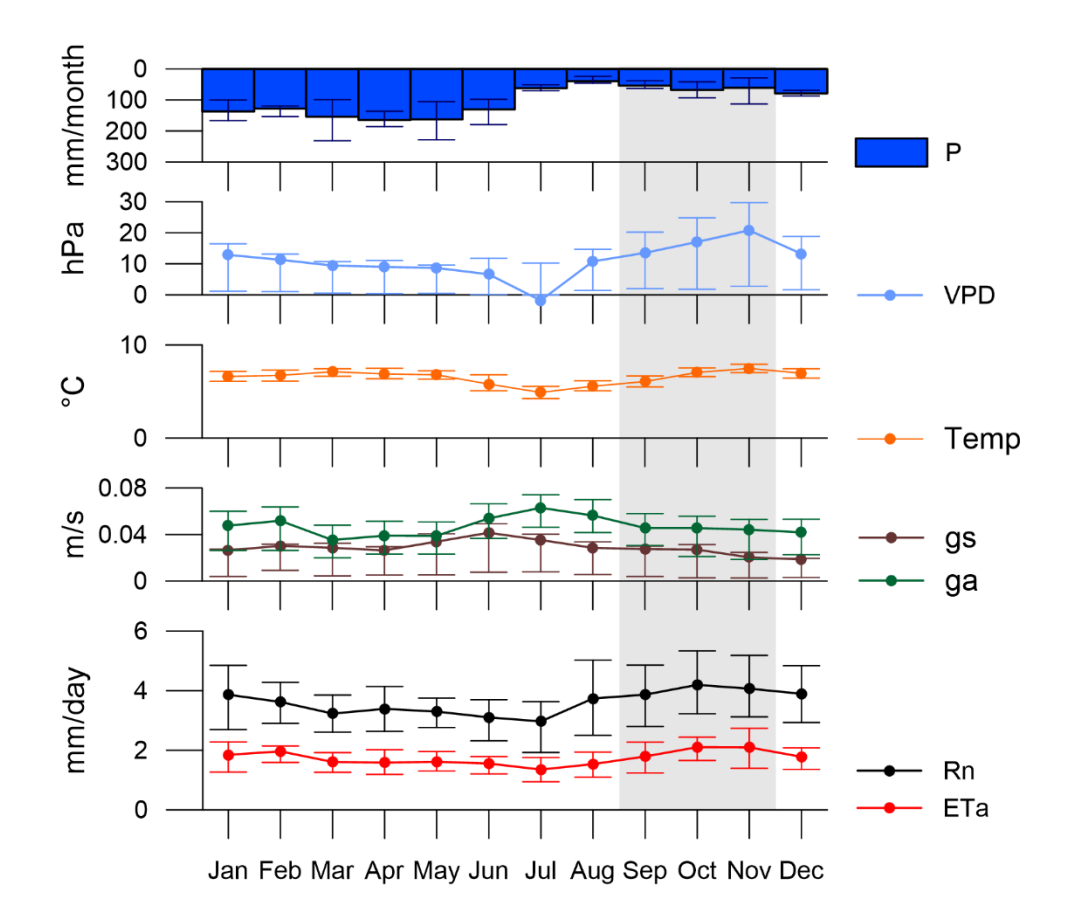


Figure 5.1. Seasonality of the average values of actual evapotranspiration (ETa), precipitation (P), vapour pressure deficit (VPD), temperature (Temp), surface conductance (g_s) , aerodynamic conductance (g_a) and net radiation (Rn). Precipitation bars correspond to the minimum and maximum monthly value. Bars for the remaining variables correspond to the first and the third quartile of the daily values. The grey shadow covers the dry periods of September, October and November according to the Budyko analysis.

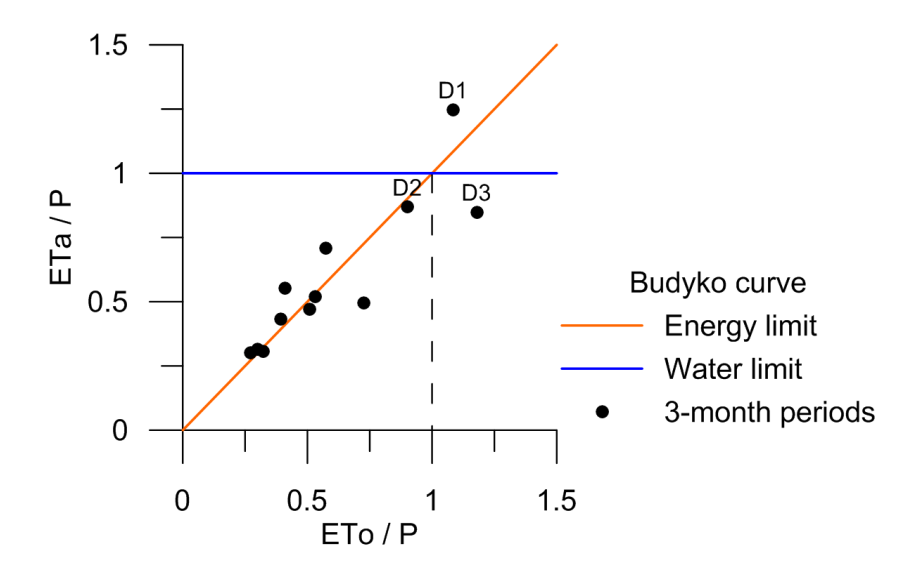


Figure 5.2. Evapotranspiration ratio (ETa/P) as a function of the dryness index (ETo/P) for three-month periods. D1, D2 and D3 correspond to dry periods (09/2016 - 11/2016, 09/2017 - 11/2017) and 09/2018 - 11/2018).

Table 5.2. Annual averages, seasonal averages, and percentage increase during dry months compared to the wet months value of the actual evapotranspiration (ETa) and its main controlling variables: precipitation (P), net radiation (Rn), vapour pressure deficit (VPD), temperature (Temp), surface conductance (g_s) and aerodynamic conductance (g_a). Bold numbers are seasonal daily averages that are significantly different from each other at the 0.05 significance level according to the t-test. Dry periods correspond to the D1, D2 and D3 points in Figure 5.2 (09/2016 – 11/2016, 09/2017 – 11/2017 and 09/2018 – 11/2018).

	P	ETa	Rn	VPD	Temp	\mathbf{g}_{s}	$\mathbf{g}_{\mathbf{a}}$
	(mm/day)	(mm/day)	(mm/day)	(hPa)	°C	(m/s)	(m/s)
Year	3.34	1.70	3.61	10.92	6.50	0.003	0.0041
Wet	4.45	1.66	3.32	6.16	6.39	0.003	0.0036
Dry	2.01	1.97	4.04	17.10	6.87	0.002	0.0041
Increment		19 %	22 %	178 %	8 %	-30 %	15 %

5.3.2 Evapotranspiration controls

We have seen that variables such as P, Rn, VPD, Temp, and gs changed significantly as well as ETa from wet to dry periods. In order to investigate controls of variables on ETa, a multiple linear regression (equation 5) was performed for the 112 events found during the 3-year monitoring period. ETa is expressed in function of net radiation (Rn) in mm/day, wind speed (u₂) in m/s, aerodynamic conductance (g_a) in m/s and surface conductance (g_s) in m/s. Rn explained 53 % of the variance, u₂ explained 16 %, g_a explained 7 % and g_s explained 4 %.

$$ETa = 0.413Rn - 0.192u_2 + 10.599g_a + 6.175g_s + 0.363$$
 (5)

The residual standard error of the MLR was 0.2 mm/day and the coefficient of determination 0.81. The linear relationship between ETa and the predictors was tested and regression residuals were checked for normality and homoscedasticity (Appendix A). Other variables used initially as predictors were dropped for collinearity between them or poor variance explanation (Appendix A). The validation dataset was compared with predicted values of ETa using the MLR in equation 5. The predicted values were highly correlated (r = 0.8) with a small bias (pbias = 5 %). The Pearson's correlation coefficient of the 10 - fold cross validation was 0.88, proving independency of the model from the dataset. ETa observations and estimations for the validation events are shown in Figure 5.3. The 95 % confidence intervals are shown as well for each fitted value.

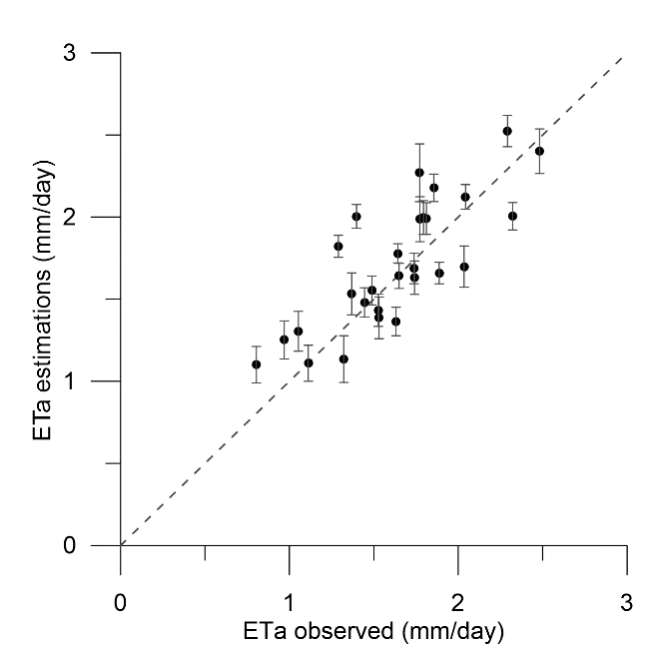


Figure 5.3. Actual evapotranspiration observations and estimations for the validation events. Bars correspond to the 95 % confidence intervals.

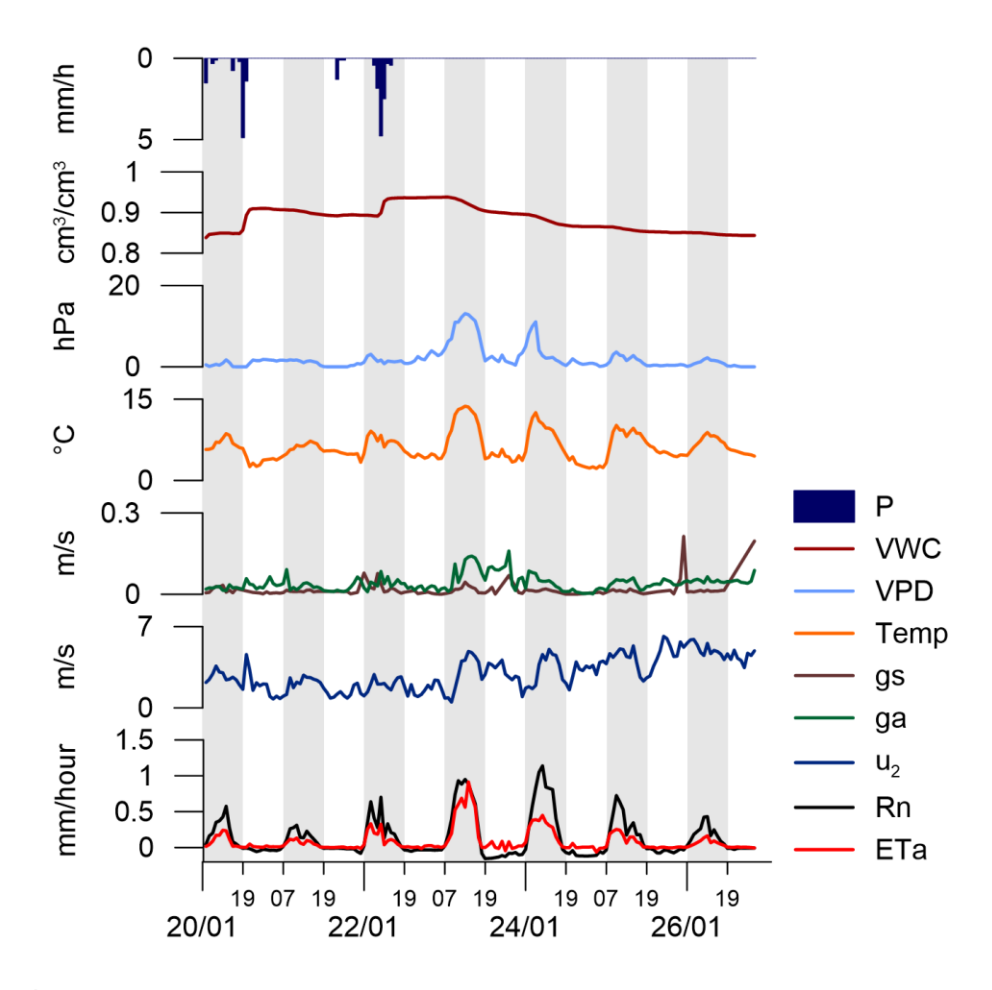


Figure 5.4. Wet event including the following variables: precipitation (P), soil volumetric water content (VWC), vapour pressure deficit (VPD), temperature (Temp), surface conductance (g_s) , aerodynamic conductance (g_a) , wind speed (u_2) , net radiation (Rn) and actual evapotranspiration (ETa). Shadow bars show daylight hours from 7 am to 7 pm.

Evapotranspiration takes place during 12 hours at daylight from around 7 a.m. to 7 p.m. (Figure 5.4). The event showed in Figure 5.4, corresponds to a common event in which the main controlling variable, Rn, has the same variability as ETa. Also, VPD and Temp vary similar to ETa. Right after rain stops, ETa is higher due to a higher evaporation of the intercepted water (water is not reaching the soil, see the VWC signal in Figure 5.4). After that, ETa values correspond mainly to transpiration (VWC signal decreases only during daytime), and ETa variation is again similar to the variation of Rn, VPD and Temp.

5.4 Discussion

The annual water budget (P-ETa-Q) closes in -69 mm, meaning that precipitation was underestimated with at least 69 mm, assuming that other variables are negligible at this site and that ETa from the supersite represents ETa at the M1 microcatchment. These assumptions are plausible since groundwater contribution to discharge are minimal (Mosquera et al., 2016) and M1 vegetation, soil and climate are very similar to the supersite.

The relatively low ETa, in combination with almost no zero-precipitation days (Padrón et al., 2015) and the high soil water retention capacity play an important role in the high water storage of the páramo environment.

Controls and quantification of ETa components are important for process understanding and for improving local, regional and global ETa modelling. We identified the main controllers on ETa at a paramo representative site and quantified transpiration during dry periods. In the following paragraphs, we contrast our findings to similar sites and provide insights on the ETa and T processes.

The Budyko framework applied to this study showed that the wet paramo is mainly controlled by energy and not by water (annual ETa/ETo ratio was on average 0.99). The continuous rainfall at the study site and the soil water retention capacity allow high soil moisture values (mean = 0.81, Figure 5.1) which rarely drop to field capacity (VWC = 0.7) and never drop to wilting point (VWC = 0.45). Every year, only the months of September, October and November had a higher dryness index, although the evaporative fraction remained constant. One of those periods was above the water limit in Figure 5.2, plausible because all precipitation was not measured (e.g. fog and dew) or because water storage contribution is important and the 3-month period used is not long enough to take this into account. On the other hand, two points showed ETa values higher than ETo (points above the energy line in Figure 5.2). Other energy-limited regions have shown an increasing gap between ETo and ETa, suggesting the influence of additional variables controlling ETa (Anabalón & Sharma, 2017). The variation of the evaporative index is controlled by the available energy, while climate and vegetation type act as additional controls (Williams et al., 2012). Given that the two points correspond to the periods between June and August 2016 and 2017, in which ga increases (Figure 5.1), this variable might be controlling ETa over those periods as well as u_2 that has the same seasonality as g_a .

The main controllers on ETa for this energy-limited site are in accordance with other studies that have analysed controls on ETa at the Tropics. We found that Rn is the main controller on ETa, followed by u₂, g_a and g_s and an annual evaporative fraction (ETa/Rn) of 0.47. The evaporative fraction remained valid for wet and dry periods. It is expected that Rn controls ETa in wet environments in the tropics; however, the evaporative fraction and consistency between wet and dry periods vary among sites (Hasler & Avissar, 2007). Fisher et al. (2009) studied evapotranspiration in the tropics, finding Rn as the main controller and a higher

evaporative fraction of 0.72. Rn explained 87 % of the monthly ETa variance in the Amazonian sites, VPD explained 14 %, the normalized difference vegetation index (NDVI) 9 % and wind speed 4 %. However, VPD and NDVI were more important for less wet tropical sites. Also, Wieser et al. (2008) found Rn, photosynthetically active radiation (PAR) and VPD as linear controllers on ETa in an energy-limited site at the Austrian Alps. The secondary controls on ETa at our study site were u2, ga and gs. The first two are atmospheric controls, and the only biotic control on ETa is g_s. We found that g_s had a significant 30 % drop in the dry season which is typical for tropical sites (Costa et al., 2010). Further work on leaf phenology effects on ETa are needed to understand better the control on ETa by vegetation. The significant seasonal variability of ETa, Rn, VPD, and g_s but not significant for ga was also found for other equatorial sites (Costa et al., 2010). Another interesting finding, related to the MLR predictors, is that although VPD varies similar to ETa, it does not inhibit evapotranspiration at least for the range of VPD values seen in this study (Figure 5.1). Many events in which ETa values were equal or higher than the mean, VPD values were lower than the mean. VPD and Temp vary similar to ETa on an event scale, as shown in Figure 5.4. In fact, VPD is collinear to Rn but explains less variance than Rn, only 1 % (Appendix A). Knowing that VPD is a function of relative humidity (RH) and Temp, the plausible explanation for the absence of VPD in the controllers on ETa could be the following. In short canopies, such as tussock grasslands, the air adjacent to the leaves is not well mixed with the air above the canopy (decoupling conditions between the vegetation and the atmosphere); and therefore, ETa is more controlled by Rn than by RH (Chapin, Matson, & Vitousek, 2011). In addition, Temp did not pass the stepwise variables selection (Appendix A). VPD and Temp are therefore, controlled by Rn, but have minimal control over ETa.

5.5 Conclusions

Our study on the controls on evapotranspiration and transpiration at high Andean grasslands led to the following conclusions: (1) the site is energy-limited and driven mainly by net radiation (annual ETa/Rn was on average 0.47), leaving wind speed, surface conductance and aerodynamic conductance (biotic control) as secondary controls, and (2) ETa increased significantly during dry periods in 19 % (between September and November) and although Rn remained the main controller, the secondary controls appeared especially important during these periods.

EC measurements provide point-source information of tussock grasslands. Although tussock grasslands cover around 80 % of the páramo, ETa has not been measured on cushion plants, polylepis and pine forests. Their contribution to ETa needs further assessment, since regional estimates on ETa would enlighten the water consumption at this very important region for water resources. Additionally, quantification of fog and dew is needed at the páramo to better close the water balance and improve explanation of the evapotranspiration process.

Conclusions

6.1 Synthesis

This dissertation unveiled the evapotranspiration process of the Andean páramo grassland through the quantification of its components, the analysis of measurement and estimation methods and the assessment of its controls. It is the first time that interception and transpiration were quantified, clarifying questions that emerged with the first studies of this important biome, back in the nineties. Methods for the measurement and estimation of evapotranspiration were analysed and their accuracy and possibilities for implementation assessed. Ultimately the controls on evapotranspiration were discussed.

The components of evapotranspiration of páramo grassland were mainly evaporation from intercepted water and transpiration. Bare soil conditions were not present at the study area thus soil evaporation was negligible. Canopy interception reached 100 to 80 % of the total precipitation on small events (P < 2 mm) and it decreased up to 10 % during large events (P > 2 mm). The canopy storage capacity of tussock grasslands (i.e. the maximum amount of water that vegetation at the páramo was able to retain) was 2 mm. Although low cumulative precipitation, low intensity, and long duration favoured interception loss, no clear relationships with meteorological variables were found. For all the events, only cumulative precipitation was found to be important. However, a multiple linear regression equation (R^2 = 0.9) was identified to estimate interception loss in function of cumulative precipitation per event and relative humidity, which is valid for events when 1.7 < P < 8.5 mm. Transpiration measurements were on average 1.5 mm/day (range from 0.7 to 2.7 mm/day). During dry periods, only transpiration was expected to occur. However, due to the humid climate at the high Andean mountain range, some days without rain the páramo grassland still captures dew and/or fog, which during daytime evaporates. The combination of evaporation due to interception during wet and dry periods represents a high contribution to the evapotranspiration process.

The most accurate method to measure evapotranspiration, with the finest temporal resolution, was the eddy-covariance method. However, besides its high cost, its implementation, operation, maintenance and further data processing are complex. Hydrological models, such

Conclusions

as the PDM and HBV-light, proved to be robust for estimating evapotranspiration during wet and dry periods. Furthermore, these methods can properly assess the hydrology of the site, are freely available, require only few data as input and are easy to implement. Also, the Penman-Monteith equation was calibrated and their estimates were highly accurate on a daily scale. For monthly timescales, the volumetric lysimeters implemented in this study are an affordable alternative technique that still gives a complete understanding of the water exchange between the vegetation and the atmosphere. It is important to note that although the water balance has been used as a reference method for estimating evapotranspiration (e.g. to which remote sensing products have been compared to), this study revealed that it is not a suitable method at daily timescale (r = -0.41 and pbias = 10%) unless accurate daily estimations or measurements of the soil water storage are provided.

Hydrological models were accurate since at the páramo the most important components of the water cycle were precipitation, discharge and evapotranspiration. Additional processes such as groundwater recharge or percolation are, therefore, minimal or non-existent. The relatively low evapotranspiration found in this study (annual ETa/P = 0.5) is in accordance with an energy-limited site where enough water is available for evapotranspiration. Therefore, net radiation is the primary control on evapotranspiration (annual ETa/Rn = 0.47). During dry periods, evapotranspiration increased significantly in about 20%. In that case, secondary controls (wind speed, surface conductance and aerodynamic conductance) were found important.

Finally, this study highlighted the importance of understanding the components of the hydrological cycle in order to better assess the functioning of the páramo ecosystem, which knowledge has increased in the past decade, but that still needs further attention, given its importance to water resources and upcoming challenges such as land use and climate change.

6.2 Future research

Ecohydrology has been a relatively recent subject of study. At the páramo, the comprehension of the water, vegetation and soil interactions still need further analysis. In this section some future studies are highlighted for which the present research opened the path.

• Evapotranspiration partitioning

Since interception loss was found to be a major component of evapotranspiration at the páramo, ETa is not a good indicator of the productive use of water through plant uptake or soil evaporation. A separate assessment of evaporation and transpiration is, therefore, necessary. In this study, an effort was made towards evapotranspiration partitioning; however, due to the available data, only the event-scale approach was possible. Mathematical models or lysimeters measurements could be used for daily evapotranspiration partitioning. Better yet, stable isotope techniques could enlighten on the hypothesis that soil water used by plants remains separated from water rapidly passing through soils (Good et al., 2015).

• Fog and dew measurements

It was noted in this study, that precipitation measured with appropriate sensors, such as disdrometers, are needed to capture light precipitation and drizzle very common at the páramo. In fact, it was proved that interception was only accurately measured when disdrometer observations were used. However, the quantification of dew and fog need further assessment in this environment where those processes are common as well. Interception of dew and fog by vegetation are part of the evaporation and they could also contribute to soil moisture. Thus, their assessment is key for further hydrological process understanding and modelling. In addition, they might become important water sources, especially during dry periods.

• Improvement of evapotranspiration estimates

Regarding the methods for estimating evapotranspiration, the water balance, lysimeters and energy balance evidence was given that these methods are not suitable at daily scale. However, they could be applied in the future considering the following. The measurement of the change in soil water storage should be improved in order to apply the water balance method. Lysimeters could be improved by converting them into weighing lysimeters;

Conclusions

therefore, increasing their accuracy. The energy balance could be used by improving the estimation of the sensible heat flux, through a different mathematical method or with the application of the Bowen ratio method.

• Evapotranspiration from other vegetation types

An important limitation of this study is the point-measurement approach due to lack of data. Eddy-covariance measurements represented evapotranspiration at tussock grasslands. Although that vegetation type covers more than 80 % of páramo sites, evapotranspiration has not been measured on cushion plants, polylepis and pine forests. Their contribution to evapotranspiration need further assessment, since regional estimates on ETa would enlighten the water consumption at this very important region for water resources.

• Improvements on hydrological and climate models

We have seen in this study that the páramo is an energy-limited environment rather than a water-limited one. However, temperature increase and changes in duration and intensity of precipitation (predicted by climate change scenarios) will lead to changes in the evapotranspiration between wet and dry periods. The assessment of the impact of these changes at the páramo need to be addressed since dry periods might shift this environment to a water-limited one. This might have severe implications on the soil that is key to hydrological regulation (water storage and yield). However, the complex orography of the páramo requires fine spatial resolution from regional climate models. In view of the higher computational capabilities available today, the few studies on climate change predictions at the páramo need to be updated. Analogously, this study laid the groundwork for hydrological models that need to estimate accurately evapotranspiration and its components. Improved climate and hydrological models will unveil the impacts of climate change, the vulnerability of the páramo and will lead towards climate action.

References

- Agam, N., Evett, S. R., Tolk, J. A., Kustas, W. P., Colaizzi, P. D., Alfieri, J. G., ... Chávez, J. L. (2012). Evaporative loss from irrigated interrows in a highly advective semi-arid agricultural area. *Advances in Water Resources*, *50*, 20–30. https://doi.org/10.1016/j.advwatres.2012.07.010
- Akaike, H. (1974). A new look at the statistical model identification. *IEEE Transactions on Automatic Control*, 19(6), 716–723. https://doi.org/10.1109/TAC.1974.1100705
- Allen, R. G., Clemmens, A. J., Burt, C. M., Solomon, K., & O'Halloran, T. (2005). Prediction Accuracy for Projectwide Evapotranspiration Using Crop Coefficients and Reference Evapotranspiration. *Journal of Irrigation and Drainage Engineering*, 131(1), 24–36. https://doi.org/10.1061/(ASCE)0733-9437(2005)131:1(24)
- Anabalón, A., & Sharma, A. (2017). On the divergence of potential and actual evapotranspiration trends: An assessment across alternate global datasets. *Earth's Future*, *5*(9), 905–917. https://doi.org/10.1002/2016EF000499
- Aparecido, L. M. T., Teodoro, G. S., Mosquera, G., Brum, M., Barros, F. de V., Pompeu, P. V., ... Oliveira, R. S. (2018). Ecohydrological drivers of Neotropical vegetation in montane ecosystems. *Ecohydrology*, *11*(3), e1932. https://doi.org/10.1002/eco.1932
- Ataroff, M., & Naranjo, M. E. (2009). Interception of water by pastures of Pennisetum clandestinum Hochst. ex Chiov. and Melinis minutiflora Beauv. *Agricultural and Forest Meteorology*, 149(10), 1616–1620. https://doi.org/10.1016/j.agrformet.2009.05.003
- Baldocchi, D. D. (2003). Assessing the eddy covariance technique for evaluating carbon dioxide exchange rates of ecosystems: past, present and future. *Global Change Biology*, *9*(4), 479–492. https://doi.org/10.1046/j.1365-2486.2003.00629.x
- Baloutsos, G., Baltas, E., & Bourletsikas, A. (2009). Development of a simplified model for the estimation of hydrological components in areas of maquis vegetation in Greece. WSEAS Transactions on Environment and Development. https://doi.org/refwid:33939
- Beard, J. S. (1956). Results of the mountain home rainfall interception and infiltration project in Black Wattle. *Journal of the South African Forestry Association*, *27*(1), 72–86. https://doi.org/10.1080/03759873.1956.9630785
- Beniston, M. (2003). Climate change in mountain regions: a review of possible impacts. *Climatic Change*, *59*, 5–31.
- Bergström, S. (1976). Development and Application of a Conceptual Runoff Model for Scandinavian Catchments. In *SMHI*. Norrköping.
- Beven, K. J. (2001). Rainfall-runoff modelling: the primer (1st ed.). John Wiley and

- sons, Chichester.
- Boll, J., Steenhuis, T. S., & Selker, J. S. (1992). Fiberglass wicks for sampling of water and solutes in the vadose zone. *Soil Science Society of America Journal*, 56(3), 701–707. https://doi.org/10.2136/sssaj1992.03615995005600030005x
- Bowden, W. B., Fahey, B. D., Ekanayake, J., & Murray, D. L. (2001). Hillslope and wetland hydrodynamics in a tussock grassland, South Island, New Zealand. *Hydrological Processes*, *15*(10), 1707–1730. https://doi.org/10.1002/hyp.235
- Braud, I., Fernandez, P., & Bouraoui, F. (1999). Study of the rainfall-runoff process in the Andes region using a continuous distributed model. *Journal of Hydrology*. Retrieved from http://www.sciencedirect.com/science/article/pii/S0022169498002923
- Breiman, L., & Leo. (2001). Random Forests. *Machine Learning*, *45*(1), 5–32. https://doi.org/10.1023/A:1010933404324
- Breusch, T. S., & Pagan, A. R. (1979). A Simple Test for Heteroscedasticity and Random Coefficient Variation. *Econometrica*, 47(5), 1287. https://doi.org/10.2307/1911963
- Bruijnzeel, L. A. (Sampurno). (2000). Forest Hydrology. In *The Forests Handbook, Volume 1* (pp. 301–343). https://doi.org/10.1002/9780470757062.ch12
- Brutsaert, W. (1982). *Evaporation into the Atmosphere* (1st ed). https://doi.org/10.1038/scientificamerican12121863-370
- Brye, K. R., Norman, J. M., Bundy, L. G., & Gower, S. T. (2000). Water-Budget Evaluation of Prairie and Maize Ecosystems. *Soil Science Society of America Journal*, 64(2), 715. https://doi.org/10.2136/sssaj2000.642715x
- Buytaert, W., Célleri, R., De Bièvre, B., Cisneros, F., Wyseure, G., Deckers, J., & Hofstede, R. (2006). Human impact on the hydrology of the Andean páramos. *Earth-Science Reviews*, 79(1–2), 53–72. https://doi.org/10.1016/j.earscirev.2006.06.002
- Buytaert, W., Cuesta-Camacho, F., & Tobon, C. (2011). Potential impacts of climate change on the environmental services of humid tropical alpine regions. *Global Ecology and Biogeography*, 20, 19–33. https://doi.org/10.1111/j.1466-8238.2010.00585.x
- Buytaert, W., De Bièvre, B., Wyseure, G., & Deckers, J. (2005). The effect of land use changes on the hydrological behaviour of Histic Andosols in south Ecuador. *Hydrological Processes*, *19*, 3985–3997.
- Buytaert, W., Deckers, J., Dercon, G., De Bièvre, B., Poesen, J., & Govers, G. (2002). Impact of land use changes on the hydrological properties of volcanic ash soils in South Ecuador. *Soil Use and Management*, *18*, 94–100.
- Buytaert, W., Iñiguez, V., Célleri, R., De Bièvre, B., Wyseure, G., & Deckers, J. (2006). Analysis of the water balance of small páramo catchments in south Ecuador. In *Environmental role of wetlands in headwaters* (pp. 271–281). https://doi.org/10.1007/1-4020-4228-0_24
- Cabral, O. M. R., da Rocha, H. R., Gash, J. H., Freitas, H. C., & Ligo, M. A. V.

- (2015). Water and energy fluxes from a woodland savanna (cerrado) in southeast Brazil. *Journal of Hydrology: Regional Studies*, *4*, 22–40. https://doi.org/10.1016/j.ejrh.2015.04.010
- Cabral, O. M. R., Rocha, H. R., Gash, J. H. C., Ligo, M. A. V., Freitas, H. C., & Tatsch, J. D. (2010). The energy and water balance of a Eucalyptus plantation in southeast Brazil. *Journal of Hydrology*, 338(3–4), 208–216. https://doi.org/10.1016/j.jhydrol.2010.04.041
- Campbell, D. I., & Murray, D. L. (1990). Water balance of snow tussock grassland in New Zealand. *Journal of Hydrology*, *118*(1–4), 229–245. https://doi.org/10.1016/0022-1694(90)90260-5
- Campbell Scientific, I. (2012). CS616 and CS625Water Content Reflectometers. Instruction Manual.
- Carrillo-Rojas, G., Silva, B., Córdova, M., Célleri, R., & Bendix, J. (2016). Dynamic mapping of evapotranspiration using an energy balance-based model over an andean páramo catchment of southern ecuador. *Remote Sensing*, 8(2), 160. https://doi.org/10.3390/rs8020160
- Carrillo-Rojas, G., Silva, B., Rollenbeck, R., Célleri, R., & Bendix, J. (2019). The breathing of the Andean highlands: Net ecosystem exchange and evapotranspiration over the paramo of southern Ecuador. *Agricultural and Forest Meteorology*, 265, 30–47. https://doi.org/10.1016/j.agrformet.2018.11.006
- Chapin, F. S., Matson, P. A., & Vitousek, P. M. (2011). Principles of Terrestrial Ecosystem Ecology. In *Principles of Terrestrial Ecosystem Ecology*. https://doi.org/10.1007/978-1-4419-9504-9
- Chen, Y.-Y., & Li, M.-H. (2016). Quantifying Rainfall Interception Loss of a Subtropical Broadleaved Forest in Central Taiwan. *Water*, 8(1), 14. https://doi.org/10.3390/w8010014
- Clark, K., Torres, M., West, A., Hilton, R., New, M., Horwath, A., ... Malhi, Y. (2014). The hydrological regime of a forested tropical Andean catchment. *Hydrology and Earth System Sciences*, *18*, 5377–5397. https://doi.org/10.5194/hess-18-5377-2014
- Clark, O. (1940, February 1). Interception of Rainfall by Prairie Grasses, Weeds, and Certain Crop Plants on JSTOR. https://doi.org/10.2307/1948607
- Coners, H., Babel, W., Willinghöfer, S., Biermann, T., Köhler, L., Seeber, E., ... Leuschner, C. (2016). Evapotranspiration and water balance of high-elevation grassland on the Tibetan Plateau. *Journal of Hydrology*, *533*, 557–566. https://doi.org/10.1016/j.jhydrol.2015.12.021
- Córdova, M., Carrillo-Rojas, G., & Célleri, R. (2013). Errores en La Estimación De La Evapotranspiración De Referencia De Una Zona De Páramo Andino Debidos Al Uso De Datos Mensuales, Diarios Y Horarios. *Aqua-LAC*, *5*(2), 14–22. https://doi.org/10.12776/amsc.v3.110
- Córdova, M., Carrillo-Rojas, G., Crespo, P., Wilcox, B., & Célleri, R. (2015). Evaluation of the Penman-Monteith (FAO 56 PM) Method for Calculating Reference Evapotranspiration Using Limited Data. *Mountain Research and*

- Development, 35(3), 230–239. https://doi.org/10.1659/MRD-JOURNAL-D-14-0024.1
- Correa, A., Windhorst, D., Crespo, P., Célleri, R., Feyen, J., & Breuer, L. (2016). Continuous versus event-based sampling: how many samples are required for deriving general hydrological understanding on Ecuador's páramo region? *Hydrological Processes*, *30*(22), 4059–4073. https://doi.org/10.1002/hyp.10975
- Correa, A., Windhorst, D., Tetzlaff, D., Crespo, P., Célleri, R., Feyen, J., & Breuer, L. (2017). Temporal dynamics in dominant runoff sources and flow paths in the Andean Páramo. *Water Resources Research*, *53*(7), 5998–6017. https://doi.org/10.1002/2016WR020187
- Costa, M. H., Biajoli, M. C., Sanches, L., Malhado, A. C. M., Hutyra, L. R., da Rocha, H. R., ... de Araújo, A. C. (2010). Atmospheric versus vegetation controls of Amazonian tropical rain forest evapotranspiration: Are the wet and seasonally dry rain forests any different? *Journal of Geophysical Research*, 115(G4), G04021. https://doi.org/10.1029/2009JG001179
- Cramer, R. D., Bunce, J. D., Patterson, D. E., & Frank, I. E. (1988). Crossvalidation, Bootstrapping, and Partial Least Squares Compared with Multiple Regression in Conventional QSAR Studies. *Quantitative Structure-Activity Relationships*, 7(1), 18–25. https://doi.org/10.1002/qsar.19880070105
- Crespo, P., Feyen, J., Buytaert, W., Bücker, A., Breuer, L., Frede, H., & Ramírez, M. (2011). Identifying controls of the rainfall–runoff response of small catchments in the tropical Andes (Ecuador). *Journal of Hydrology*, *407*(1), 164–174. https://doi.org/10.1016/j.jhydrol.2011.07.021
- Criss, R. E., & Winston, W. E. (2008). Do Nash values have value? Discussion and alternate proposals. *Hydrological Processes*, 22(14), 2723–2725. https://doi.org/10.1002/hyp.7072
- Crouse, R. P., Corbett, E. S., & Seegrist, D. W. (1966). Methods of measuring and analyzing rainfall interception by grass. *International Association of Scientific Hydrology.* Bulletin, 11(2), 110–120. https://doi.org/10.1080/02626666609493463
- De'ath, G., & Fabricius, K. (2000). Classification and regression trees: A powerful yet simple technique for ecological data analysis. *Ecology*, *81*(11). Retrieved from http://doi.wiley.com/10.1890/0012-9658(2000)081[3178:CARTAP]2.0.CO;2
- Domingo, F., Sánchez, G., Moro, M. J., Brenner, A. J., & Puigdefábregas, J. (1998). Measurement and modelling of rainfall interception by three semi-arid canopies. *Agricultural and Forest Meteorology*, 91(3), 275–292. https://doi.org/10.1016/S0168-1923(98)00068-9
- Falge, E., Baldocchi, D., Olson, R., Anthoni, P., Aubinet, M., Bernhofer, C., ... Wofsy, S. (2001). Gap filling strategies for defensible annual sums of net ecosystem exchange. *Agricultural and Forest Meteorology*, *107*(1), 43–69. https://doi.org/10.1016/S0168-1923(00)00225-2
- Fan, C., Li, C., Jia, K., Sun, B., Shi, X., & Gao, H. (2015). Grass canopy interception of Hulun watershed under different grazing systems. *Acta Ecologica Sinica*, 35(14), 4716–4724. Retrieved from

- http://jglobal.jst.go.jp/en/public/20090422/201602217037735104
- FAO/ISRIC/ISSS. (1998). World Reference Base for Soil Resources. Rome: FAO.
- Fisher, J. B., Malhi, Y., Bonal, D., Da Rocha, H. R., De Araújo, A. C., Gamo, M., ... Von Randow, C. (2009). The land-atmosphere water flux in the tropics. *Global Change Biology*, 15, 2694–2714. https://doi.org/10.1111/j.1365-2486.2008.01813.x
- Fisher, J. B., Melton, F., Middleton, E., Hain, C., Anderson, M., Allen, R., ... Wood, E. F. (2017). The future of evapotranspiration: Global requirements for ecosystem functioning, carbon and climate feedbacks, agricultural management, and water resources. *Water Resources Research*, *53*, 2618–2626. https://doi.org/10.1002/2016WR020175
- Foley, J. A., Ramankutty, N., Brauman, K. A., Cassidy, E. S., Gerber, J. S., Johnston, M., ... Zaks, D. P. M. (2011). Solutions for a cultivated planet. *Nature*, 478(337). https://doi.org/10.1038/nature10452
- Foster, P. (2001). The potential negative impacts of global climate change on tropical montane cloud forests. *Earth-Science Reviews*, *55*, 73–106.
- Frasson, R. P. de M., da Cunha, L. K., & Krajewski, W. F. (2011). Assessment of the Thies optical disdrometer performance. *Atmospheric Research*, 101(1), 237–255. https://doi.org/10.1016/j.atmosres.2011.02.014
- Fritschen, L. J., & Simpson, J. R. (1989). Surface Energy and Radiation Balance Systems: General Description and Improvements. *Journal of Applied Meteorology and Climatology*, 28, 680–689.
- Gash, J. (1979). An analytical model of rainfall interception by forests. *Royal Meteorological Society, Quarterly Journal*, 105, 43–75. Retrieved from http://iss.iae.kyoto-u.ac.jp/iss/eng/lecture/sidle_2007/lect4/GashInterceptionModel.pdf
- Gebler, S., Hendricks Franssen, H. J., Pütz, T., Post, H., Schmidt, M., & Vereecken, H. (2015). Actual evapotranspiration and precipitation measured by lysimeters: A comparison with eddy covariance and tipping bucket. *Hydrology and Earth System Sciences*, *19*, 2145–2161. https://doi.org/10.5194/hess-19-2145-2015
- Genxu, W., Guangsheng, L., & Chunjie, L. (2012). Effects of changes in alpine grassland vegetation cover on hillslope hydrological processes in a permafrost watershed. *Journal of Hydrology*, *444*(445), 22–33. Retrieved from http://agris.fao.org/agris-search/search.do?recordID=US201400181649
- Good, S. P., Noone, D., & Bowen, G. (2015). Hydrologic connectivity constrains partitioning of global terrestrial water fluxes. *Science*, *349*(6244), 175–177. https://doi.org/10.1126/science.aaa5931
- Gu, S., Tang, Y., Cui, X., Du, M., Zhao, L., Li, Y., ... Zhao, X. (2008). Characterizing evapotranspiration over a meadow ecosystem on the Qinghai-Tibetan Plateau. *Journal of Geophysical Research Atmospheres*, 113(D08118). https://doi.org/10.1029/2007JD009173
- Harden, C. (2001). Soil erosion and sustainable mountain development. *Mountain Research and Development*, 21(1), 77–83. https://doi.org/10.1659/0276-

- 4741(2001)021[0077:SEASMD]2.0.CO;2
- Harden, C., & Scruggs, P. (2003). Infiltration on mountain slopes: a comparison of three environments. *Geomorphology*. Retrieved from http://www.sciencedirect.com/science/article/pii/S0169555X03001296
- Hasler, N., & Avissar, R. (2007). What Controls Evapotranspiration in the Amazon Basin? *Journal of Hydrometeorology*, *8*(3), 380–395. https://doi.org/10.1175/JHM587.1
- Hastie, T., Tibshirani, R., & Friedman, J. (2010). The Elements of Statistical Learning: Data Mining, Inference, and Prediction. In *Springer Series in Statistics* (Vol. 173). https://doi.org/10.1111/j.1467-985X.2010.00646_6.x
- Hofstede, R., Calles, J., López, V., Polanco, R., Torres, F., Ulloa, J., ... Cerra, M. (2014). Los páramos Andinos ¿Qué Sabemos? Estado de conocimiento sobre el impacto del cambio climático en el ecosistema páramo. In *UICN* (IUCN). Quito, Ecuador.
- Hofstede, R., Segarra, P., & Mena, P. (2003). Los Páramos del Mundo. Quito: Global Peatland Initiative/NC-IUCN/EcoCiencia, Quito.
- Holdsworth, D. K., & Mark, A. F. (1990). Water and nutrient input:output budgets: effects of plant cover at seven sites in upland snow tussock grasslands of eastern and central Otago, New Zealand. *Journal Royal Society of New Zealand*, 20(1), 1–24. https://doi.org/10.1080/03036758.1990.10426730
- Hsieh, C.-I., Lai, M.-C., Hsia, Y.-J., & Chang, T.-J. (2008). Estimation of sensible heat, water vapor, and CO2 fluxes using the flux-variance method. *International Journal of Biometeorology*, *52*(6), 521–533. https://doi.org/10.1007/s00484-008-0149-4
- Iniguez, V., Morales, O., Cisneros, F., Bauwens, W., & Wyseure, G. (2016). Analysis of the drought recovery of Andosols on southern Ecuadorian Andean paramos. HYDROLOGY AND EARTH SYSTEM SCIENCES, 20(6), 2421–2435. https://doi.org/10.5194/hess-20-2421-2016
- Jensen, M. E., Burmann, R. D., & Allen, R. G. (1990). Evaporation and irrigation water requirements. In *ASCE manual and reports on engineering practice*.
- Jones, H. (2013). Plants and Microclimate. In *Plants and Microclimate: A Quantitative Approach to Environmental Plant Physiology*. https://doi.org/10.1017/CBO9780511845727
- Jones, & Hulme. (1996). Calculating regional climatic time series for temperature and precipitation: methods and illustrations. *International Journal of Climatology*, 16(4), 361–377. https://doi.org/10.1002/(SICI)1097-0088(199604)16:4<361::AID-JOC53>3.0.CO;2-F
- Jones, J. (1987). The effects of soil piping on contributing areas and erosion patterns. *Earth Surface Processes and Landforms*, *12*(3), 229–248. https://doi.org/10.1002/esp.3290120303
- Jones, J., & Connelly, L. (2002). A semi-distributed simulation model for natural pipeflow. *Journal of Hydrology*, 262(1), 28–49. https://doi.org/10.1016/S0022-1694(02)00018-5

- Katul, G., Goltz, S. M., Hsieh, C. I., Cheng, Y., Mowry, F., & Sigmon, J. (1995). Estimation of surface heat and momentum fluxes using the flux-variance method above uniform and non-uniform terrain. *Boundary-Layer Meteorology*, *74*(3), 237–260. https://doi.org/10.1007/BF00712120
- Khan, B. R., Mainuddin, M., & Molla, M. N. (1993). Design, construction and testing of a lysimeter for a study of evapotranspiration of different crops. *Agricultural Water Management*, 23(3), 183–197. https://doi.org/10.1016/0378-3774(93)90027-8
- Klaassen, W., Bosveld, F., & de Water, E. (1998). Water storage and evaporation as constituents of rainfall interception. *Journal of Hydrology*, *212–213*, 36–50. https://doi.org/10.1016/S0022-1694(98)00200-5
- Kljun, N., Calanca, P., Rotach, M. W., & Schmid, H. P. (2015). A simple two-dimensional parameterisation for Flux Footprint Prediction (FFP). Geoscientific Model Development, 8(11), 3695–3713. https://doi.org/10.5194/gmd-8-3695-2015
- Knowles, J. F., Burns, S. P., Blanken, P. D., & Monson, R. K. (2015). Fluxes of energy, water, and carbon dioxide from mountain ecosystems at Niwot Ridge, Colorado. *Plant Ecology & Diversity*, 8(5–6), 663–676. https://doi.org/10.1080/17550874.2014.904950
- Koichiro, K., Yuri, T., Nobuaki, T., & Isamu, K. (2001). Generation of stemflow volume and chemistry in a mature Japanese cypress forest. *Hydrological Processes*, *15*(10), 1967–1978. https://doi.org/10.1002/hyp.250
- Kool, D., Agam, N., Lazarovitch, N., Heitman, J. L., Sauer, T. J., & Ben-Gal, A. (2014). A review of approaches for evapotranspiration partitioning. *Agricultural and Forest Meteorology*, 184, 56–70. https://doi.org/10.1016/j.agrformet.2013.09.003
- Krstajic, D., Buturovic, L. J., Leahy, D. E., & Thomas, S. (2014). Cross-validation pitfalls when selecting and assessing regression and classification models. *Journal of Cheminformatics*, *6*(1), 10. https://doi.org/10.1186/1758-2946-6-10
- Lanzinger, E., Theel, M., & Windolph, H. (2006). Rainfall Amount and Intensity measured by the Thies Laser Precipitation Monitor. *TECO-2006 WMO Technical Conference on Meteorological and Environmental Instruments and Methods of Observation*, 9. Retrieved from https://www.wmo.int/pages/prog/www/IMOP/publications/IOM-94-%0ATECO200 6/3%283%29_Lanzinger_Germany.pdf
- Lawrence, D. M., Thornton, P. E., Oleson, K. W., & Bonan, G. B. (2007). The Partitioning of Evapotranspiration into Transpiration, Soil Evaporation, and Canopy Evaporation in a GCM: Impacts on Land–Atmosphere Interaction. *Journal of Hydrometeorology*, 8(4), 862–880. https://doi.org/10.1175/JHM596.1
- Leyton, L., Reynold, E. R. C., & Thompson, F. B. (1967). Rainfall interception in forest and moorland. *International Symposium on Forest Hydrology*, *163*, 168. Retrieved from https://scholar.google.com.ec/scholar?hl=es&q=Rainfall+interception+in+forest+ and+moorland.+leyton+1967&btnG=&lr=#0

- Llambí, L. D., Soto-W, A., Célleri, R., Bièvre, B. De, Ochoa, B., & Borja, P. (2012). Ecología, hidrología y suelos de páramos. In Proyecto Páramo Andino (Ed.), *Proyecto Páramo Andino*. Ecuador: CONDENSAN.
- Llorens, P., Poch, R., Latron, J., & Gallart, F. (1997). Rainfall interception by a Pinus sylvestris forest patch overgrown in a Mediterranean mountainous abandoned area I. Monitoring design and results down to the event. *Journal of Hydrology*. Retrieved from http://www.sciencedirect.com/science/article/pii/S0022169496033343
- Lockwood, J. G., & Sellers, P. J. (1982). Comparisons of Interception Loss from Tropical and Temperate Vegetation Canopies. *Journal of Applied Meteorology*, 21(10), 1405–1412. https://doi.org/10.1175/1520-0450(1982)021<1405:COILFT>2.0.CO;2
- Maffei, M. (2012). Performance of Hargreaves equation in the estimating of reference evapotranspiration (ETo) in a zone of Andean paramo in Trujillo state, Venezuela. *Revista de La Facultad de Agronomía de La Universidad de Los Andes*, 29, 378–394.
- Marc, V., & Robinson, M. (2007). The long-term water balance (1972-2004) of upland forestry and grassland at Plynlimon, mid-Wales. *Hydrology and Earth System Sciences*, 11, 44–60. https://doi.org/10.5194/hess-11-44-2007
- Mauder, M., Cuntz, M., Drüe, C., Graf, A., Rebmann, C., Schmid, H. P., ... Steinbrecher, R. (2013). A strategy for quality and uncertainty assessment of long-term eddy-covariance measurements. *Agricultural and Forest Meteorology*, 169, 122–135. https://doi.org/10.1016/j.agrformet.2012.09.006
- Mayocchi, C. L., & Bristow, K. L. (1995). Soil surface heat flux: some general questions and comments on measurements. *Agricultural and Forest Meteorology*, 75(1–3), 43–50. https://doi.org/10.1016/0168-1923(94)02198-S
- Moehrlen, C., Kiely, G., & Pahlow, M. (1999). Long term water budget in a grassland catchment in Ireland. *Physics and Chemistry of the Earth, Part B: Hydrology, Oceans and Atmosphere*, 24(1–2), 23–29. https://doi.org/10.1016/S1464-1909(98)00006-9
- Moisen, G. (2008). Classification and regression trees. *Ecological Informatics*, 582–588. Retrieved from https://www.treesearch.fs.fed.us/pubs/30645
- Monson, R., & Baldocchi, D. (2014). Terrestrial Biosphere-Atmosphere Fluxes. In Terrestrial Biosphere-Atmosphere Fluxes. https://doi.org/10.1017/CBO9781139629218
- Moore, R. J. (1985). The probability-distributed principle and runoff production at point and basin scales. *Hydrological Sciences Journal*, *30*, 273–297. https://doi.org/10.1080/02626668509490989
- Moore, R. J., & Clarke, R. T. (1981). A distribution function approach to rainfall runoff modeling. *Water Resources Research*, *13*, 1367–1382. https://doi.org/10.1029/WR017i005p01367
- Mosquera, G. M., Célleri, R., Lazo, P. X., Vaché, K. B., Perakis, S. S., & Crespo, P. (2016). Combined use of isotopic and hydrometric data to conceptualize

- ecohydrological processes in a high-elevation tropical ecosystem. *Hydrological Processes*, *30*(17), 2930–2947. https://doi.org/10.1002/hyp.10927
- Mosquera, G. M., Lazo, P. X., Célleri, R., Wilcox, B. P., & Crespo, P. (2015). Runoff from tropical alpine grasslands increases with areal extent of wetlands. *CATENA*, *125*, 120–128. https://doi.org/10.1016/j.catena.2014.10.010
- Muñoz, P., Célleri, R., & Feyen, J. (2016). Effect of the resolution of tipping-bucket rain gauge and calculation method on rainfall intensities in an andean mountain gradient. *Water (Switzerland)*, *8*(11), 534. https://doi.org/10.3390/w8110534
- Nisbet, T. (2005). Water use by trees. Edinburgh.
- Novick, K., Brantley, S., Miniat, C. F., Walker, J., & Vose, J. M. (2014). Inferring the contribution of advection to total ecosystem scalar fluxes over a tall forest in complex terrain. *Agricultural and Forest Meteorology*, 185, 1–13. https://doi.org/10.1016/j.agrformet.2013.10.010
- Ochoa-Sánchez, A., Crespo, P., Carrillo-Rojas, G., Sucozhañay, A., & Célleri, R. (2019). Actual Evapotranspiration in the High Andean Grasslands: A Comparison of Measurement and Estimation Methods. *Frontiers in Earth Science*, 7(55). https://doi.org/10.3389/feart.2019.00055
- Ochoa-Sánchez, A., Crespo, P., & Célleri, R. (2018). Quantification of rainfall interception in the high Andean tussock grasslands. *Ecohydrology*, *11*(3), e1946. https://doi.org/10.1002/eco.1946
- Ochoa-Tocachi, B. F., Buytaert, W., Antiporta, J., Acosta, L., Bardales, J. D., Célleri, R., ... De Bièvre, B. (2018). High-resolution hydrometeorological data from a network of headwater catchments in the tropical Andes. *Scientific Data*, *5*, 180080. Retrieved from http://dx.doi.org/10.1038/sdata.2018.80
- Oki, T., & Kanae, S. (2006). Global hydrological cycles and world water resources. *Science*, *313*(5790), 1068–1072. https://doi.org/10.1126/science.1128845
- Padrón, R. S., Wilcox, B. P., Crespo, P., & Célleri, R. (2015). Rainfall in the Andean Páramo: New Insights from High-Resolution Monitoring in Southern Ecuador. *Journal of Hydrometeorology*, 16(3), 985–996. https://doi.org/10.1175/JHM-D-14-0135.1
- Papale, D., Reichstein, M., Aubinet, M., Canfora, E., Bernhofer, C., Kutsch, W., ... Yakir, D. (2006). Towards a standardized processing of Net Ecosystem Exchange measured with eddy covariance technique: algorithms and uncertainty estimation. *Biogeosciences*, 3(4), 571–583. https://doi.org/10.5194/bg-3-571-2006
- Penuelas, J., Rutishauser, T., & Filella, I. (2009). Phenology Feedbacks on Climate Change. *Science*, *324*(5929), 887–888. https://doi.org/10.1126/science.1173004
- Pepin, N., Bradley, R. S., Diaz, H. F., Baraer, M., Caceres, E. B., Forsythe, N., ... Yang, D. Q. (2015). Elevation-dependent warming in mountain regions of the world. *Nature Climate Change*, *5*(5), 424–430. https://doi.org/10.1038/nclimate2563
- Pereira, F. L., Gash, J. H. C., David, J. S., David, T. S., Monteiro, P. R., & Valente, F. (2009). Modelling interception loss from evergreen oak Mediterranean

- savannas: Application of a tree-based modelling approach. *Agricultural and Forest Meteorology*, 149(3), 680–688. https://doi.org/10.1016/j.agrformet.2008.10.014
- Perrin, J. L., Bouvier, C., Janeau, J. L., Ménez, G., & Cruz, F. (2001). Rainfall/runoff processes in a small peri-urban catchment in the Andes mountains. The Rumihurcu Quebrada, Quito (Ecuador). *Hydrological Processes*, *15*, 843–854.
- Poss, J. A., Russell, W. B., Shouse, P. J., Austin, R. S., Grattan, S. R., Grieve, C. M., ... Zeng, L. (2004). A volumetric lysimeter system (VLS): An alternative to weighing lysimeters for plant-water relations studies. *Computers and Electronics in Agriculture*, 43(1), 55–68. https://doi.org/10.1016/j.compag.2003.10.001
- Poulenard, J., Podwojewski, P., Janeau, J. L., & Collinet, J. (2001). Runoff and soil erosion under rainfall simulation of andisols from the Ecuadorian páramo: effect of tillage and burning. *Catena*, *45*, 185–207.
- Ramírez, D. A., Bellot, J., Domingo, F., & Blasco, A. (2007). Stand transpiration of Stipa tenacissima grassland by sequential scaling and multi-source evapotranspiration modelling. *Journal of Hydrology*, 342(1–2), 124–133. https://doi.org/10.1016/j.jhydrol.2007.05.018
- Rana, G., & Katerji, N. (2000). Measurement and estimation of actual evapotranspiration in the field under Mediterranean climate: A review. *European Journal of Agronomy*, 13(2–3), 125–153. https://doi.org/10.1016/S1161-0301(00)00070-8
- Reichstein, M., Falge, E., Baldocchi, D., Papale, D., Aubinet, M., Berbigier, P., ... Valentini, R. (2005). On the separation of net ecosystem exchange into assimilation and ecosystem respiration: review and improved algorithm. *Global Change Biology*, 11(9), 1424–1439. https://doi.org/10.1111/j.1365-2486.2005.001002.x
- Ren, Z., Li, Z., Liu, X., Li, P., Cheng, S., & Xu, G. (2018). Comparing watershed afforestation and natural revegetation impacts on soil moisture in the semiarid Loess Plateau of China. *Scientific Reports*, 8(1), 2972. https://doi.org/10.1038/s41598-018-21362-5
- Rincón, Y., Ataroff, M., & Rada, F. (2005). Dinamica hídrica de un pastizal de Pennisetum clandestinum Hochst ex. Chiov (pasto kikuyo) bajo distintos niveles de corte. In *Dinámica Hídrica en Sistemas Neotropicales. Investigaciones en Dinámica Hídrica de la red RICAS.* Mérida, Venezuela.
- Rose, C. W., & Sharma, M. L. (1984). Summary and recommendations of the Workshop on Evapotranspiration from plant communities. *Agricultural Water Management*, 8(1–3), 325–342. https://doi.org/10.1016/0378-3774(84)90061-1
- Rowley, J. (1970). Lysimeter and interception studies in narrow-leaved snow tussock grassland. *New Zealand Journal of Botany*, *8*(4), 478–493. https://doi.org/10.1080/0028825X.1970.10430158
- Royston, J. P. (1982). An Extension of Shapiro and Wilk's W Test for Normality to Large Samples. *Applied Statistics*, *31*(2), 115. https://doi.org/10.2307/2347973
- Rutter, A. J., Kershaw, K. A., Robins, P. C., & Morton, A. J. (1971). A predictive

- model of rainfall interception in forests, 1. Derivation of the model from observations in a plantation of Corsican pine. *Agricultural Meteorology*, 9, 367–384. https://doi.org/10.1016/0002-1571(71)90034-3
- Saleska, S. R. (2003). Carbon in Amazon Forests: Unexpected Seasonal Fluxes and Disturbance-Induced Losses. *Science*, *302*(5650), 1554–1557. https://doi.org/10.1126/science.1091165
- Savenije, H. H. G. (2004). The importance of interception and why we should delete the term evapotranspiration from our vocabulary. *Hydrological Processes*, *18*(8), 1507–1511. https://doi.org/10.1002/hyp.5563
- Scherrer, S., & Naef, F. (2003). A decision scheme to indicate dominant hydrological flow processes on temperate grassland. *Hydrological Processes*, *17*(2), 391–401. https://doi.org/10.1002/hyp.1131
- Seibert, J., & Vis, M. J. P. (2012). Teaching hydrological modeling with a user-friendly catchment-runoff-model software package. *Hydrology and Earth System Sciences*, *16*, 3315–3325. https://doi.org/10.5194/hess-16-3315-2012
- Serrano-Ortiz, P., Sánchez-Cañete, E. P., Olmo, F. J., Metzger, S., Pérez-Priego, O., Carrara, A., ... Kowalski, A. S. (2016). Surface-Parallel Sensor Orientation for Assessing Energy Balance Components on Mountain Slopes. *Boundary-Layer Meteorology*, *158*(3), 489–499. https://doi.org/10.1007/s10546-015-0099-4
- Sucozhañay, A., & Célleri, R. (2018). Impact of Rain Gauges Distribution on the Runoff Simulation of a Small Mountain Catchment in Southern Ecuador. *Water*, 10(1169). https://doi.org/10.3390/w10091169
- Sun, X., Onda, Y., Kato, H., Gomi, T., & Komatsu, H. (2015). Effect of strip thinning on rainfall interception in a Japanese cypress plantation. *Journal of Hydrology*, 525, 607–618. https://doi.org/10.1016/j.jhydrol.2015.04.023
- Uchida, T., Tromp-van Meerveld, I., & McDonnell, J. J. (2005). The role of lateral pipe flow in hillslope runoff response: an intercomparison of non-linear hillslope response. *Journal of Hydrology*, 311(1), 117–133. https://doi.org/10.1016/j.jhydrol.2005.01.012
- UN. (2018). Transforming Our World: The 2030 Agenda for Sustainable Development. In *A New Era in Global Health* (p. 41). https://doi.org/10.1891/9780826190123.ap02
- van den Bergh, T., Inauen, N., Hiltbrunner, E., & Körner, C. (2013). Climate and plant cover co-determine the elevational reduction in evapotranspiration in the Swiss Alps. *Journal of Hydrology*, *500*, 75–83. https://doi.org/10.1016/j.jhydrol.2013.07.013
- Van Halsema, G. E., & Vincent, L. (2012). Efficiency and productivity terms for water management: A matter of contextual relativism versus general absolutism. Agricultural Water Management. https://doi.org/10.1016/j.agwat.2011.05.016
- Venables, W. N., & Ripley, B. D. (2002). *Modern Applied Statistics with S* (4th ed.). https://doi.org/10.1007/978-0-387-21706-2
- Wagener, T., Boyle, D. P., Lees, M. J., Wheater, H. S., Gupta, H. V., & Sorooshian,

- S. (2001). A framework for development and application of hydrological models. *Hydrology and Earth System Sciences*, *5*, 13–26. https://doi.org/10.5194/hess-5-13-2001
- Walter, I. A., Allen, R. G., Elliott, R., Jensen, M. E., Itenfisu, D., Mecham, B., ... Martin, D. (2000). ASCE's Standardized Reference Evapotranspiration Equation. *Watershed Management and Operations Management 2000*, 10. https://doi.org/10.1061/40499(2000)126
- Wan, Z., Zhang, K., Xue, X., Hong, Z., Hong, Y., & Gourley, J. J. (2015). Water balance-based actual evapotranspiration reconstruction from ground and satellite observations over the conterminous United States. *Water Resources Research*, *51*(8), 6485–6499. https://doi.org/10.1002/2015WR017311
- Wesson, K. H., Katul, G., & Lai, C.-T. (2001). Sensible heat flux estimation by flux variance and half-order time derivative methods. *Water Resources Research*, 37(9), 2333–2343. https://doi.org/10.1029/2001WR900021
- Wieser, G., Hammerle, A., & Wohlfahrt, G. (2008). The Water Balance of Grassland Ecosystems in the Austrian Alps. *Arctic, Antarctic, and Alpine Research*, 40(2), 439–445. https://doi.org/10.1657/1523-0430(07-039)[WIESER]2.0.CO;2
- Wilcox, B. P., Dowhower, S. L., Teague, W. R., & Thurow, T. L. (2006). Long-term water balance in a semiarid shrubland. *Rangeland Ecology and Management*, 59(6), 600–606. https://doi.org/10.2111/06-014R3.1
- Williams, C. A., Reichstein, M., Buchmann, N., Baldocchi, D., Beer, C., Schwalm, C., ... Schaefer, K. (2012). Climate and vegetation controls on the surface water balance: Synthesis of evapotranspiration measured across a global network of flux towers. Water Resources Research, 48(6). https://doi.org/10.1029/2011WR011586
- Wilson, C. M., & Smart, P. L. (1984). Pipes and pipe flow process in an upland catchment, Wales. *CATENA*, *11*(2–3), 145–158. https://doi.org/10.1016/0341-8162(84)90004-3
- Xiao, Q, McPherson, E., Ustin, S., & Grismer, M. (2000). Winter rainfall interception by two mature open-grown trees in Davis, California. *Hydrological Processes*, 14(4), 763–784. Retrieved from http://www.academia.edu/download/42741864/Xiao_winter_20rainfall_2000.pdf
- Xiao, Qingfu, McPherson, E. G., Xiao, Q., & McPherson, E. G. (2011). Rainfall interception of three trees in Oakland, California. *Urban Ecosystems*, *14*(4), 755–769. Retrieved from https://www.treesearch.fs.fed.us/pubs/39932
- Zehetner, F., & Miller, W. P. (2006). Erodibility and runoff-infiltration characteristics of volcanic ash soils along an altitudinal climosequence in the Ecuadorian Andes. *Catena*, *65*, 201–210.
- Zhang, Q., Manzoni, S., Katul, G., Porporato, A., & Yang, D. (2014). The hysteretic evapotranspiration-Vapor pressure deficit relation. *Journal of Geophysical Research:* Biogeosciences, 119(2), 125–140. https://doi.org/10.1002/2013JG002484

Appendix A

Multiple linear regression model (MLR)

The following variables were intended as predictors: net radiation (mm/day), relative humidity (%), temperature (°C), wind speed (m/s), vapour pressure deficit (hPa), precipitation (mm/day), mean soil volumetric water content and at the initial time of the event (cm³/cm³), aerodynamic conductance (m/s), surface conductance (m/s), dew temperature (°C), beam radiation (MJ/m²/day) and diffuse radiation (MJ/m²/day).

1. Selection of predictors with the stepwise function in R version 3.3.2, package stats

The following variables were selected via the stepwise function: Net radiation (Rn) in mm/day, aerodynamic conductance (g_a) in m/s, surface conductance (g_s) in m/s, dew temperature (T_{dew}) in ${}^{\circ}C$, vapour pressure deficit (VPD), initial soil volumetric water content (VWC_{ini} in cm³/cm³) and wind speed (u_2) in m/s.

2. Collinearity between variables

As seen in Figure A1, VPD is linearly related with Rn. VPD explains 1 % of the variance in the MLR. T_{dew} also explains 1 % of the variance, thus it was not taken into account. VWC_{ini} accounts for 1.5 % and since the VWC at Andosols is never equal or below wilting point, VWC_{ini} was not considered. Finally, the four variables Rn, u_2 , g_a , g_s were chosen.

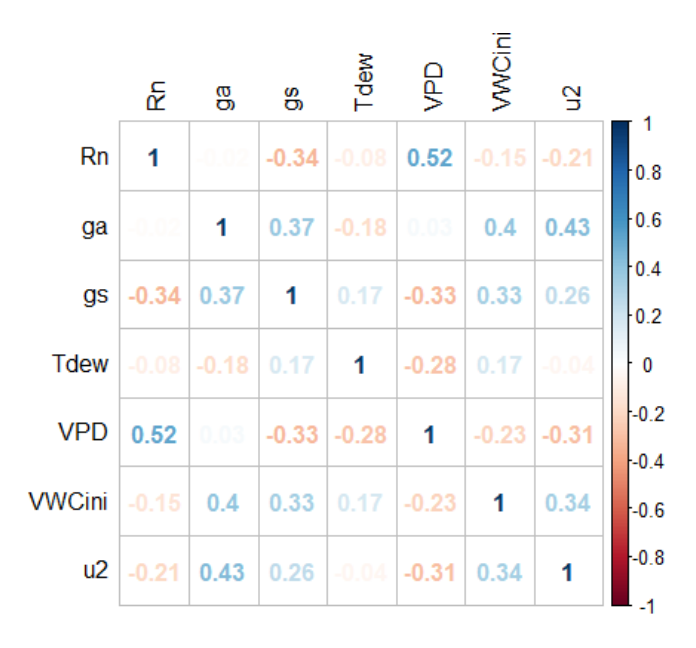


Figure A1. Collinearity between variables chosen with the stepwise method

3. Linear relationship between ETa and the predictors

Figure A2 shows the residuals and predictors which are around zero and vary constantly over the x-axis.

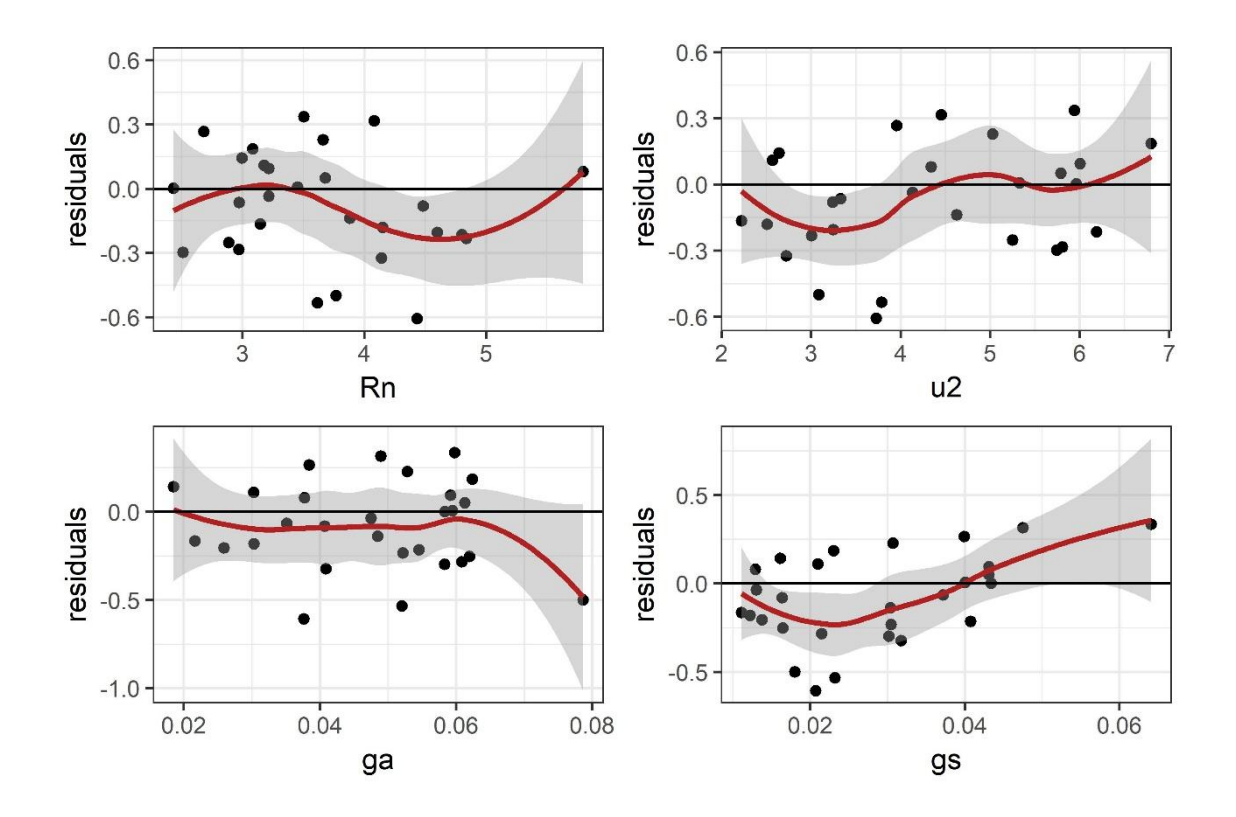


Figure A2. Model residuals vs. predictors

4. Normality of residuals

The Shapiro test (p-value of 0.7834) and the q-q plot in Figure A3 confirm normality.

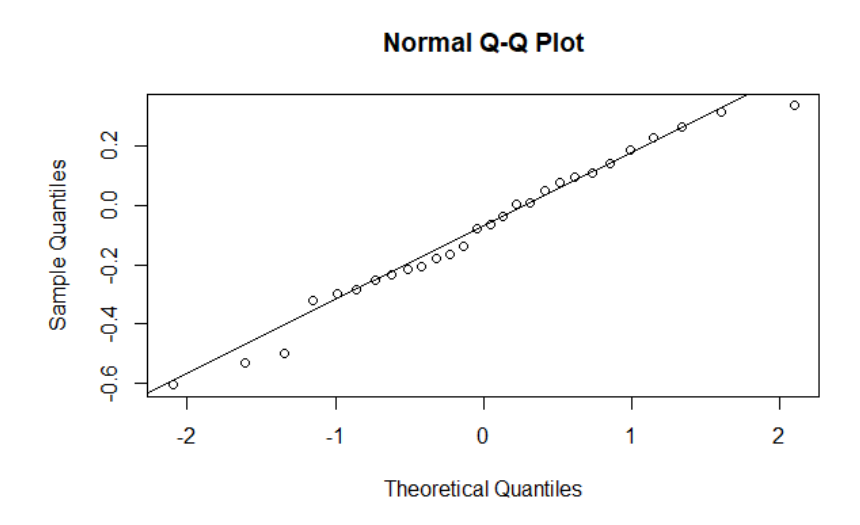


Figure A3. Q-Q plot of the model residuals

5. Homoscedasticity of residuals

Figure A4 shows dispersion plots between the model residuals and the fitted values of ETa. Residuals are randomly distributed around zero and they constantly along the x-axis. Additionally, the studentized Breusch-Pagan test had a p-value = 0.1846. There is no evidence of lack of homoscedasticity.

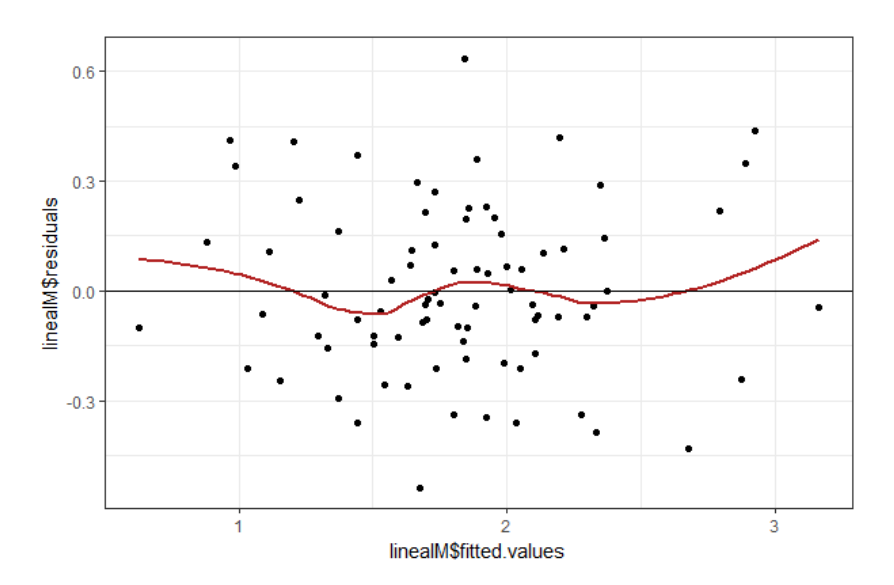


Figure A4. Model residuals vs. fitted values of ETa

About the author

Ana Elizabeth Ochoa Sánchez was born in Cuenca, Ecuador on January 24th, 1986. She graduated as Civil Engineer from the Faculty of Engineering, University of Cuenca, Ecuador in 2009. She graduated in 2012 as Master of Science in Water Resources Engineering from the Interuniversity Programme in Water Resources Engineering (IUPWARE) at the KU Leuven and Vrije Universiteit Brussel. From 2012 to 2015, she worked as a researcher in two projects related to climate change modelling and river modelling; both of them at the Department of Water Resources and Environmental Sciences (iDRHICA) at the University of Cuenca. In 2015, she started the Doctoral Programme in Water Resources.

Peer review publications

Ochoa-Sánchez, A., Crespo, P., Carrillo-Rojas, G., Marín, F., Célleri, R. Controls on Andean grasslands evapotranspiration and quantification of transpiration at event scale. Hydrological Processes, in review, 2019.

Carrillo-Rojas, G., Schulz, H.M., Orellana-Alvear, J., <u>Ochoa-Sánchez, A.,</u> Trachte, K., Célleri, R., Bendix, J. Atmosphere-surface fluxes modelling for the high Andes: The case of páramo catchments of Ecuador. Science of the Total Environment, accepted, 2019.

Montenegro, P., <u>Ochoa-Sánchez, A.</u>, Célleri, R. Impact of tussock grass removal on the soil water dynamics of a tropical mountain hillslope. Ecohydrology, 2019;e2146. doi: 10.1002/eco.2146, 2019.

Ochoa-Sánchez, A., Crespo, P., Carrillo-Rojas, G., Sucozhañay, A., Célleri, R. Actual evapotranspiration in the high Andean grasslands: a comparison of measurement and estimation methods. Frontiers in Earth Science, 7:55. doi: 10.3389/feart.2019.00055, 2019.

Ochoa, A., Timbe, L., Sánchez, E., Vázquez-Patiño, A., and Samaniego, E.: Unidimensional, non-stationary modeling of a high mountain river in southern Ecuador. Maskana, 9 (2). doi: 10.18537/mskn.09.02.2018, 2018.

Ochoa-Sánchez, A., Crespo, P., Célleri, R.: Quantification of rainfall interception in the high Andean tussock grasslands. Ecohydrology, 2018;e1946. doi: 10.1002/eco.1946, 2018.

Ochoa, A., Campozano, L., Sánchez, E., Gualán, R., and Samaniego, E.: Evaluation of Downscaled Estimates of Monthly Temperature and Precipitation for a Southern Ecuador Case Study. Int. J. Climatol., 36: 1244–1255. doi: 10.1002/joc.4418, 2015.

Ochoa, A., Pineda, L., Crespo, P., and Willems, P.: Evaluation of TRMM 3B42 precipitation estimates and WRF retrospective precipitation simulation over the Pacific—Andean region of Ecuador and Peru. Hydrol. Earth Syst. Sci., 18, 3179-3193. doi:10.5194/hess-18-3179-2014, 2014.

Book chapter

Correa, A., Ochoa-Tocachi, B., <u>Ochoa-Sánchez, A.</u>, Zogheib, C., Tovar, C., Buytaert, W. A concerted research effort to leapfrog hydrological understanding of South American hydrology: the case of the páramos, in Breña, A. and Birkel, C. (ed.) Tropical Hydrology: Processes and Patterns. American Geophysical Union, in review, 2019.

Conferences

International Mountain Conference. Innsbruck, September 2019. Ochoa-Sánchez, A., Crespo, P., Carrillo-Rojas, G., Sucozhañay, A. and Célleri, R. Understanding actual evapotranspiration of Tropical Andean grasslands: a comparison of measurement and estimation methods.

SaWaM project workshop. Loja, May 2019. <u>Ochoa-Sánchez, A</u>. Rainfall research: processes, downscaling and modelling.

EGU General Assembly 2019. Viena, April 2019. Ochoa-Sánchez, A., Crespo, P., Carrillo-Rojas, G., Sucozhañay, A., Célleri, R. Actual evapotranspiration at the Andean grasslands: comparison of daily and hourly measurements and estimates.

EGU General Assembly 2019. Viena, April 2019. Carrillo-Rojas, G., Schulz, H.M., Orellana-Alvear, J., Ochoa-Sánchez, A., Trachte, K., Célleri, R., Bendix, J. Modelling of land surface-atmosphere exchanges of energy and evapotranspiration for the páramo highlands of southern Ecuador.

Environmental changes in biodiversity hotspot ecosystems of South Ecuador: RESPonse and feedback effECTs (RESPECT). Ochoa-Sánchez, A., Crespo, P., Carrillo-Rojas, G., Sucozhañay, A., Célleri, R. Actual evapotranspiration in the high Andean grasslands. Loja, October 2018.

Jornadas de Bioética y Medio Ambiente. Cuenca, April 2018. Ochoa-Sánchez, A. Estudio de los Recursos Hídricos con miras a un desarrollo sustentable y principios éticos del uso del agua.

IUPWARE International Alumni Event 2018. Cuenca, March 2018. Ochoa-Sánchez, A., Crespo, P., Célleri, R. Rainfall interception in the high Andean grasslands.

Día Mundial del Agua. Cuenca, March 2018. <u>Ochoa-Sánchez, A.</u>, Crespo, P., Célleri, R. Cuantificación de la intercepción de lluvia en el pajonal altoandino.

Chapman Conference on Emerging Issues in Tropical Ecohydrology. Cuenca, June 2016. Palomeque, X., Ochoa-Sánchez, A., Chica, E., López, J., Crespo, P., Célleri, R. Exploring the potential of native trees for restoration of highland ecosystem in the Andes under climate change predictions.

Doctoral Courses

- Spatial Analysis with Geographical Information Systems, 2016.
- Advanced Statistics, 2016.
- Numerical methods, 2016.
- Scientific writing, 2016.
- Water Resources Planning and Management, 2016.
- Optional course: Random Forest and Decision Trees, 15 horas, 2018. Cuenca, Ecuador.